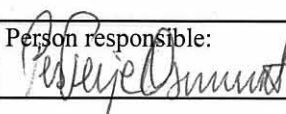


NGU Report 2010.015

The Fongen–Hyllingen layered intrusion,
Trondheim region, Norway: an excursion guide

Report no.: 2010.015		ISSN 0800-3416	Grading: Open
Title: The Fongen–Hyllingen layered intrusion, Trondheim region, Norway: an excursion guide			
Authors: J. Richard Wilson		Client: NGU	
County: Sør-Trøndelag		Commune: Selbu	
Map-sheet name (M=1:250.000) Trondheim, Røros		Map-sheet no. and -name (M=1:50.000)	
Deposit name and grid-reference:		Number of pages: 146	Price (NOK): 585,-
		Map enclosures:	
Fieldwork carried out:	Date of report: April 2010	Project no.: 325100	Person responsible: 
<p>Summary:</p> <p><i>The Fongen-Hyllingen complex, situated 60 km southeast of Trondheim, Norway, comprises the 160 km² Fongen-Hyllingen layered mafic intrusion (FHI) and the slightly younger, minor (3 km²) mafic to ultramafic Treknattan intrusion. The FHI was emplaced synorogenically in the Scandinavian Caledonides ~435 Ma ago. Folding and subsequent uplift and erosion allow access to the floor, walls and roof of the magma chamber. The complex itself has been affected to some extent by deformation and metamorphism, but sufficient primary features remain to study magma chamber processes in detail.</i></p> <p><i>Lateral correlation along ~40 km of strike length through ~6 km of layered cumulates has allowed reconstruction of the form and evolution of the magma chamber. The magma was emplaced into deformed and metamorphosed pelitic and basaltic rocks. There are abundant inclusions, particularly of metabasaltic hornfels, and the magma was contaminated by assimilation of ~8% of metapelitic material. Modal layering is exceptionally well developed in much of the FHI, and there are a wide variety of erosional structures. There is a very wide compositional range: olivine Fo₇₅₋₀; plagioclase An₆₇₋₁; Ca-rich pyroxene Mg#₈₀₋₀; Ca-poor pyroxene is also present locally. The sequence of appearance of cumulus minerals in the more evolved rock is: FeTi-oxides, calcic amphibole, apatite, biotite, zircon, quartz, alkali feldspar and allanite. The most evolved rocks (quartz-bearing syenites) are in direct contact with country rock amphibolites at the roof. The average composition of the cumulates is dioritic. The parental magma was broadly of andesitic composition.</i></p> <p><i>The FHI has been divided into four evolutionary stages on the basis of mineral chemical variations in a series of profiles normal to modal layering. Stage I (<350 m thick) comprises a basal reversal; Stage II (<2400 m) has fairly constant mineral compositions, with slightly more evolved rocks at the top; Stage III (<500 m) comprises a major compositional regression, ending with the most primitive compositions in FHI. In Stage IV (<1500 m) mineral compositions become more evolved upwards, ending with quartz-bearing syenites at the roof. Olivine-rich units in the lower part of Stage IV reflect minor events of magma addition.</i></p> <p><i>A vital feature of FHI is the presence of systematic lateral compositional variations in mineral chemistry with more evolved compositions along the strike of modal layering approaching the southern margin. These discordant relations between modal and cryptic layering developed as a result of the crystallisation of compositionally zoned magma along an inclined floor.</i></p>			
Keywords: layered intrusion	cryptic layering	fractionation	
gabbro	modal layering	assimilation	
synorogenic	Caledonides	inclusions	

CONTENTS

1. REGIONAL GEOLOGY, DESCRIPTION AND EVOLUTION OF THE FONGEN-HYLLINGEN COMPLEX	17
1.1. Introduction	17
1.2. Early studies of the Fongen-Hyllingen Complex	18
1.3. Regional setting of the Fongen-Hyllingen Complex	18
1.4. Isotopic age dating	21
1.5. Metamorphism and deformation	21
1.6. Main features of the Fongen-Hyllingen Intrusion	24
1.6.1. Layering features	24
1.6.2. Inclusions	25
1.6.3. Cumulate stratigraphy	25
1.6.4. Subdivision of the layered series into Stages	28
1.6.5. Lateral correlation of Stages	28
1.6.6. Isotopic variation in the Hyllingen Series	29
1.6.7. Parental magma composition, fractionation trend and conditions of crystallisation	29
1.6.8. The origin of discordant relations between modal and cryptic layering	31
2. GEOLOGICAL EXCURSION	36
2.1. Practical information	36
3. EXCURSION STOPS	37
3.1. Introduction to Stops 1 – 7	38
3.2. Stop 1: Southwest of Gjetleken	38
3.2.1. Location	38
3.2.2. Introduction	38
3.2.3. Description	38
3.2.4. Significance of the outcrops	42
3.3. Stop 2: Northwest of Gjetleken	45
3.3.1. Location	45
3.3.2. Introduction	45
3.3.3. Description	45
3.3.4. Significance of the outcrops	46
3.4. Stop 3: Southwest of Skjellåfjellet	47
3.4.1. Location	47
3.4.2. Introduction	47
3.4.3. Description	48
3.4.4. Significance of the outcrops	48
3.5. Stop 4: Waterfall at westernmost of 5 lakes	49
3.5.1. Location	49
3.5.2. Introduction	49
3.5.3. Description	49
3.5.4. Significance of the outcrops	52
3.6. Stop 5: ~1.5 km south of Hyllingen summit	55
3.6.1. Location	55
3.6.2. Introduction	55
3.6.3. Description	56
3.6.4. Significance of the outcrops	56
3.7. Stop 6: ~1.2 km south of Hyllingen summit	56
3.7.1. Location	56

3.7.2. Introduction	56
3.7.3. Description	56
3.7.4. Significance of the outcrops	57
3.8. Stop 7: Southern Ysterhøgda	58
3.8.1. Location	58
3.8.2. Introduction	58
3.8.3. Description	58
3.8.4. Significance of the outcrops	59
3.9. Introduction to Stops 8 - 12	61
3.10. Stop 8: Top of Gjetleken	62
3.10.1. Location	62
3.10.2. Introduction	63
3.10.3. Description	63
3.10.4. Significance of the outcrops	65
3.11. Stop 9: ~1 km northeast of Gjetleken	65
3.11.1. Location	65
3.11.2. Introduction	65
3.11.3. Description	66
3.11.4. Significance of the outcrops	66
3.12. Stop 10: ~1 km east-northeast of Gjetleken	67
3.12.1. Location	67
3.12.2. Introduction	67
3.12.3. Description	67
3.12.4. Significance of the outcrops	67
3.13. Stop 11: Tverfortfjellet	70
3.13.1. Location	70
3.13.2. Introduction	70
3.13.3. Description	71
3.13.4. Significance of the outcrops	72
3.14. Stop 12: Synste Skjellåa	73
3.14.1. Location	73
3.14.2. Introduction	73
3.14.3. Description	73
3.14.4. Significance of the outcrops	73
3.15. Introduction to Stops 13 - 16	73
3.16. Stop 13: Road 705 at Gressli	73
3.16.1. Location	73
3.16.2. Introduction	74
3.16.3. Description	74
3.16.4. Significance of the outcrops	78
3.17. Stop 14: Gresslivola	78
3.17.1. Location	78
3.17.2. Introduction	79
3.17.3. Description	79
3.17.4. Significance of the outcrops	79
3.18. Stop 15: NNE of Gresslivola	82
3.18.1. Location	82
3.18.2. Introduction	82
3.18.3. Description	82
3.18.4. Significance of the outcrops	83
3.19. Stop 16: Sæteråtjørna	83

3.19.1. Location.....	83
3.19.2. Introduction	84
3.19.3. Description	84
3.19.4. Significance of the outcrops	84
3.20. Introduction to Stops 17 - 24.....	85
3.21. Stop 17: Ramskar	86
3.21.1. Location.....	86
3.21.2. Introduction	86
3.21.3. Description	87
3.21.4. Significance of the outcrops	89
3.22. Stop 18: Angular discordance	90
3.22.1. Location.....	90
3.22.2. Introduction	90
3.22.3. Description	91
3.22.4. Significance of the outcrop	92
3.23. Stop 19: Fongen: the eastern ridge	93
3.23.1. Location.....	93
3.23.2. Introduction	93
3.23.3. Description	93
3.23.4. Significance of the outcrops	96
3.24. Stop 20: Modal layering profile	96
3.24.1. Location.....	96
3.24.2. Introduction	96
3.24.3. Description	96
3.24.4. Significance of the outcrops	99
3.25. Stop 21: The “summit inclusion”	100
3.25.1. Location.....	100
3.25.2. Introduction	100
3.25.3. Description	101
3.25.4. Significance of the outcrops	109
3.26. Stop 22: Fongen summit	112
3.26.1. Location.....	112
3.26.2. Introduction	112
3.26.3. Description	112
3.27. Stop 23: Impact structure	113
3.27.1. Location.....	113
3.27.2. Introduction	113
3.27.3. Description	114
3.27.4. Significance of the outcrops	114
3.28. Stop 24: Shear Zone west of Ramsjø lake.....	115
3.28.1. Location.....	115
3.28.2. Introduction	116
3.28.3. Description	116
3.29. Introduction to Stops 25 – 27	119
3.30. Stop 25: Ramåa (NW of Litlefongen)	119
3.30.1. Location.....	119
3.30.2. Introduction	119
3.30.3. Description	120
3.30.4. Significance of the outcrops	121
3.31. Stop 26: North of Ramåa (A)	122
3.31.1. Location.....	122

3.31.2. Introduction	123
3.31.3. Description	123
3.31.4. Significance of the outcrops	124
3.32. Stop 27: North of Ramåa (B)	125
3.32.1. Location.....	125
3.32.2. Introduction	125
3.32.3. Description	125
3.32.4. Significance of the outcrops	127
3.33. Introduction to Stops 28-31	128
3.34. Stop 28: Load features A.....	128
3.34.1. Location.....	128
3.34.2. Introduction	129
3.34.3. Description	129
3.35. Stop 29: Slump structures in an olivine-rich unit.....	130
3.35.1. Location.....	130
3.35.2. Introduction	130
3.35.3. Description	130
3.35.4. Significance of the outcrops	131
3.36. Stop 30: Load features B.....	131
3.36.1. Location.....	131
3.36.2. Introduction	131
3.36.3. Description	132
3.36.4. Significance of the outcrops	134
3.37. Stop 31: Olivine-rich unit 7 (The Kvassåsen unit).....	134
3.37.1. Location.....	134
3.37.2. Introduction	134
3.37.3. Description	136
3.37.4. Significance of the outcrops	139
4. ACKNOWLEDGEMENTS	141
5. REFERENCES.....	142

FIGURES

- Fig.1. Geological map of the Trondheim region showing the location of the Fongen-Hyllingen Intrusion (FHI). Based on Roberts & Wolff (1981).19
- Fig.2. The relationship of the Fongen-Hyllingen Complex to geological events in the Trondheim region. Data is taken from Olesen et al. (1973), Furnes et al. (1980), Roberts & Sturt (1980) and Wolff & Roberts (1980). The timing of intrusion of the FHI has recently been revised to close to 435 Ma (see text). Palaeomagnetic studies of the FHI have been carried out by Abrahamsen et al. (1979).20
- Fig.3A. Location of Fig.3 in Norway. B. Country rock lithology in the vicinity of the Fongen-Hyllingen Complex. The approximate locations of sample profiles A, B and C used in Fig.5 are shown. C. Contact and regional metamorphism. Based largely on Olesen et al. (1973).23
- Fig.4. PT diagram for metamorphic events involving the Fongen-Hyllingen Complex showing (a) contact metamorphism at 3.5 ± 0.5 kb (b) regional metamorphism in amphibolite facies at 5-6 kb (c) retrograde metamorphism in greenschist facies at 3-4 kb and 350-450°C (d) retrograde metamorphism in prehnite-pumpellyite facies at 2-3 kb and 200-250°C.24
- Fig.5. Cumulate stratigraphy of the Fongen-Hyllingen Intrusion based on fig.3 in Wilson & Sørensen (1996). The approximate locations of sample profiles A, B and C are shown in Fig.3B. Lateral compositional variations result in a slight gap between the top of Profile B and the base of Profile C.....26
- Fig.6. Compositional variations of major silicates in the Fongen-Hyllingen Intrusion. The most calcic plagioclase in Fig.5 is An₅₇. More calcic compositions (up to An₆₇) have been found in the Hyllingen Series (Modified after Wilson et al. 1981b and Wilson & Larsen, 1985). The most magnesian olivine found in the FHI is Fo₇₅. The most iron-rich Ca-poor pyroxenes are replaced by grunerite (Fe-Mg-Mn amphibole).27
- Fig.7. Compositional variations in a profile (close to EE' in Enclosure 1) through the Hyllingen Series. From left to right: stratigraphic thickness (using the Stage III/IV boundary as datum); inclusions (in brown); Mg# in Ca-rich pyroxene; An% in plagioclase; initial Sr-isotopic ratio; e_{Nd} values; subdivision into evolutionary stages.28
- Fig.8A. Distribution of cumulus apatite and zircon in the Hyllingen Series. B. Contoured compositional variation of Mg# in Ca-rich pyroxene in the Hyllingen Series. Plagioclase compositions show a similar variation to Ca-rich pyroxene. Based on fig.11 in Wilson & Larsen (1985).30
- Fig.9A. The nature of discordant relations between modal and cryptic layering in the Hyllingen Series. Cryptic layering is illustrated by the compositional variation of olivine and entry of cumulus apatite when olivine reaches ~Fo₃₇. B. Modal and cryptic layering are interpreted as representing isochrons and isotherms respectively. C. Development of the discordant relations by crystallisation of compositionally zoned magma along an inclined floor. Cryptic layering probably dips at an angle (a) between that of the crystallisation front and the horizontal. D. Crystallisation during elevation of the resident zoned magma by influx of dense magma along the magma chamber floor will give rise to a compositional regression. The angle b will depend on the relative rates of influx and crystallisation. Hypothetical compositional variations through profiles X, Y and Z are32

shown in Fig.9E. E. Hypothetical compositional profiles (X, Y and Z) through a regression like that in Fig.9D. The compositional variation of olivine is shown in three profiles, together with the entry of apatite at Fo ₃₇ . Note that (a) the compositional regression develops concordant to modal layering. (b) Compositions become more evolved along modal layering from X to Z (up-slope in Fig.9D). (c) The Z-shaped pattern of distribution shown by the entry of cumulus apatite (compare with Fig.8A). Some of the consequences of crystallisation along a sloping floor have been discussed by Huppert et al. (1987).	33
Fig.10. Schematic illustration of the southern end of the Fongen-Hyllingen magma chamber during crystallisation of compositionally zoned magma along an inclined floor. During magma chamber expansion by influx of dense magma elevating the magma column, the first magma to come in contact with the new floor at the leading edge is the evolved magma at the magma chamber roof. Crystallisation during continued influx results in a compositional reversal up through Stage I (HS-I) as denser, more primitive magma layers come in contact with the crystallisation front. Away from the leading edge, more primitive magma is crystallising at the same time to produce Stage II (HS-II).....	33
Fig.11A-E: Schematic development of the Fongen-Hyllingen magma chamber. The Treknattan Intrusion formed during stage E. F: The form of the Fongen-Hyllingen layered intrusion after deformation. See text for further explanation.	35
Fig.12. Simplified geological map of the Fongen-Hyllingen complex which comprises the Fongen-Hyllingen layered intrusion (FHI) and the small Treknattan intrusion. The FHI has been subdivided into stages on the basis of mineral compositions in a series of profiles normal to modal layering; these allow lateral correlation. The locations of Stops 1 – 31 and the Trondheim Turistforening huts (Grasslihytta, Ramsjøhytta and Schulzhytta) are shown.	38
Fig.13. Locations of Stops 1 to 6. This map has been extracted from Enclosure 1. The boundaries between Stages II, III and IV are shown by dotted lines.....	40
Fig.14. Photomicrograph of metabasalt from the inner contact metamorphic aureole at Stop 1. The mineralogy is dominated by hornblende (Hb) with minor plagioclase (Pl). There are veins of calcite (Cc) and epidote (Ep). PPL. (FH 06-01).....	41
Fig.15. View to the north from just south of the bridge at Stop 1. The outcrops by the bridges and on the banks of the stream are of metabasaltic country rocks. Marginal diorites belonging to the Fongen-Hyllingen Intrusion outcrop ~250 m to the north along the stream.....	42
Fig.16. Photomicrograph of coarse grained dioritic from the Fongen-Hyllingen marginal facies near Stop 1. The large hornblende (Hb) contains ilmenite dust. The evolved composition of this rock from Stage I is evident from the presence of quartz (Q) and apatite (Ap). Pl = plagioclase. PPL. (FH 06-08).	43
Fig.17. The southern part of the Hyllingen Series showing the locations of: a) profiles B' to H in Fig.18; b) profiles H2 and H3 in Fig.40; c) Stops 1 – 12.	44
Fig.18. Subdivision of stratigraphic columns through the Hyllingen Series based on lithology and compositional evolution as shown by, for example, An% in plagioclase, Fo% in olivine and Mg# in pyroxenes. B. Correlation of profiles in the lower part of the Hyllingen Series showing modal layering, raft-like metabasaltic inclusions, presence of zircon, and Mg# in	

clinopyroxene. Stage I comprises a basal reversal. The Stage I/II boundary is located where Mg#cpx ceases to increase upwards. This boundary is not clear in profiles G and H where two possible interpretations are shown. Stage I is entirely located in un-layered diorites in the northern profiles i.e. modal layering first develops when the basal regression has ceased. Mg#cpx values remain more or less constant with stratigraphic height in the lower part of Stage II. The numbers in brackets below each profile are the average Mg#cpx values and standard deviations for the individual profiles. Two values are given for profiles G and H representing the upper and lower placings of the Stage I/II boundary respectively. It is important to observe that these compositions become quite systematically more evolved towards the south, from Mg#cpx_{~59} in profile B' to Mg#cpx_{~45} in profile H. The basal regression is also shown by other mineral compositions. For example, the profile C regression covers the ranges clinopyroxene Mg#cpx₂₀₋₅₇, plagioclase An₃₅₋₄₇, and olivine Fo₄₋₃₀, accompanied by the upward disappearance of zircon and apatite. Along the boundary between the layered series and the marginal diorite a thickness of ~600 m of layered rocks wedge out to the south over a distance of ~4 km, a discordance of ~7°.....45

- Fig.19. Photomicrograph of olivine diorite from Stop 2 near the base of Stage II in the Hyllingen Series. Olivine, plagioclase, Ca-rich pyroxene, magnetite and apatite are cumulus phases. Brown hornblende is intercumulus. The identified olivine grain has a narrow corona of orthopyroxene followed by green hornblende. PPL. (FH 06-2).....46
- Fig.20. View to the north from near Stop 2. Modal layering (striking ~north-south and dipping to the east) in brown-weathering un-metamorphosed rocks is visible to the right of the person. The grey colour in the right centre is developed in metamorphosed equivalents (in amphibolite facies). The shallow eastward dip of the layering is apparent in the summit of Hyllingen (1205 m) in the distance (about 4 km away).....47
- Fig.21. Metabasaltic hornfels inclusion at Stop 3 with a granoblastic texture consisting of small rounded grains of plagioclase, Ca-rich and Ca-poor pyroxene and minor FeTi-oxide. Pyroxene hornfels facies. PPL. (FH 06-3a).....48
- Fig.22. Contact metamorphosed plagioclase-pyrrhic basalt at Stop 3. The relict plagioclase phenocryst consists of several sub-grains. The main mafic minerals are Ca-rich and Ca-poor pyroxenes together with brown hornblende. PPL. (FH 06-3c)49
- Fig.23. Several nested trough structures in olivine gabbro at Stop 4. Photograph taken looking north. Stratigraphic up is to the right.....50
- Fig.24. Modally layered, brownish olivine gabbro is cut by a series of grey veins at Stop 4. These are fractures on either side of which the rock has been metamorphosed to an amphibolite facies mineral assemblage. This static metamorphism is locally widespread in the Hyllingen Series.51
- Fig.25. Alteration of brown-weathering gabbro to grey-weathering metagabbro is obviously related hydration on either side of a thin vein.52
- Fig.26. Oikocrysts of calcic amphibole in gabbro near Stop 4.53
- Fig.27. Scan of thin section (2 x 3.4 cm) of olivine-bearing gabbro with a large, optically continuous, oikocryst of brown hornblende. Near Stop 4. PPL. (WF-183).54
- Fig.28. Bleached plagioclase-rich layer at Stop 5.....55

Fig.29. Rounded olivines and magnetite enclosed by brown hornblende in the lower of two large trough structures at Stop 6. PPL. (FH06-6).	57
Fig.30. View to the north from near Stop 6 looking along the strike of modal layering. The summit of Fongen (1441 m) is visible in the distance.	58
Fig.31. Location of Stop 7. This map has been extracted from Enclosure 1. The boundary between Stages III and IV is shown by a dotted line.	59
Fig.32. Sharp contact at the roof of the Fongen-Hyllingen layered intrusion between pink quartz-bearing syenites below and country rock metabasaltic hornfels above. The syenite is extremely evolved with low-temperature end-member mineral compositions.	60
Fig.33. Quartz-bearing syenite from just below the roof at the top of the Hyllingen Series at Stop 7. The mafic minerals include ferroedenite (Fe-ed), allanite (Al), biotite (Bi), zircon (Z) and hedenbergite (not in photo). Felsic minerals are mainly albite and K-feldspar with minor quartz. PPL. (FH 06-16a).	61
Fig.34. Metabasaltic country rock from ~1 m above the roof contact in the eastern Hyllingen area (Stop 7). The rock consists dominantly of granular hornblende and plagioclase (lower part of photo) with veins of coarser grained clinopyroxene and plagioclase (upper part). PPL. (FH 06-16b).	61
Fig.35. Locations of Stops 8-12. The boundaries between Stages II, III and IV are shown with dotted lines.	62
Fig.36. Modally layered metagabbro with a coronitic texture near Stop 8. Brown cores of cummingtonite (replacing Ca-poor pyroxene and/or olivine) are surrounded by black hornblende (green in thin section). See also Fig.37.	64
Fig.37. Cummingtonite metagabbro from near Stop 8. A Ca-poor pyroxene grain has been replaced by a granular aggregate of cummingtonite/grunerite (Cu) rimmed by greenish hornblende (green Hb) where the pyroxene was adjacent to plagioclase. This kind of corona structure is commonly developed in the FHI. Ca-rich pyroxene has been partially pseudomorphed to tremolite/actinolite (uralite; Ur). Primary igneous brown hornblende remains largely unaltered. There are many small apatite grains. This coronitic metagabbro contains four different amphiboles. PPL. (FH 92).	65
Fig.38. Rusty-weathering rocks at the tip near the entrance to the old copper mine at Stop 9.	66
Fig.39. Looking north along the strike of modal layering from near Stop 10.	68
Fig.40. Compositional variation of Ca-rich pyroxene and Sr- and Nd-isotopic variations in Stage III in profiles F1 (in the northern Fongen area), H2 and H3. Locations of H2 and H3 are shown on Fig.17. Adapted from fig.7 in Sørensen & Wilson (1995) where the Nd-isotopes are discussed. Brown intervals to the left are metabasaltic inclusions.	69
Fig.41. Comparison of Mg-number in Ca-rich pyroxene (cpx), plagioclase An%, Sr_i and e_{Nd} at the base and top of Stage III in profiles F1 (northern Fongen), H2 (near Stop 4) and H3 (near Stop 10). Arrows point from data at the base to the top. So the length of the arrow shows the magnitude of the regression. Dashed lines connecting points from different profiles illustrate lateral compositional variations. Note that the scale for Sr_i has been reversed. Adapted from fig.8 in Sørensen & Wilson (1995) where the Nd-isotopes are discussed.	70
Fig.42. Garnet-rich diorite resulting from the assimilation of metapelitic material near Stop 11.	71

Fig.43. Metapelitic hornfels from near Tverfortfjellet (Stop 11). Sillimanite (Sil) is partially altered to muscovite. Biotite (Bi) is abundant. The colourless groundmass consists largely of plagioclase and quartz. PPL. (FH 06-13).....	72
Fig.44. Location of Stop 13.....	74
Fig.45. Layered metagabbro on the right is dragged into a shear zone at Stop 13. Within the shear zone the rocks are foliated amphibolites with tonalitic and granitic veins.	75
Fig.46. Foliated amphibolite at Stop 13 cut by tonalitic and granitic veins, some of which are pegmatitic. The arrowhead is in a near-vertical fine-grained felsic dyke that cuts across all other lithologies. The hammer shaft to the left of the arrowhead is 40 cm long.....	76
Fig.47. Microphotograph of amphibolite from Stop 13 (Fig.46). Original igneous plagioclases retain some of their integrity whereas the mafic minerals now consist of green hornblende, ilmenite and minor biotite. PPL. (FH07-6a).	77
Fig.48. Microphotograph of foliated amphibolite from the outcrop shown in Fig.47 at Stop 13. The texture is much finer grained than in Fig.47 and the foliation (E-W in the picture) is obvious. The mineral assemblage is the same as that in Fig.47. PPL. (FH07-6b).....	78
Fig.49. Locations of Stops 14 to 16 in the Gresslivola area. This map has been extracted from Enclosure 1.	80
Fig.50. Microphotographs of cummingtonite metagabbro in plane polarised light (above) and cross-polarised light (below). (Sample FH07-7 from the Gresslivola area).....	81
Fig.51. Serpentinised, brownish, olivine-rich layer (to right of hammer) in grey metagabbro striking towards the summit of Melshogna to the north. The olivine-rich layer has been slightly offset by a minor fault.....	82
Fig.52. Stop 15. Granitic pegmatite with large, thin flakes of biotite.....	83
Fig.53. Stop 16. Foliated amphibolite within a shear zone. An agmatitic structure is developed in which blocks and streaks of grey amphibolite are separated by veins of tonalite and granite.	84
Fig.54. Stop 16. Relict modal layering is preserved in this block of metagabbro that is enclosed by strongly foliated felsic rocks.....	85
Fig.55. View of Fongen from the east across Ramsjø lake. The summit (1441 m) is ~5 km away. The Trondheim Turistforening tourist hut “Ramsjøhytta” is on the left. The pass “Ramskaret” is just off the photo to the right. Stops 18 – 23 are on the ridge to the right of the summit. Stop 22 is at the summit. The summit of Fongskaftet is behind the large hut to the left of Fongen. The overall ~20-30° southerly dip of the layering in this area can be discerned below Fongen summit.....	87
Fig.56. Locations of Stops 17 to 23.	87
Fig.57. Plagioclase-phyric metabasaltic dyke in the Ramskar area (Stop 17).	88
Fig.58. Brecciated metapelitic hornfels with granitic veins from the inner contact metamorphic aureole at Stop 17.	89
Fig.59. PT diagram for contact metamorphism in metapelites around the Fongen-Hyllingen layered intrusion. The Al_2SiO_5 phase boundaries (with some degree of uncertainty in blue lines), first occurrence of almandine (+ alm; by a variety of mineral reactions), staurolite stability field, first occurrence of orthoclase (kf) (by the reaction muscovite = K-feldspar + Al_2SiO_5) and the onset of partial melting (PM) are from fig.7.8 in Bucher & Frey (1994). The cordierite stability field has been expanded towards	

higher pressures than shown in fig.8 in Bucher & Frey (1994) as would be appropriate for slightly more magnesian compositions than used by these authors. The + oa (= orthoamphibole-in) and + opx (orthopyroxene-in) curves have been moved to temperatures intermediate between those shown in figs.7.8 and 7.13 in Bucher & Frey (1994). The contact metamorphism took place below ~4 kb because of the presence of a wide andalusite zone, but the lower limit is hard to constrain. A pressure of 3.5 ± 0.5 kb seems a reasonable estimate. It must be borne in mind that the FHI has a thickness of ~6 km.	90
Fig.60. Angular unconformity in layered metagabbro at Stop 18. Up is to the left.....	91
Fig.61. Load features at the top of a plagioclase-rich layer just below the unconformity in Fig.60. Up is to the left.....	92
Fig.62. Strongly disturbed modal layering caused by the impact of a large inclusion on the magma chamber floor.	93
Fig.63. Modal layering truncated by disturbed layered rocks. This is again caused by the impact on the floor of an inclusion falling from the roof.	94
Fig.64. Metabasaltic hornfels inclusion with dendritic olivine porphyroblasts. The olivines are altered to amphibole along a vein just above the pen.....	94
Fig.65. Chilled contact between a basaltic dyke (left) and metabasalt in an inclusion. Both are now in pyroxene hornfels facies.	95
Fig.66. Fold structures in an inclusion of metapelitic hornfels. The light layers consist largely of plagioclase and quartz and the dark layers of orthopyroxene and green spinel.	95
Fig.67. The modally layered sequence at Stop 20 has been studied in detail by Josephsen (2003). The section in Fig.68 is marked.	97
Fig.68. Detailed stratigraphic log through a 6.5 m-thick profile normal to the layering at Stop 20. The lower ~3 m of the profile are on the left and the upper ~3.5 m on the right. From left to right: Stratigraphic height relative to the top of a striking olivine-rich layer (Fig.67); layer number (L1-L73); indication of the type of layer – isomodal (blue), normally graded (red) or inversely graded (yellow); illustration of the lithological variation of the profile in grey tones; location of thin sections for point counting; modal variation.....	98
Fig.69. Fo-An-Di phase diagram at 1 atmosphere from Morse (1980). The bulk modal compositions of different intervals are plotted together with some relevant contours.	99
Fig.70. The basal contact of the summit inclusion is concordant with modal layering in the underlying cumulates. Stop 21.....	100
Fig.71. Stop 21. Modally layered cumulates to the left are overlain concordantly by the summit inclusion.	101
Fig.72. Vertical section through the summit inclusion.	102
Fig.73. Metabasaltic hornfels with gabbroic streaks in the summit inclusion.	103
Fig.74. Layered gabbroic interval in the summit inclusion.....	103
Fig.75. Globular metabasaltic hornfels in a gabbroic matrix in the summit inclusion.	104
Fig.76. Granoblastic metabasaltic hornfels with porphyroblasts of olivine and brown hornblende.....	105
Fig.77. Scans of thin sections (2 x 3.5 cm). Left: Contact between globular metabasaltic hornfels and gabbroic matrix. Sample from outcrop in Fig.75.	

Right: Metabasaltic hornfels with gabbroic streaks. Sample from outcrop in Fig.73.....	106
Fig.78. Plagioclase grain enclosing granules of clinopyroxene (top; CPL) and a clinopyroxene grain enclosing small granules of plagioclase (bottom; PPL). Fields of view ~2 x 3 mm. (DH13).	107
Fig.79. Compositions of pyroxenes, olivine and plagioclase in the summit inclusion. The compositions of the same minerals in FHI cumulates immediately under the inclusion are shown for comparison.....	108
Fig.80. Total alkali vs silica plot for 14 essentially homogeneous samples from the summit inclusion (orange area). They all lie in the basalt field and are more primitive than the composition of the FHI parental magma (FH from Abu El-Rus et al., 2007).....	109
Fig.81. Simplified model for generation of metabasaltic inclusions in the FHI. Intrusion of a wedge-shaped, sill-like body into Fundsjø Group metabasalts. Continued influx and magma chamber expansion results in the magma penetrating the roof. During continued influx some of the sill-like bodies at the roof merge. Raft-like portions of the roof become totally engulfed in magma. The raft-like inclusions may remain interlinked in three dimensions. The crystallisation front moves upwards throughout this process.	110
Fig.82. Model for genesis of the extreme textural variations in the summit inclusion involving the flux of heat (red arrows) and fluids. The summit inclusion initially formed part of the roof and was only heated from below (during stage A in Fig.81). As magma penetrated above the inclusion it became heated from both sides (during stages B & C in Fig.81). The boundaries between the different textural types and the orientation of layering in the summit inclusion are parallel with its contacts and probably developed along isothermal surfaces.....	111
Fig.83. Stop 22. The author at the main cairn on the top of Fongen (1434 m). The view is to the east.	113
Fig.84. Stop 23. Impact structure formed by a metabasaltic inclusion. A sketch of the structure as seen normal to the layering is shown in Fig.85 which identifies inclusion A. The small inclusion C is near the hammer at the top of the photograph.	115
Fig.85. Stop 23. Sketch of the impact structure in Fig.84.....	115
Fig.86. Location of Stop 24. Two different views of the elongate EW metabasaltic inclusion at 1098 m are shown in Figs.87 & 89.....	116
Fig.87. View of Fongskaftet from the NE showing the location of the shear zone at Stop 24 illustrated in Fig.88 and a ridge formed of a metabasaltic inclusion (~60 m high). A view of this ridge from above is shown in Fig.89.....	117
Fig.88. Stop 24. Shear zone cutting through layered gabbro.	118
Fig.89. The elongate east-west metabasaltic inclusion (the highest point of which is at 1098 m) in Fig.86 forms a striking ridge which is ~700 m long. The ridge seen from a different angle is shown in Fig.87.....	118
Fig.90. Location of Stop 25.....	120
Fig.91. Hornblende plagioclase pegmatite at Stop 25. Relatively fine-grained (A) or coarse-grained, massive (B) bands rich in hornblende are roughly perpendicular to prismatic hornblendes. Some of the elongate hornblendes branch from right to left, implying that they grew in that direction.....	120

Fig.92. A skeletal structure is sometimes developed in hornblende crystals in the hornblende plagioclase pegmatite at Stop 25.....	121
Fig.93. Brownish olivine gabbro showing alteration to grey metagabbro ca. 1.5 km northwest of Stop 25.	122
Fig.94. Location of Stops 26 and 27 in the Treknattan Intrusion.....	123
Fig.95. Olivine cumulates of the Treknattan intrusion at Stop 26. Sub-rounded blocks of greyish-brown, plagioclase-rich olivine cumulates are enclosed in brown olivine cumulates with less intercumulus plagioclase. In the picture this is most obvious to the right of the hammer.	124
Fig.96. Olivine cumulates of the Treknattan Intrusion at Stop 27. The hammer shaft is on a large plagioclase oikocryst. The irregular-shaped, brownish patches represent oikocrysts of clinopyroxene and/or hornblende.	126
Fig.97. View of the Treknattan area to the ESE from Stop 27. The highest point is the summit of Fongen (1441 m). The Treknattan Intrusion is poorly exposed in the Ramåa valley. On the southern side of the valley the intrusion extends towards the summit of Fongen mountain. The olivine-rich rocks of the Treknattan body, that are more easily weathered than the layered gabbros and metabasaltic inclusions of the FHI, occupy the saddle-shaped area in the centre of the picture.	127
Fig.98. Locations of Stops 28 to 30.	128
Fig.99. Stop 28. The olivine-rich unit in the foreground is ~1.2 m thick. The view to the north includes the summits of Fongen (left; ~4.5 km away) and Fongskaftet (right centre; ~3 km away).	129
Fig.100. Stop 28. Polygonal patterns in the plane of the layering in an olivine-rich unit. The lighter-coloured polygonal shapes consist of discrete, altered plagioclases in a darker, olivine-rich matrix. The “cells” are separated by continuous dunitic rims.	130
Fig.101. Stop 29. Fold structure in the troctolitic upper part of an olivine-rich unit.....	131
Fig.102. Stop 30. A series of “mushroom” structures in a ~6 cm-thick layer in an olivine-rich unit.	132
Fig.103. Schematic model showing possible development of the deformation structures in Figs100 & 102. 1 = largely consolidated gabbro. 2 = plagioclase-rich crystal mush. 3 = olivine-rich crystal mush (in contact with magma in A). The progressive deformation caused by density contrast between layers 2 and 3 is shown in stages from A to C. Stage B is equivalent to that in Fig.102, whereas stage C is equivalent to that in Fig.100. The diagram is very similar to those shown by Ankatell et al. (1970) for the experimental deformation of water-saturated sediments in a non-mobile system with reversed density gradients.	133
Fig.104. Location of Stop 31.....	135
Fig.105. Simplified geological map of the area containing olivine-rich units 1-7. Based on Enclosure 1 and Meyer & Wilson (1999). Sample profiles A – D have been studied by Meyer & Wilson (1999).	136
Fig.106. View to the north from near Stop 31 along the strike of olivine-rich unit 7. The approximate location of unit 7 is marked with a dashed line. The most olivine-rich part of unit 7 (sub-unit e in Fig.107) forms the brown-weathering rocks. Unit 7 dips to the east along its entire strike length.....	137
Fig.107. Lithological variations in unit 7 established on the basis of 17 logs. Datum is the lower level of the pyroxenite (chC) that defines the base of the unit. Unit 7 has been divided into 8 sub-units on the basis of the	

lithology and scale of layering. Vertical exaggeration = x 20. Cumulus phase notation: p = plagioclase; c = Ca-rich pyroxene; o = olivine; h = Ca-poor pyroxene; m = magnetite; C = cumulate. Abbreviations after C = intercumulus status. Numbers 1-17 are the log numbers. Stop 31 is in the vicinity of log 6.	138
Fig.108. Stop 31. Sub-unit e in olivine-rich unit 7 consists largely of alternating layers of dunite (dark brown) and troctolite (paler brown). Small-scale modal layering is beautifully developed. Looking south; stratigraphic up is to the left.....	139
Fig.109. Stop 31. Laterally persistent small scale layering in sub-unit e in olivine-rich unit 7. Stratigraphic up is to the right. Two small trough-like features are developed to the left of the hammer. Olivine in the dark-brown layers has been partially altered to serpentine. These layers weather out preferentially so that the paler brown, plagioclase-bearing layers stand out to give a striking ribbed appearance to the outcrops. Thin veins of serpentine are aligned at a slight angle to the modal layering below the hammer and elsewhere.	140
Fig.110. Relatively pervasive alteration of olivine to serpentine in one of the olivine-rich units. Largely unaltered olivine remains brown. Serpentine is white. Magnetite produced during the metamorphic reaction forms black, metallic veins. Oikocrysts of Ca-rich pyroxene stand out as small resistant spheres.	141

1. REGIONAL GEOLOGY, DESCRIPTION AND EVOLUTION OF THE FONGEN-HYLLINGEN COMPLEX

1.1. Introduction

It is largely through field studies of igneous intrusions that knowledge of magma chamber processes can be advanced. Layered intrusions can be particularly rewarding in this respect because the layering allows "stratigraphic" aspects to be considered, such as the direction of younging, lateral correlation and estimates of thicknesses. Fractional crystallisation is commonly efficient in their development and a wide compositional range of products may be produced, for example from ultramafic to felsic. Layered intrusions can crystallise from a single batch of magma in a closed chamber, or from successive influxes when information can be obtained as to how magma is repeatedly emplaced. Layered intrusions can be economically important, particularly for chrome, nickel, platinum group elements and gold.

Until the late 1970's it was widely accepted that crystal settling and large scale thermal convection played vital roles during the cooling of large magma bodies, as persuasively argued in the classic book on layered igneous rocks by Wager & Brown (1968). However, a compelling combination of field, experimental and theoretical considerations (Campbell, 1978; McBirney & Noyes, 1979; Irvine, 1980; Irvine et al., 1983; Martin et al., 1987; Parsons, 1987) implied that other processes must be considered, and *in situ* crystallisation, magma stratification and the ponding of dense magma at the floor were among the ideas proposed.

Detailed investigations of any intrusion will usually increase our knowledge of how nature works. Research on Fongen-Hyllingen has revealed features that are not only significant on a local scale but are important in terms of magma chamber processes in general (Sparks, 1985). Studies of the complex by an Aarhus-based group began in the early 1970's and progressed while ideas on the origins of layered igneous rocks were changing drastically, and investigations of Fongen-Hyllingen have contributed significantly to this discussion (Wilson & Sørensen, 1996). Until the mid 1980's, studies of layered intrusions traditionally only considered compositional variations normal to the layering, from the floor to the roof of the magma chamber; lateral variations were assumed to be negligible. Probably the most important feature that has emerged from studies of Fongen-Hyllingen is that lateral variations can be very significant, and must be considered if fundamental magma chamber processes, such as crystallisation mechanisms and magma emplacement, are to be understood.

The Fongen-Hyllingen Complex (FHC) comprises the main (~160 km²) Fongen-Hyllingen layered mafic intrusion (FHI) and the small (~3 km²) Treknattan Intrusion. The latter, that consists largely of dunitic and troctolitic rocks (Stops 26 and 27), was intruded into the layered rocks of the northernmost part of the FHI before regional amphibolite facies metamorphism. It has been described by Sørensen & Wilson (1996) and will not be presented here, apart from briefly under Stops 26 and 27. The complex is named after the mountains Fongen (1441 m) in the north and Hyllingen (1205 m) in the south.

This contribution presents the first detailed map of the entire Fongen-Hyllingen Complex (Enclosure 1) and a review of its geology. A recent review has been published in Danish by Wilson et al. (2004).

1.2. Early studies of the Fongen-Hyllingen Complex

The complex is located ~60 km south east of Trondheim in Norway (Fig.1). The area has long been known for its sulphide mineralization and an economic find was made at Rødhammaren, near the south west margin of the intrusion, in 1774. The presence of a large gabbro body was noted by Hørbye (1861), and some of its geological aspects were mentioned by Möhl (1877) and Homan (1890). In 1889, Vogt described a graptolite locality (*Dictyonema flabelliforme*, Tremadocian, lower Ordovician) in contact metamorphosed rocks near the southern end of the intrusion. In 1896, Törnebohm presented a geological map of the Trondheim area. The importance of his mapping and interpretation of the geology of Scandinavia is emphasised since Gee (1975a) essentially used Törnebohm's map in a regional geological synthesis.

The first mention of the Fongen gabbro in the 20th century was by Carstens (1920). Kisch (1962) was the first to contribute with detailed mapping and a geological description of part of the FHI in an area mostly south of the Nea river (fig.1 in Enclosure 1). The southern part of the complex (Hyllingen) was subsequently mapped by Nilsen (1973) and the northern part (Fongen) by Olesen (1974). The latter was part of a regional study presented by Olesen et al. (1973). Since 1973 a series of students from the Department of Earth Sciences, University of Aarhus, have carried out M.Sc. or Ph.D. projects on the complex (fig.1 in Enclosure 1). The results of these studies are presented here.

1.3. Regional setting of the Fongen-Hyllingen Complex

The FHC is located in the Meråker nappe that is the uppermost part of the Trondheim Nappe Complex (Gee, 1975b) in the Scandinavian Caledonides (Fig.1). These nappes are believed to have been transported many tens of kilometers to the east so that the present location of the FHI is now far from its original site relative to the nappes below and above the Meråker unit. It is the largest mafic intrusion in the central Scandinavian Caledonides into which it was emplaced synorogenically (Fig.2). All of the country rocks adjacent to the complex belong to the Fundsjø Group. The *Dictyonema* occurrence times the Fundsjø Group as Tremadocian, and overlying sediments in the Kjølhøgen region (~50 km north of Fongen) contain graptolites of Silurian (Llandoveryan) age (Gee, 1975b). Rock belonging to the Trondheim Nappe Complex are unconformably overlain by plant-bearing sediments of Lower Devonian age at Røragen, ~50 km south of Hyllingen. These were deposited after uplift and erosion of the Scandinavian Caledonides.

The Fundsjø Group comprises broadly metabasaltic and metapelitic lithologies. These were folded and metamorphosed (D1) prior to the emplacement of a swarm of basaltic dykes, many of which are plagioclase-phyric (Stops 1, 3 and 17). The FHC was emplaced in the vicinity of the lithological contact between the metapelites and metabasalts. The FHI contains contact metamorphosed inclusions (Stops 3, 4, 9, 12, 19, 21, 22 and 23) of folded metapelites and plagioclase-phyric metabasalts (as well as many aphyric

metabasalts) and was clearly emplaced after the dyke swarm. Olesen et al. (1973) found evidence for emplacement after the early stages of D2 deformation (Fig.2). The peak of

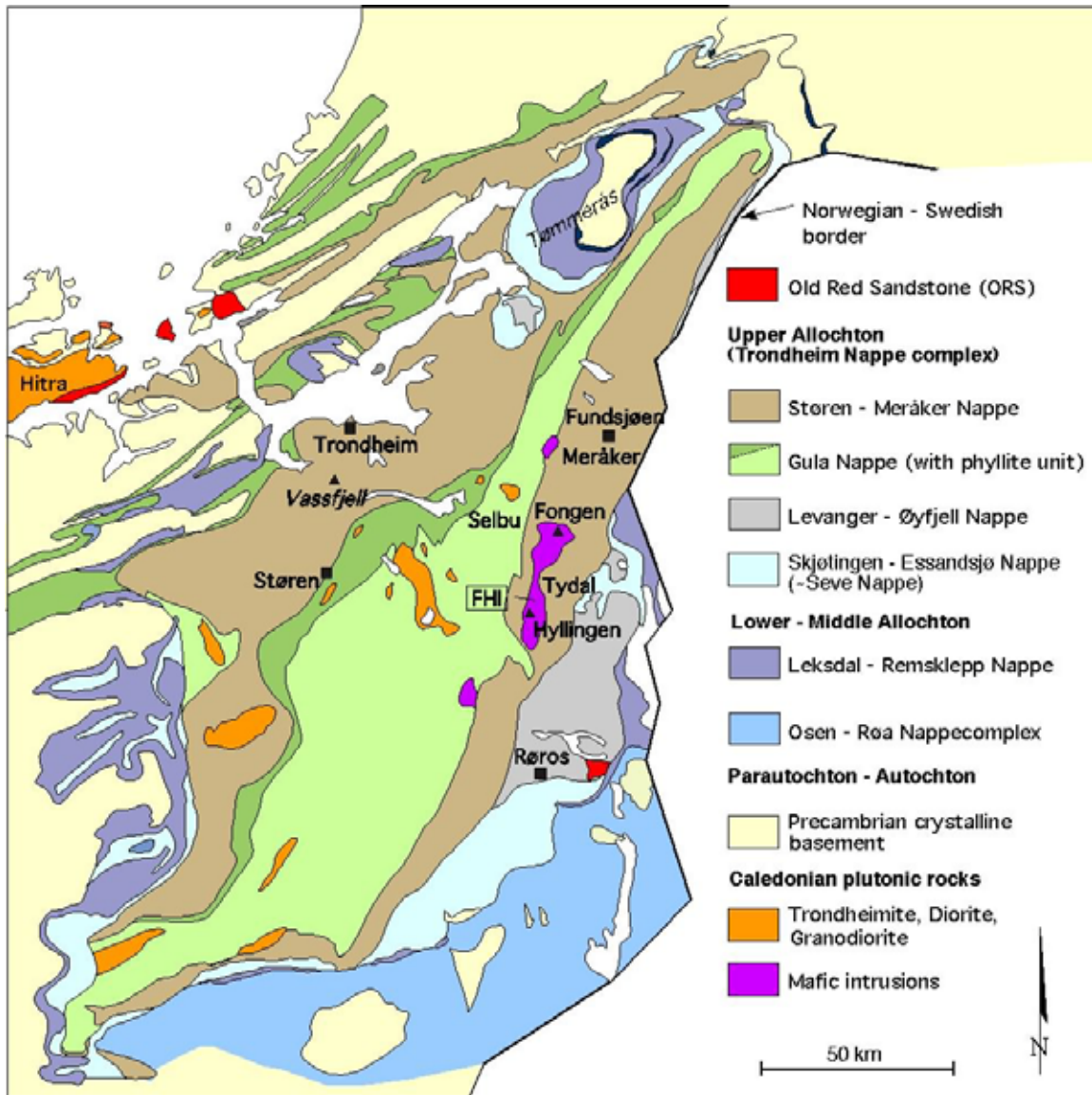


Fig.1. Geological map of the Trondheim region showing the location of the Fongen-Hyllingen Intrusion (FHI). Based on Roberts & Wolff (1981).

the regional deformation and metamorphism (the Scandian orogenic phase) took place after crystallisation of the complex, during which mafic country rocks were transformed to foliated amphibolites and pelites to schists. The Fongen-Hyllingen Complex acted as a huge resistant block during the Scandian orogeny and largely escaped deformation, except in shear zones (Stops 13, 16 and 24) that are locally developed throughout, but are particularly widespread on either side of the Nea river (Enclosure 1; Stops 13 and 16). Regional metamorphism is pervasive in shear zones and sporadically developed throughout the complex, as will be described later. The inner part of the contact metamorphic aureole also locally escaped this regional overprint (Stop 17).

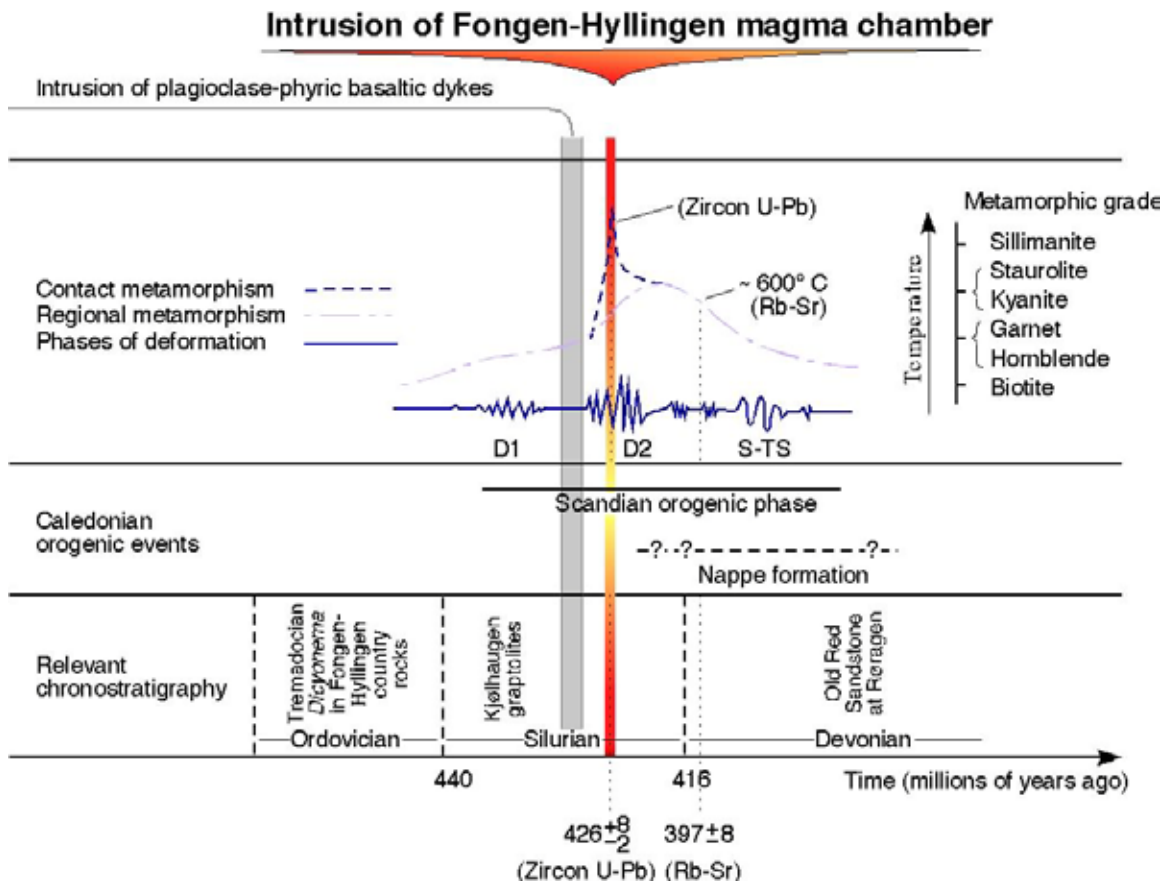


Fig.2. The relationship of the Fongen-Hyllingen Complex to geological events in the Trondheim region. Data is taken from Olesen et al. (1973), Furnes et al. (1980), Roberts & Sturt (1980) and Wolff & Roberts (1980). The timing of intrusion of the FHI has recently been revised to close to 435 Ma (see text). Palaeomagnetic studies of the FHI have been carried out by Abrahamsen et al. (1979).

The form of the FHC and its envelope were strongly influenced by the late Caledonian Selbu-Tydal synform (S-TS in Fig.2). The synformal axis passes roughly north-south through the north-east part of the FHI (Fig.3 and Enclosure 1). Prior to this folding, modal layering in the FHI was close to horizontal. Since we know the direction of younging in the FHI we can refer to the folds here as synclines and anticlines. The fold axis plunges to the south and is responsible for the southern dip of modal layering in cross sections AA' and BB' (Enclosure 1). The asymmetric bowl-shape in the east-west cross section CC' in Enclosure 1 is also due to the syncline. Its effect becomes stronger to the south, as illustrated in cross section DD'. Layering in the western Melshogna area is very steep and is locally slightly overturned; the orientation of the modal layering indicates the presence of a minor syncline to the east of Melshogna that is followed by an anticline. The main synclinal axis is located near the eastern end of DD' and has folded the layered rocks into a tight isoclinal syncline whose eastern flank is overturned. The axial trace of the syncline continues to the south where it is located to the east of the FHI

and is responsible for the consistent eastward dip of modal layering in the Hyllingen area (EE' in Enclosure 1). There are some east-west trending folds in the north Ruten area that are particularly revealed by the orientation of some laterally continuous olivine-rich units (Stop 28). No such east-west structures are evident in the adjacent country rocks, and no regional fold phase has an appropriate orientation. The relationship of these east-west folds to the north-south structures has not been established and their origin remains unresolved.

Deformation of the FHI and subsequent uplift and erosion mean that the section now exposed provides unique access to a magma chamber, allowing us to study its walls and roof and a ~6 km-thick sequence of layered rocks.

1.4. Isotopic age dating

Isotope dating has provided a more precise age for the FHI and has contributed to our knowledge of the timing of regional events during the Caledonian orogeny in Norway. Final differentiates from the eastern Hyllingen area (Stop 7) have given a zircon U-Pb age of $426 \pm 8/-2$ Ma which has been interpreted as reflecting the timing of crystallisation of these rocks (Wilson et al. 1983). A more recent U-Pb zircon age determination on the same rocks by Nilsen et al. (2007) has provided a date of 437.8 ± 2.3 Ma. Together these two determinations imply that crystallisation of the final differentiates of the FHI took place at close to 435 Ma. The same rocks gave a Rb-Sr whole rock isochron age of 405 ± 9 Ma (Wilson & Pedersen 1982), revised to 397 ± 8 Ma by Sørensen & Wilson (1995). This date is considered to represent post-metamorphic cooling of the FHI; the Rb-Sr system must have remained open to diffusion for a long period of time in these extremely evolved rocks and did not become closed until long after the peak of regional metamorphism (Fig.2).

1.5. Metamorphism and deformation

The FHC has a well-developed contact metamorphic aureole (Fig.3C; Stop 17). Based on mineral parageneses in metapelitic rocks, Olesen et al. (1973) suggested that intrusion took place at 5-6 kb. Since then the location of the triple point for the Al_2SiO_5 polymorphs has been revised (Bucher & Frey, 1994) and emplacement probably took place at 3.5 ± 0.5 kb (Fig.4). The complex contains hornfelsed, folded country rocks (Stop 19) and cross-cuts at least an early metamorphic foliation, intrusion taking place during an early stage of the main penetrative deformation (D2 of Olesen et al., 1973) (Fig.2). Metamorphism of the FHC is locally developed in undeformed rocks where primary igneous textures are largely preserved (referred to as metagabbros/metadiorites) and in shear zones where primary textures have been destroyed to produce foliated amphibolites (Stops 13, 16 and 24). Penetrative deformation is most widespread in the narrow, central part of the FHI (Enclosure 1).

(a) *Metagabbros in amphibolite facies.* Rocks retaining their primary igneous mineralogy typically have a brownish weathering colour and crumble readily, whereas metagabbros have greyish weathering surfaces and are less friable (Stops 1 and 26). Macroscopic evidence for metamorphism is commonly seen by the development of coronitic textures where original Ca-poor pyroxene or olivine in a plagioclase matrix has been replaced by

cummingtonite/grunerite with a mantle of dark green to black hornblende (Stops 8 and 14). Fractures in the gabbroic rocks are commonly fringed by a mm- to dm-thick zone in which the mafic phases have been partially or completely hydrated to amphiboles and plagioclase has been saussuritized. The fractures do not appear to have any systematic orientation and closely spaced fractures can result in the entire rock becoming altered to metagabbro. This metamorphism is essentially dependant on the availability of a hydrous fluid which has partially or completely converted the anhydrous mafic phases to amphibole(s). A consequence of these reactions is that modal layering is commonly more obvious in metamorphosed than in unmetamorphosed rocks since the colour contrast between mafic and felsic layers is increased; brown-weathering mafic phases alter to macroscopically black amphiboles and plagioclase becomes whitened by saussuritization.

Olivine, which is dominantly present in olivine-rich units in the Ruten area and olivine-rich lithologies in the Treknattan Intrusion, locally shows partial to complete alteration to serpentine + magnetite (Stops 28-31).

(b) Foliated amphibolites. Foliated amphibolites in which igneous textures are obliterated occur in shear zones which are locally developed in the northern (Fongen) part of the FHI (Stop 24), common in the central area on either side of the Nea valley (Stops 13 and 16), and relatively rare in the southern (Hyllingen) area (Enclosure 1). Gneissic structures are locally developed in the shear zones with segregation into felsic (dominantly tonalitic) and mafic (hornblende-rich) zones. Boudin-like structures can be developed in which blocks of amphibolite, sometimes with traces of relict modal layering showing that the blocks are rotated, are separated by a network of felsic veins which are also commonly intensely deformed. Large sheets of granitic pegmatite are locally developed in the foliated amphibolites (Stop 15).

(c) Greenschist facies rocks. Greenschist facies mineral assemblages are sporadically developed in connection with fractures and minor faults. Pale green chlorite (in veins up to a few mm-thick) replaces mafic phases along fractures in gabbro, metagabbro and foliated amphibolite. In some cases the alteration along these local fractures covers a wider zone (cm-dm) and plagioclases are extensively saussuritized as well as chlorite replacing the mafic minerals.

(d) Prehnite-pumpellyite facies rocks. In the Hyllingen area plagioclase-rich layers are locally altered to a distinct white colour. In one instance (Stop 5) a strikingly white ~70 cm-thick anorthositic layer can be followed for ~300 m along strike. The bleaching is due to the extensive alteration of plagioclase to prehnite and pumpellyite. Cm-thick fractures with sub-greenschist facies assemblages extend from the bleached plagioclase-rich layer into overlying and underlying metagabbros. In addition to this bleaching related to plagioclase-rich rocks, pale green and white, fine-grained (<1 mm) rocks, consisting largely of prehnite and pumpellyite, are locally developed associated with fractures in gabbro, metagabbro and foliated amphibolite.

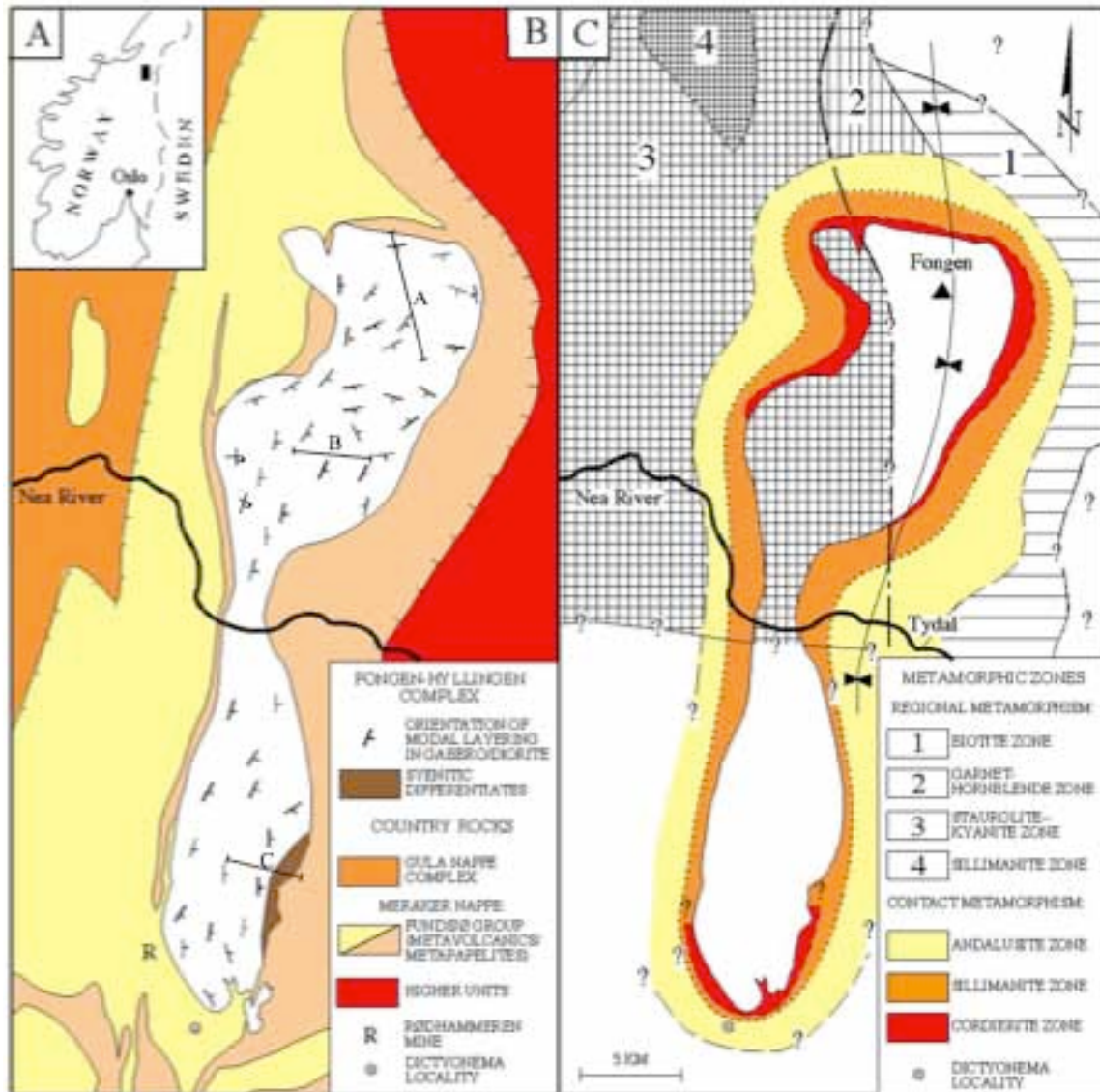


Fig.3A. Location of Fig.3 in Norway. B. Country rock lithology in the vicinity of the Fongen-Hyllingen Complex. The approximate locations of sample profiles A, B and C used in Fig.5 are shown. C. Contact and regional metamorphism. Based largely on Olesen et al. (1973).

The main penetrative deformation in amphibolite facies involved formation of kyanite in some of the metapelites (Fig.3) and probably took place at 5-6 kb (Fig.4). The subsequent greenschist facies metamorphism took place at 3-4 kb and the prehnite-pumpellyite event at 2-3 kb. The amphibolite facies metamorphism took place during the main Scandian orogenic event (at 430-425 Ma). The greenschist event probably records retrograde metamorphism during nappe emplacement, whereas the prehnite-pumpellyite event could represent retrograde metamorphism during a late phase of nappe emplacement or a local Late Devonian post-orogenic event.

Emplacement of the FHC was followed by several phases of folding, the most important of which was the Selbu-Tydal fold phase of Olesen et al. (1973) (Fig.2). The FHC is located partly in the core and partly on the western limb of the Tydal synform (Fig.3C), and the form of the complex is largely controlled by this fold (Wilson & Olesen, 1975).

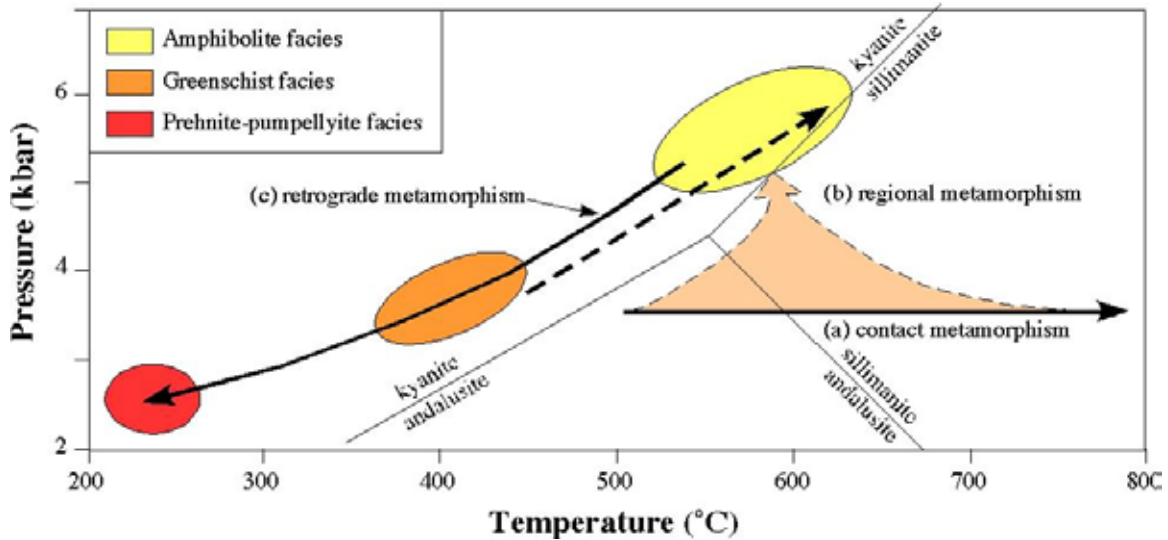


Fig.4. PT diagram for metamorphic events involving the Fongen-Hyllingen Complex showing (a) contact metamorphism at 3.5 ± 0.5 kb (b) regional metamorphism in amphibolite facies at 5-6 kb (c) retrograde metamorphism in greenschist facies at 3-4 kb and $350-450^{\circ}\text{C}$ (d) retrograde metamorphism in prehnite-pumpellyite facies at 2-3 kb and $200-250^{\circ}\text{C}$.

1.6. Main features of the Fongen-Hyllingen Intrusion

This region of Norway has been recently glaciated and most of the area above the tree line is superbly exposed. The intrusion is named after the major mountains in the northern (Fongen) and southern (Hyllingen) parts (Enclosure 1). A zone of medium- to coarse-grained non-layered dioritic rocks occurs along most of the country rock contact (Stops 1, 12 and 25); no chilled margin is developed. A possible feeder to part of the intrusion may be preserved in the extreme northwest (Wilson et al., 1981a). The rest of the intrusion consists dominantly of modally layered gabbroic and dioritic rocks which comprise the layered series. The FHI contains abundant country rock inclusions (Enclosure 1).

1.6.1. Layering features

The layered series rocks are generally medium-grained with a grain size in the range 1-3 mm. Small-scale modal layering is widely developed with layers from 2-30 cm-thick (Stop 20). Igneous lamination, defined by the planar orientation of plagioclase laths and/or tabular pyroxenes in the plane of the modal layering, is locally developed. Individual layers can seldom be followed along strike for more than ~30 m before they taper out. In the Ruten area, however, olivine-rich units can be traced along strike for up to 3 km (Enclosure 1; Stops 28-31). Magmatic load casts have been described from one of these units (Thy & Wilson, 1980; Stops 28 and 30). Trough structures and local

discordances are sporadically preserved throughout the FHI and are evidence for the intermittent action of magmatic currents (Stops 4, 6 and 18).

1.6.2. Inclusions

A major feature of the FHI is the presence of abundant country rock inclusions, many of which are raft-like and concordant or subconcordant to modal layering. Metabasaltic hornfels inclusions dominate but metapelitic hornfels are locally present, consistent with the nature of the country rocks. The inclusions are most abundant in the lower portions of the layered series (Enclosure 1). In the western Hyllingen area, raft-like inclusions occupy ~22% of the area and measure up to about 1500 x 100 m (average 200 x 25 m). Where exposure and topography allow detailed observations it emerges that the inclusions may form a three-dimensional network (e.g. in the vicinity of Fongen mountain in Enclosure 1). The raft-like inclusions are believed to represent blocks of the roof that became partially enveloped by magma as the chamber expanded in response to magma addition (Habekost & Wilson, 1989; Stop 21). The layered rocks show local evidence of deformation adjacent to small inclusions (Stops 19 and 23). This deformation is believed to have developed in response to the impact of fragments of the roof that sank through the magma and impacted on the partially consolidated layered mafic rocks on the chamber floor.

1.6.3. Cumulate stratigraphy

Because of the form of the Fongen-Hyllingen Intrusion and the lateral compositional variations described later, no single profile through the layered series covers the entire stratigraphic sequence, and the composite stratigraphic column in Fig.5 has been compiled from several profiles, omitting the raft-like inclusions. The stratigraphically lowest rocks are to the north of Fongen mountain and the highest are developed at the eastern margin in the Hyllingen area. Lateral correlation between these two parts is discussed below. Texturally the rocks display cumulus/intercumulus relationships. The commonly large number of cumulus phases, however, commonly results in postcumulus overgrowth playing a large role. Calcic amphibole, however, is a common intercumulus phase through much of the layered series where it forms oikocrysts. It becomes an early crystallising phase in the upper rocks. Biotite, quartz and K-feldspar are intercumulus phases before they adopt cumulus status in the uppermost rocks. Modal layering ceases to be developed when K-feldspar becomes an early crystallising phase and the most evolved rocks are massive quartz-bearing ferrosyenites that sharply cut country rock metabasaltic hornfels at the roof (Stop 7).

Fig.5 shows a compositional reversal at the base with relatively evolved rocks (olivine ferrodiorite with An_{38} and FO_{11}) near the floor. Above this there is a ~1200 m-thick sequence of olivine ferrogabbros and gabbronorites with fairly constant mineral compositions (An_{53-46} ; FO_{40-35}). This is followed by a ~400 m-thick compositional regression (from An_{47} , FO_{37} to An_{57} , FO_{73}) in which both apatite and FeTi-oxides cease to be cumulus phases, ending with the most primitive rocks in the profile. Above this the assemblage has a fairly constant composition for ~1000 m (most of the profile B sequence in Fig.5), after which the assemblage becomes progressively more evolved through a thickness of ~1600 m with the successive entry of cumulus FeTi-oxide, calcic

amphibole, apatite, biotite, zircon, quartz, K-feldspar, and allanite. The rare mineral babingtonite has been found (Thayssen, 1998) in these quartz-bearing ferrosyenites that contain minerals with close to end-member compositions.

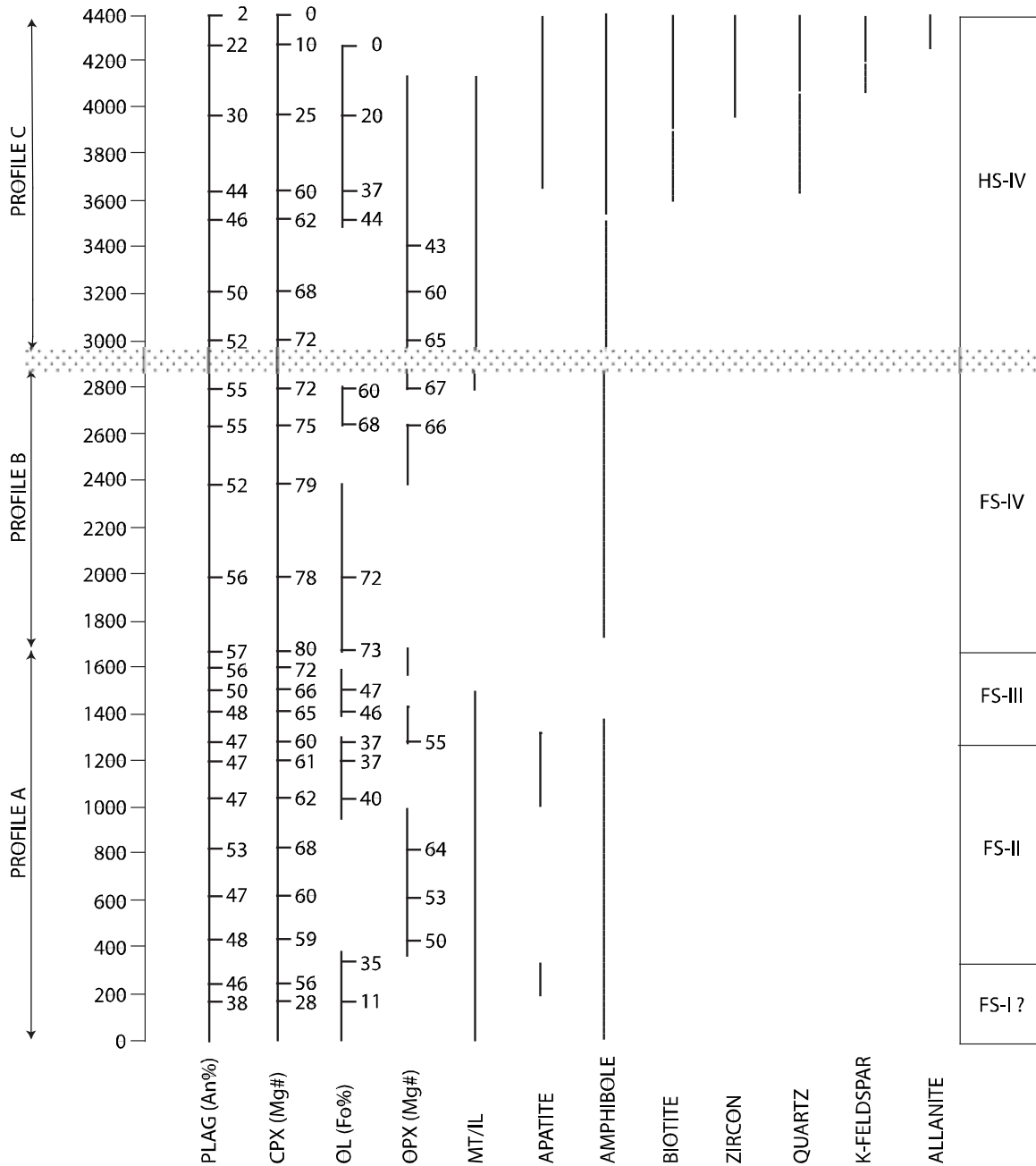


Fig.5. Cumulate stratigraphy of the Fongen-Hyllingen Intrusion based on fig.3 in Wilson & Sørensen (1996). The approximate locations of sample profiles A, B and C are shown in Fig.3B. Lateral compositional variations result in a slight gap between the top of Profile B and the base of Profile C.

Several important points emerge from Fig.5:

- a) The average composition of the layered series is broadly dioritic rather than gabbroic and plagioclase is a cumulus phase throughout so there are no thick sequences of ultramafic cumulates. This has implications for the composition of the parental magma.
- b) The most primitive rocks in Fig.5 (olivine gabbros with plagioclase An₅₇, olivine Fo₇₃ and Ca-rich pyroxene Mg#₈₀) do not occur near the base but near the middle of the cumulate stratigraphic sequence.
- c) There is a reaction relationship between olivine and Ca-poor pyroxene.
- d) Hydrous phases are present throughout most of the layered series. Ca-amphibole is commonly an intercumulus phase and becomes a cumulus phase in evolved assemblages. It is joined by biotite in the latest differentiates.
- e) The major solid solution minerals in the final differentiates have low temperature end-member compositions.
- f) The main solid solution silicates cover extremely wide compositional ranges: olivine Fo₇₃₋₀; plagioclase An₅₇₋₁; Ca-rich pyroxene Mg#₈₀₋₀ (Fig.6).
- g) The fairly constant compositions through thick sequences of cumulates and the major regression in the central part of the intrusion imply that magma replenishment played a major role in the evolution of the Fongen-Hyllingen Intrusion.

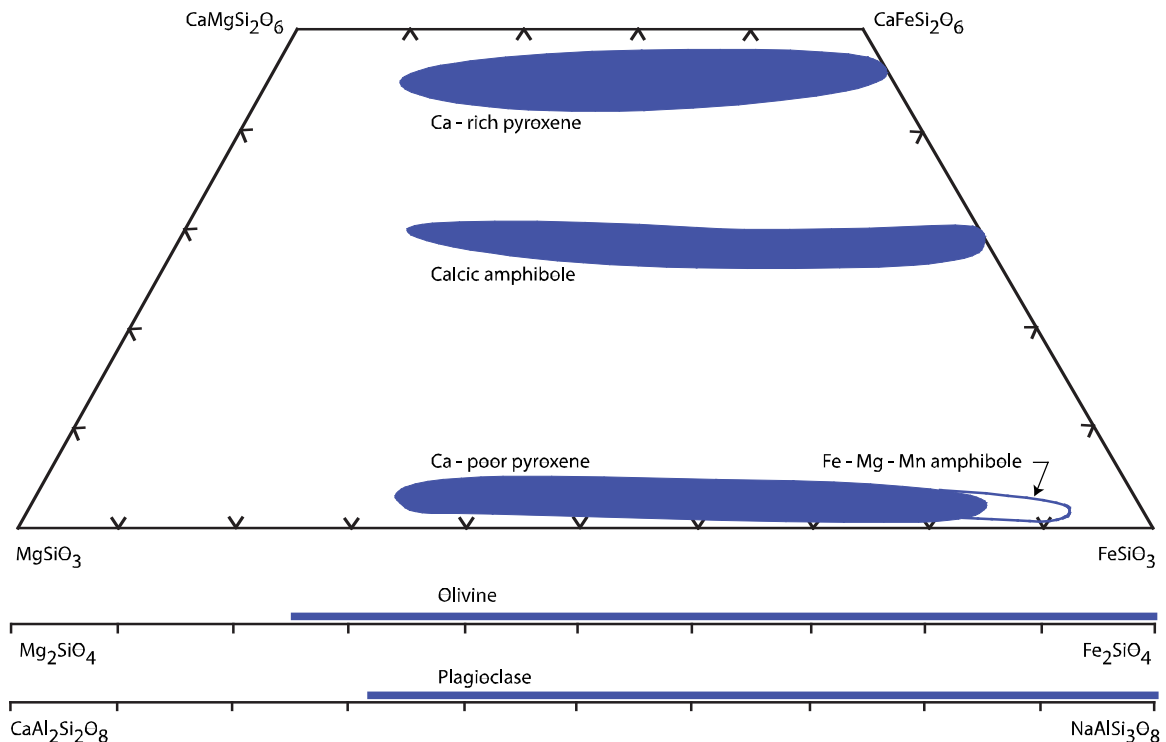


Fig.6. Compositional variations of major silicates in the Fongen-Hyllingen Intrusion. The most calcic plagioclase in Fig.5 is An₅₇. More calcic compositions (up to An₆₇) have been found in the Hyllingen Series (Modified after Wilson et al. 1981b and Wilson & Larsen, 1985). The most magnesian olivine found in the FHI is Fo₇₅. The most iron-rich Ca-poor pyroxenes are replaced by grunerite (Fe-Mg-Mn amphibole).

1.6.4. Subdivision of the layered series into Stages

The southern part of the FHI – the Hyllingen Series (Enclosure 1) – was subdivided by Wilson & Larsen (1985) into four evolutionary stages on the basis of mineral chemical variations in a series of profiles normal to modal layering (fig.2 in Enclosure 1). These are referred to here as HS-I, HS-II etc. The compositional variation with stratigraphic height outlined in fig.2 in Enclosure 1 summarises the mineral chemical data of the type shown in Fig.7. HS-I comprises a basal reversal (Wilson & Engell-Sørensen, 1986), the lower part of which consists of non-layered dioritic rocks (Stops 1, 2 and 12). Indistinct, wispy modal layering occurs 100-200 m above the base, followed after a few tens of metres by well-developed modal layering. The basal reversal of HS-I, which is ~340 m thick, therefore continues into the layered sequence. Modal layering in the Hyllingen Series is discordant to the western margin and the unlayered diorite by ~7° (Enclosure 1). HS-II (Stops 2, 4, 8 and 9) is defined by a sequence with fairly constant mineral compositions, ending with a trend to more evolved rocks. It has been divided into two parts in Fig.7: HS-IIA in which mineral compositions are fairly constant but the isotopic signature become more pristine upwards, and HS-IIB in which mineral compositions become more evolved upwards while isotopic compositions remain more or less constant. HS-III (Stops 4 and 10) comprises a remarkable, gradual regression to more primitive compositions, ending with the most primitive compositions in the profile. In HS-IV the rocks become progressively more evolved upwards (between Stops 6 and 7), ending with low temperature, end-member mineral compositions at the roof (Stop 7).

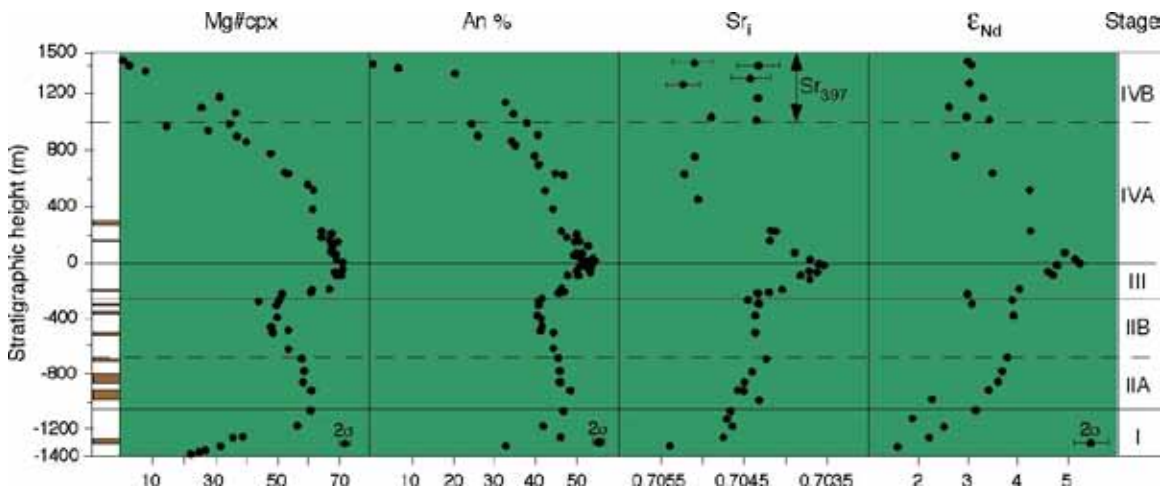


Fig.7. Compositional variations in a profile (close to EE' in Enclosure 1) through the Hyllingen Series. From left to right: stratigraphic thickness (using the Stage III/IV boundary as datum); inclusions (in brown); Mg# in Ca-rich pyroxene; An% in plagioclase; initial Sr-isotopic ratio; e_{Nd} values; subdivision into evolutionary stages.

1.6.5. Lateral correlation of Stages

The northern and southern parts of FHI are linked by a narrow zone where deformation and metamorphism are widespread (Enclosure 1). Lateral correlation between the Fongen and Hyllingen Series has been established on the basis of the strike of modal layering, the

distribution of raft-like inclusions, the general lithologies developed and specifically the lower and upper boundaries of Stage III. Details concerning this correlation are available in Wilson & Larsen (1985), Wilson & Sørensen (1995) and Meyer & Wilson (1999). The correlation achieved is illustrated in fig.2 in Enclosure 1.

A major feature to emerge from the lateral correlation is that mineral compositions become increasingly evolved along the strike of modal layering from north to south (Wilson & Larsen, 1982; 1985). For example, at the Stage II/III boundary in the Hyllingen Series, olivine, plagioclase and Ca-rich pyroxene compositions vary from Fo₂₃, An₄₆, Mg#₄₉ to Fo₃, An₂₃, Mg#₁₇ over a distance of ~7 km approaching the southern margin. At the Stage III/IV boundary the compositions vary from Fo₇₅, An₆₃, Mg#₇₉ to Fo₂₀, An₅₅, Mg#₄₆. These cryptic variations along strike are accompanied by the successive entry of cumulus apatite and zircon (Fig.8; Stops 4, 10 and 11).

The aeromagnetic map of the area (fig.3 in Enclosure 1) illustrates several features relevant for the structure and development of the FHI (Wilson, 1985). The map, which essentially shows the distribution of cumulus magnetite, clearly indicates the major magma influx associated with Stage III, correlation between the northern and southern parts of the FHI, lateral compositional variations in the Hyllingen Series, and the influence of metamorphism.

1.6.6. Isotopic variation in the Hyllingen Series

Fig.7 shows that there is generally a very close correlation between mineral chemistry and isotopic compositions. More evolved rocks have higher Sr-isotopic ratios and lower ϵ_{Nd} values, implying a close relationship between assimilation and fractional crystallisation. It is not possible to determine the precise composition of the contaminant, but it contained a large metapelitic component. The total range in Sr_i is from 0.70308 to 0.70535 and initial ϵ_{Nd} ranges from 1.58 to 5.84. The most contaminated signatures are at the base of HS-I and in the upper part of HS-IV, and the least contaminated signatures at the Stage III/IV boundary, consistent with the mineral compositional evolution. This evolution is described in more detail by Sørensen & Wilson (1995). Assimilation in the FHI has also been discussed by Tegner et al. (2005).

1.6.7. Parental magma composition, fractionation trend and conditions of crystallisation

The absence of a chilled margin and co-magmatic dykes means that it is not easy to estimate the composition of the parental magma to the FHI. An overall tholeiitic affinity is implied by the co-precipitation of Ca-rich and Ca-poor pyroxenes, a reaction relationship between olivine and Ca-poor pyroxene, and the development of quartz-bearing late differentiates. However, there are only very minor amounts of ultramafic cumulates in the most primitive rocks and the average composition of the layered series is dioritic rather than gabbroic. Wilson et al. (1981a) concluded that the fractionation trend was intermediate

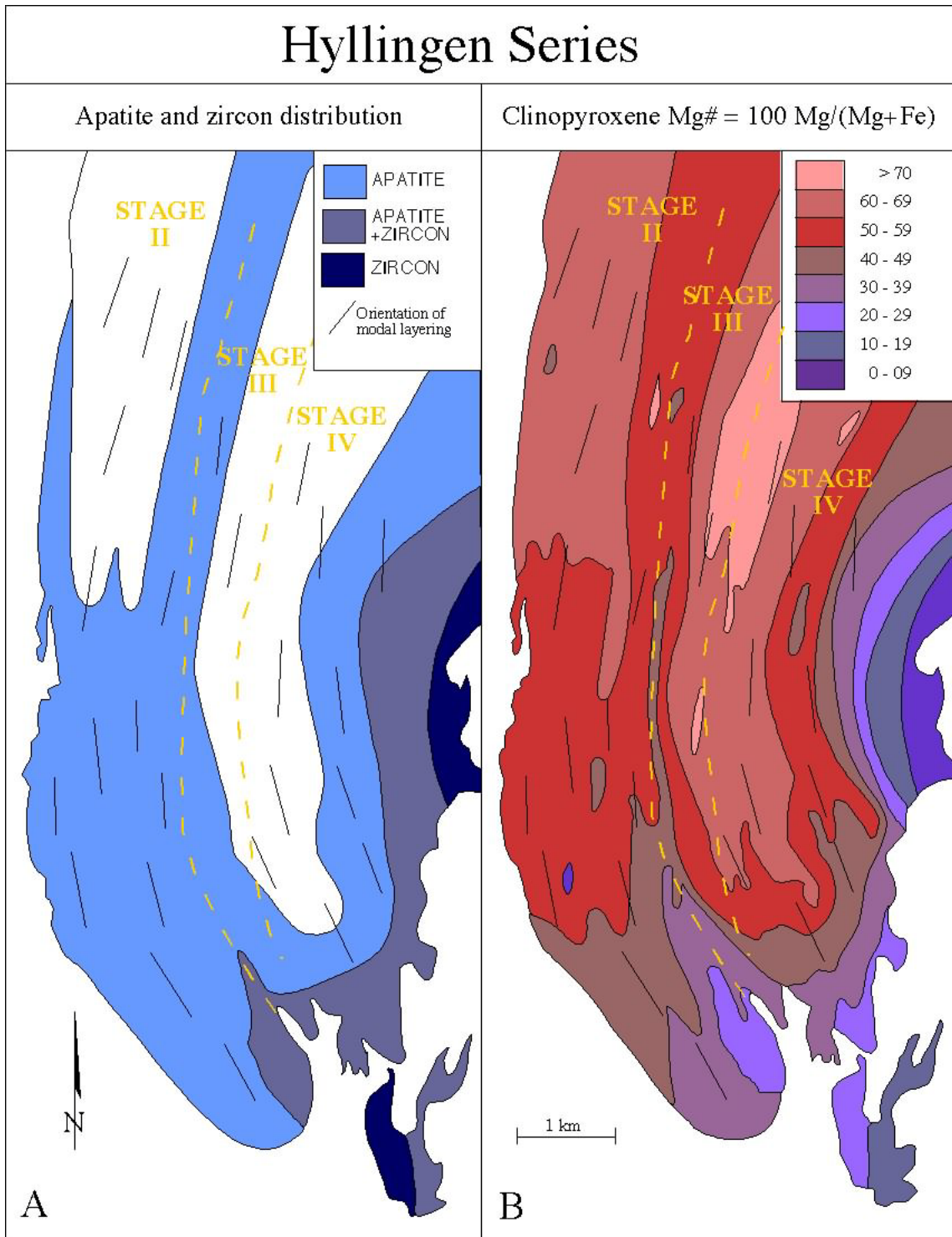


Fig.8A. Distribution of cumulus apatite and zircon in the Hyllingen Series. B. Contoured compositional variation of Mg# in Ca-rich pyroxene in the Hyllingen Series. Plagioclase compositions show a similar variation to Ca-rich pyroxene. Based on fig.11 in Wilson & Larsen (1985).

between typical tholeiitic and calc-alkaline trends, resulting from the crystallisation of (basaltic)-andesitic magma under elevated and increasing pH_2O .

Based on a summation method through Stage IV, Abu El-Rus et al. (2007) estimated that the parental magma composition lay very close to the dividing line to the basaltic, basaltic andesite, trachybasalt and basaltic trachyandesite fields in a TAS diagram. Their proposed composition is 51.7% SiO_2 , 1.68% TiO_2 , 16.34% Al_2O_3 , 2.13% Fe_2O_3 , 9.82% FeO , 0.23% MnO , 4.99% MgO , 7.44% CaO , 4.02% Na_2O , 1.29% K_2O and 0.35% P_2O_5 with a Mg# value of 47.5. This composition lies very close to the tholeiitic-alkaline dividing line in the TAS diagram. Abu El-Rus (2003) also carried out trace element modelling of the FHI. This relatively evolved parental magma composition implies that it was derived from an underlying chamber where extensive fractionation of mantle-derived magma took place prior to repeated feeding of the Fongen-Hyllingen chamber.

1.6.8. The origin of discordant relations between modal and cryptic layering

If modal layering represents the crystallisation front, the discordant relations mean that low temperature assemblages were crystallising near the southern margin at the same time as relatively high temperature assemblages were crystallising away from the margin. Cryptic layering (i.e. constant mineral compositions) and phase layering (e.g. entry of cumulus apatite) represent, as a first approximation, isochemical and isothermal surfaces. This means that at any one time, magma in contact with the floor was crystallising systematically lower temperature mineral assemblages approaching the margin (Fig.9).

The situation in Fig.9B and C clearly means that the magma cannot have been undergoing large-scale convection. It is also difficult to envisage how crystals with appropriate compositions could be transported to the magma chamber floor. Crystals nucleating, for example, in the uppermost magma layer in Fig.10 will not be in equilibrium with those in the underlying magma layers, and would dissolve in the hotter, more primitive magma during sinking. Crystal settling is therefore not an option for the origin of most of the modal layering in the Hyllingen Series and an *in situ* process is implied, like that proposed by Maaloe (1978). The model in Figs. 9 and 10 also precludes the presence of steep magma chamber walls from which crystal-laden currents could descend and deposit layered rocks on the magma chamber floor, as was suggested for the graded layers in the Skærgaard Intrusion by Wager & Brown (1968).

In Figs.9 & 10 the magma is shown as being zoned in a step-like manner, as would be the case if double-diffusive convection was active. This is partly because it is much easier to illustrate the relevant processes involved using a step-like rather than a gradational pattern. The evidence for composition zoning of the Fongen-Hyllingen magma is overwhelming, but convincing evidence for step-like magma zoning has not been found. This is possibly because the steps are so small as to be undetectable in the crystalline products.

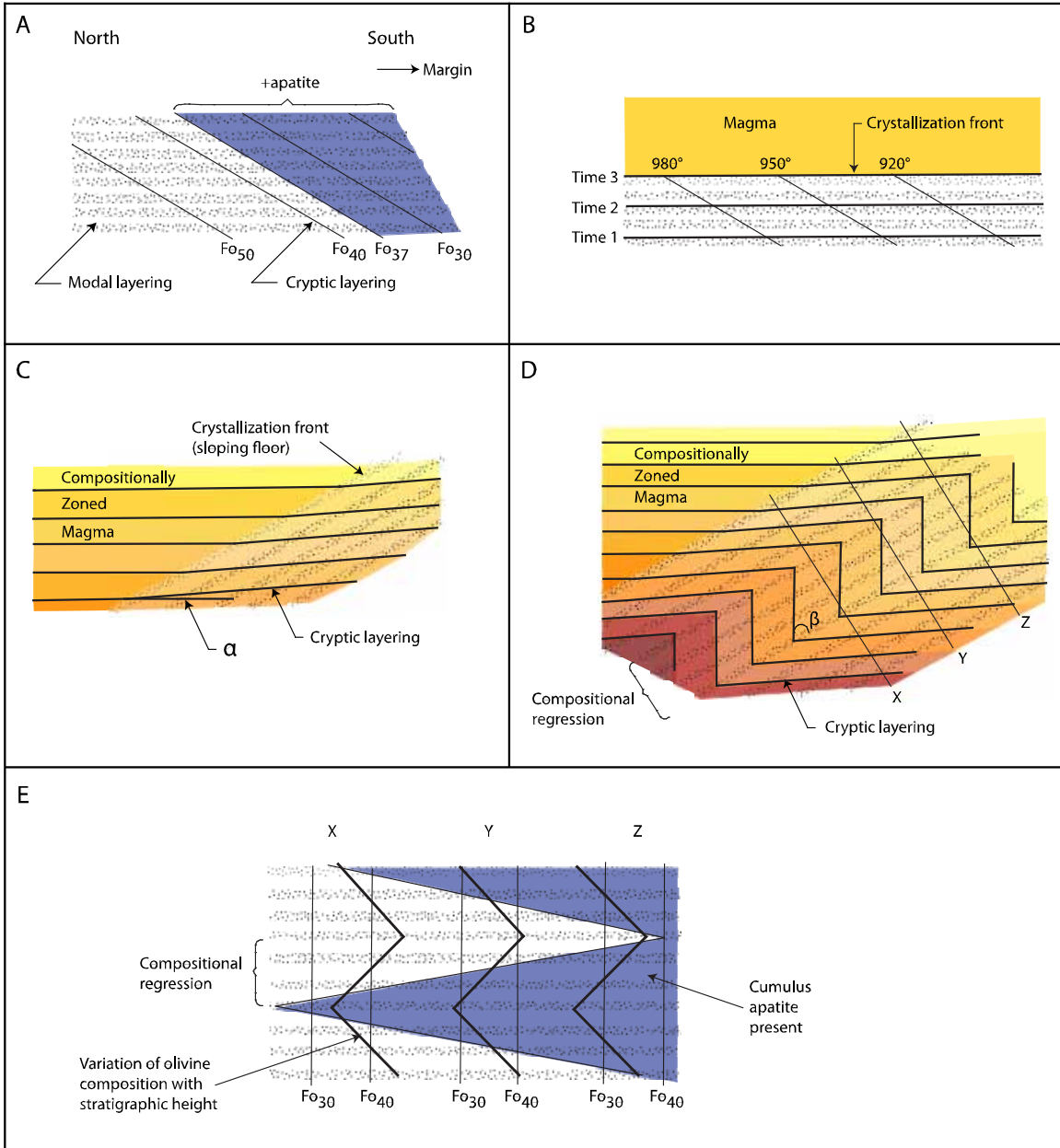


Fig.9A. The nature of discordant relations between modal and cryptic layering in the Hyllingen Series. Cryptic layering is illustrated by the compositional variation of olivine and entry of cumulus apatite when olivine reaches $\sim Fo_{37}$. B. Modal and cryptic layering are interpreted as representing isochrons and isotherms respectively. C. Development of the discordant relations by crystallisation of compositionally zoned magma along an inclined floor. Cryptic layering probably dips at an angle (α) between that of the crystallisation front and the horizontal. D. Crystallisation during elevation of the resident zoned magma by influx of dense magma along the magma chamber floor will give rise to a compositional regression. The angle β will depend on the relative rates of influx and crystallisation. Hypothetical compositional variations through profiles X, Y and Z are

shown in Fig.9E. E. Hypothetical compositional profiles (X, Y and Z) through a regression like that in Fig.9D. The compositional variation of olivine is shown in three profiles, together with the entry of apatite at Fo₃₇. Note that (a) the compositional regression develops concordant to modal layering. (b) Compositions become more evolved along modal layering from X to Z (up-slope in Fig.9D). (c) The Z-shaped pattern of distribution shown by the entry of cumulus apatite (compare with Fig.8A). Some of the consequences of crystallisation along a sloping floor have been discussed by Huppert et al. (1987).

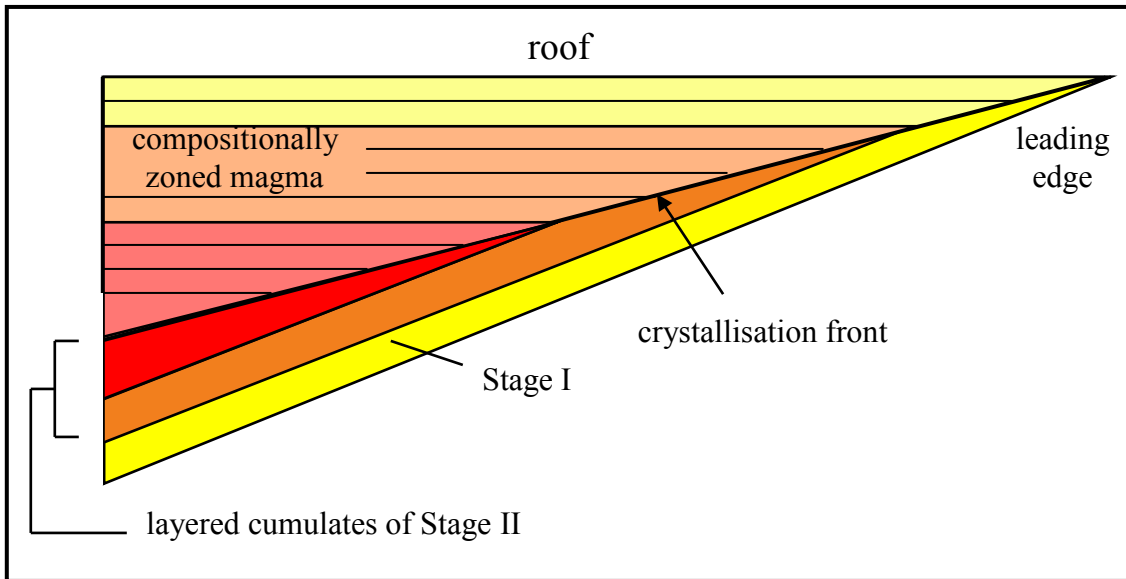


Fig.10. Schematic illustration of the southern end of the Fongen-Hyllingen magma chamber during crystallisation of compositionally zoned magma along an inclined floor. During magma chamber expansion by influx of dense magma elevating the magma column, the first magma to come in contact with the new floor at the leading edge is the evolved magma at the magma chamber roof. Crystallisation during continued influx results in a compositional reversal up through Stage I (HS-I) as denser, more primitive magma layers come in contact with the crystallisation front. Away from the leading edge, more primitive magma is crystallising at the same time to produce Stage II (HS-II).

1.6.9. Development of the Fongen-Hyllingen magma chamber

In-depth treatments of the evolution of the Fongen-Hyllingen magma chamber can be found in Wilson & Larsen (1985), Sørensen & Wilson (1995), Wilson & Sørensen (1996) and Meyer & Wilson (1999). Some of the main features are presented here.

The magma chamber started to develop in the Fongen area near the boundary between metabasaltic and metapelitic country rocks (Fig.11A). The relatively constant mineral compositions in the lower part of the Fongen Series (Fig.5) imply that crystallisation took place during magma addition. Expansion of the chamber was largely by elevation of the

roof, but magma also penetrated along cracks in the roof to form dykes and sills. At this stage of development of the FH magma chamber the roof zone consisted of a network of largely metabasaltic hornfels and magma. Metapelitic country rocks were partially melted. The crystallisation front moved upwards and engulfed the roof-rocks to form a three-dimensional network of mainly metabasaltic hornfels (Fig.11B). Some fragments of the roof rocks became detached and sank through the magma, forming impact structures in the partially consolidated floor cumulates. The repeated addition of dense, relatively primitive magma at the floor and the accumulation of evolved magma near the roof, as a result of compositional convection and accumulation of partial melts from metapelites, resulted in the magma becoming compositionally zoned.

The continued addition of new magma resulted in the chamber expanding in a wedge-form towards the south, and crystallisation of the Hyllingen Series started along the sloping floor of the wedge (Figs.10 & 11C). Stage I in the Hyllingen Series comprises a regressive sequence which developed during crystallisation of compositionally zoned magma along an inclined floor during magma chamber expansion. HS-I developed along the floor of the expanding wedge at the same time as HS-II developed on the crystallisation front away from the floor. Crystallisation of the compositionally zoned magma along an inclined floor gave rise to the most important feature of the FHI – the discordant relationship between modal and cryptic layering. During development of HS-IIA (Fig.7) the rate of crystallisation roughly balanced the rate of addition of magma to the chamber so that mineral compositions remain constant with stratigraphic height. HS-IIB developed when the rate of influx decreased or ceased so that mineral compositions became more evolved upwards.

Stage III started to develop when a new, long period of magma addition commenced which led to further expansion of the wedge-shaped chamber (Fig.11D). Crystallisation of zoned magma along an inclined floor during continual magma addition led to the compositional regression (Fig.7). The cumulates that formed at the end of Stage III are the most primitive rocks in the entire layered series.

The magma residing in the chamber crystallised during Stage IV (Fig.11D-E). There were, however, several minor influxes of magma during this phase. These influxes were responsible for formation of the laterally continuous olivine-rich units in the Ruten area (Enclosure 1; Stops 28-31) that developed by local magma mixing (Meyer & Wilson, 1999). The absence of clear regressive sequences in the southern part of the chamber demonstrates that these minor events of magma addition had little effect in distal areas. The fact that the most evolved rocks in the FHI are at the top of the stratigraphic sequence, in contact with country rocks at the roof, implies that crystallisation took place upwards from the floor and not downwards from the roof.

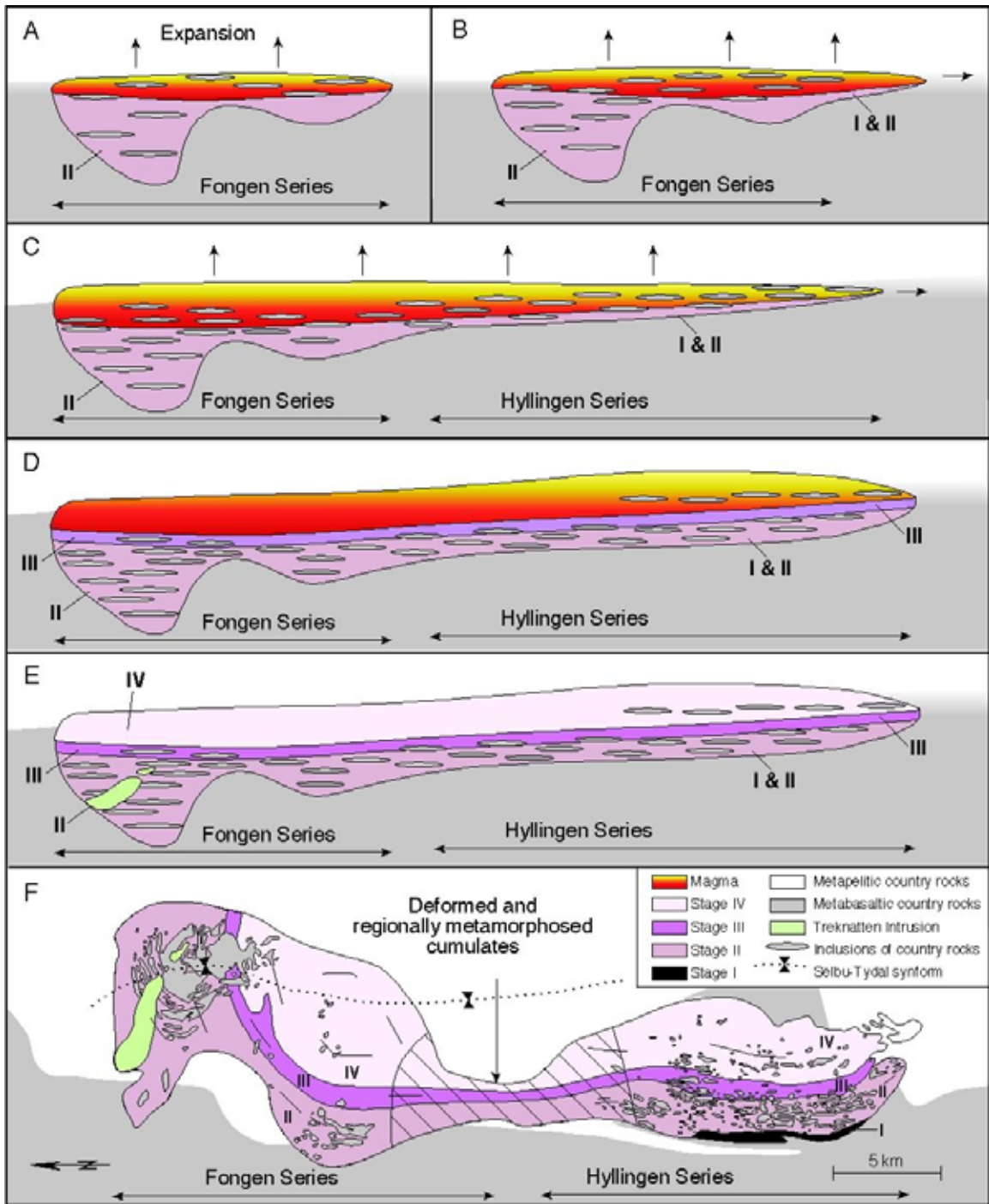


Fig.11A-E: Schematic development of the Fongen-Hyllingen magma chamber. The Treknattan Intrusion formed during stage E. F: The form of the Fongen-Hyllingen layered intrusion after deformation. See text for further explanation.

Primitive basaltic magma (the Treknattan intrusion) intruded the lower part of the FHI at some stage after this part of the intrusion had solidified (Fig.11E). Crystallisation of both the Fongen-Hyllingen layered intrusion and the Treknattan Intrusion was followed by regional deformation and metamorphism in amphibolite facies. Most of the FHI acted as a resistant block during the penetrative deformation. The central part, however, was

severely influence by deformation and metamorphism and appears to have become narrower (Fig.11E-F). Foliated amphibolites developed in shear zones and amphibolite facies mineral assemblages formed in connection with hydration along joints and minor faults. The area was subsequently folded into a series of antiforms and synforms along north-south fold axes. The hinge zone of the Selbu-Tydal synform plunges to the south and passes through the Fongen Series that has been folded into a syncline. The location of the Hyllingen Series west of the fold axis has resulted in a constant easterly dip of the layered sequence in this area. The effect of the folding and subsequent uplift and erosion has allowed access to the floor and roof of the magma chamber and has made it possible to study both vertical and lateral variations in the layered cumulates over a strike length of ~40 km.

2. GEOLOGICAL EXCURSION

2.1. Practical information

In order to visit all 31 stops described in this excursion guide would take a minimum of 6 days. Two days would be in the Hyllingen area (stops 1 - 12). One day would involve travelling from the Hyllingen to the Fongen area via Tydal (stops 13 - 16). One day would be in the Fongen area (stops 18 - 23); one day in the extreme northern part of the Fongen-Hyllingen Intrusion (stops 17 and 24 – 27); and one day in the Ruten area (stops 28 – 31). If shorter time is available the most instructive stops to visit are 1 – 7 in the Hyllingen area, 18 – 23 in the Fongen area, and 28-31 in the Ruten area.

There is no obvious tourist accommodation in the Hyllingen area, but the stops are readily accessible from the car park at Holdalsvollen, ~1.5 km west of Stop 1. In the northern part of the intrusion there are excellent tourist huts (belonging to Trondheim Turistforening) at Gressli (suitable for stops 14 - 16), Ramsjø (stops 17 - 24) and Stormoen (Schulzhytta, stops 25 - 27). The stops in the Ruten area (28 - 31) can be reached from any of these huts but involve a long walk.

The 1:50.000 topographic maps of Ålen and Tydal are essential.

3. EXCURSION STOPS

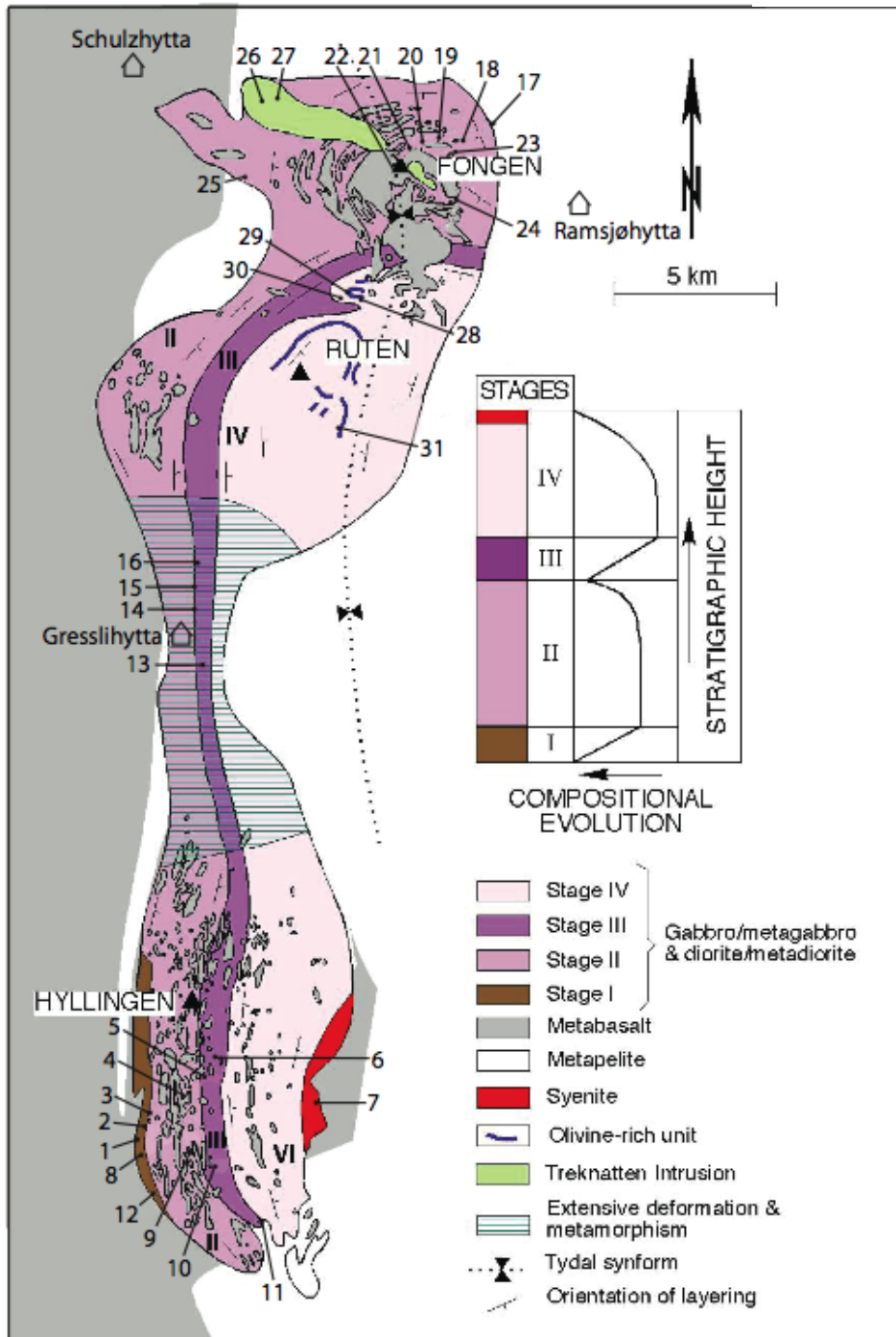


Fig.12. Simplified geological map of the Fongen-Hyllingen complex which comprises the Fongen-Hyllingen layered intrusion (FHI) and the small Treknattan intrusion. The FHI has been subdivided into stages on the basis of mineral compositions in a series of profiles normal to modal layering; these allow lateral correlation. The locations of Stops 1 – 31 and the Trondheim Turistforening huts (Grasslihytta, Ramsjøhytta and Schulzhytta) are shown.

3.1. Introduction to Stops 1 – 7

These stops provide a complete section from the floor to the roof through the Hyllingen Series (Fig.12 and Enclosure 1). Stop 1 is near the western (lower) country rock contact of the Hyllingen Series of the FHI. Stop 7 is at the roof contact. The basal contact is with metabasaltic hornfelses which are intruded by ferrodioritic rocks of the FHI that are locally pegmatitic. Sporadic modal layering is first developed ~100 m above the local floor (Stop 2). The route passes through the entire Hyllingen Series, starting with the basal reversal of Stage I. There are many inclusions of metabasaltic hornfels in Stage II (Stop 3). Mineral compositions remain fairly constant through Stage II. We pass through the compositional regression of Stage III (Stop 4), reaching the most primitive rocks in this profile at the Stage III/IV boundary. The modally layered rocks in Stage III contain several small trough-like features (Stop 4).

Some of the mafic rocks have been subjected to amphibolite facies metamorphism; this metamorphism is related to the availability of hydrous fluids (Stop 4). Low-grade metamorphism has locally influenced some of the cumulates, as is evident at Stop 5 where there is a strikingly white plagioclase-rich layer. Two large trough-like structures at Stop 6 are evidence of magmatic current activity.

Passing through Stage IV the rocks become more evolved, ending with quartz-bearing syenites with low-temperature end-member solid solution minerals at the roof (Stop 7) where the contact with metabasaltic hornfels country rocks is well exposed.

3.2. Stop 1: Southwest of Gjetleken

3.2.1. Location

Coordinates: 0623123 6980006. Ålen 1:50000 map.

3.2.2. Introduction

Stop 1 starts at a bridge where the path turns to the south and extends ~500 m to the north. This stop is located at the western, lower country rock contact of the Hyllingen Series where evolved ferrodioritic rocks are in contact with country rock metabasalts.

3.2.3. Description

Approaching Stop 1 from the west there are outcrops of amphibolite facies metabasalts along the path just east of the car park at Holdalsvollen (P – Siste mulighet!). These belong to the Fundsjø Group. Some of the metabasalts are plagioclase-phyric. Gabbroic/dioritic rocks of the FHI form the hill Gjetleken to the east of the bridge. The metabasaltic rocks (basalts and plagioclase-phyric dykes) here are well within the contact

metamorphic aureole around the FHI. The country rocks here have not been strongly affected by the regional (Scandian) deformation that took place after crystallisation of the layered intrusion. However, granular pyroxene in the fine-grained granoblastic-textured metabasaltic hornfels has largely been replaced by hornblende, and there is some epidote and carbonate. This is an overprint by the regional amphibolite facies metamorphism (here epidote-amphibolite facies) that took place during the Scandian event (Fig.14).

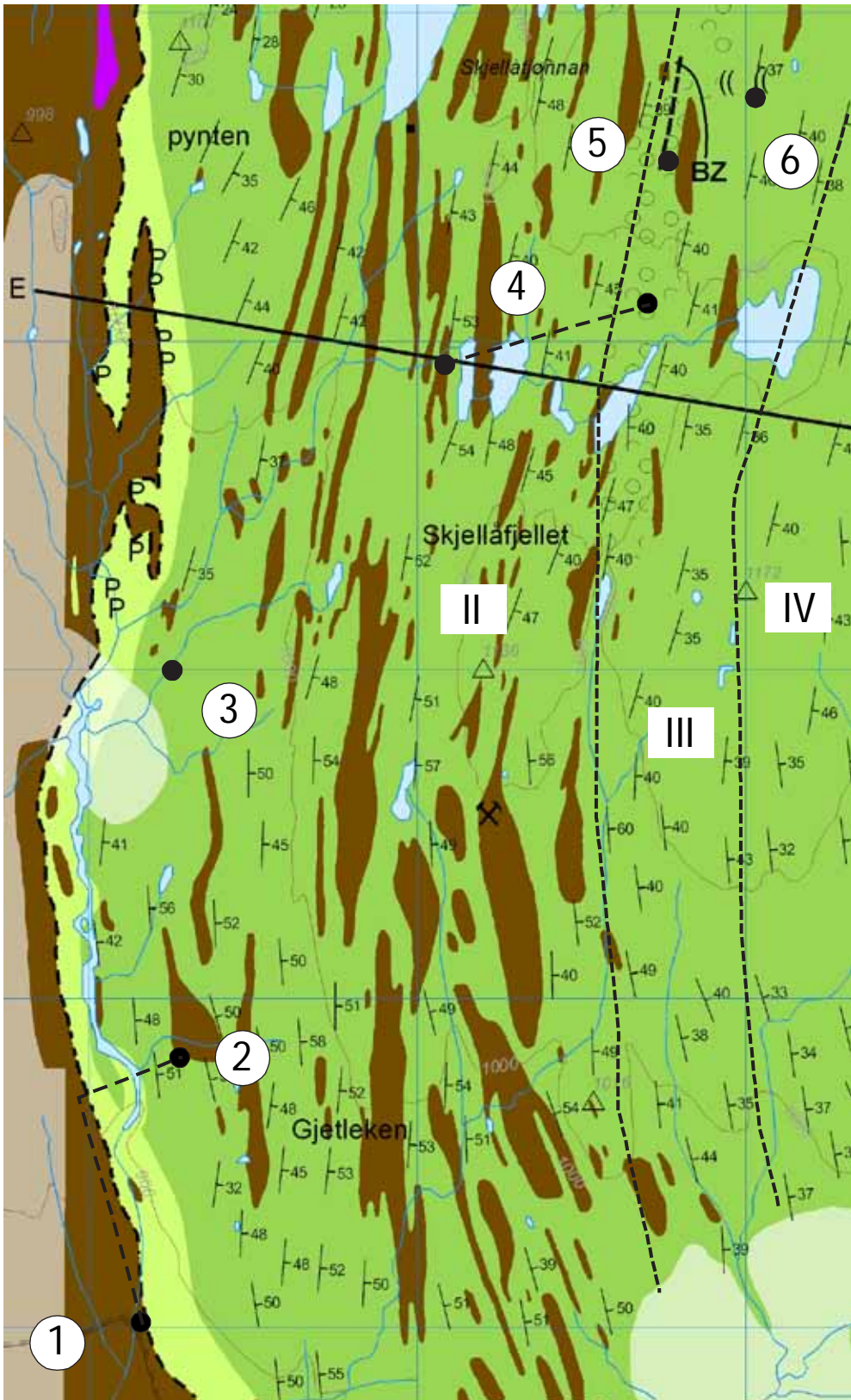


Fig.13. Locations of Stops 1 to 6. This map has been extracted from Enclosure 1. The boundaries between Stages II, III and IV are shown by dotted lines.

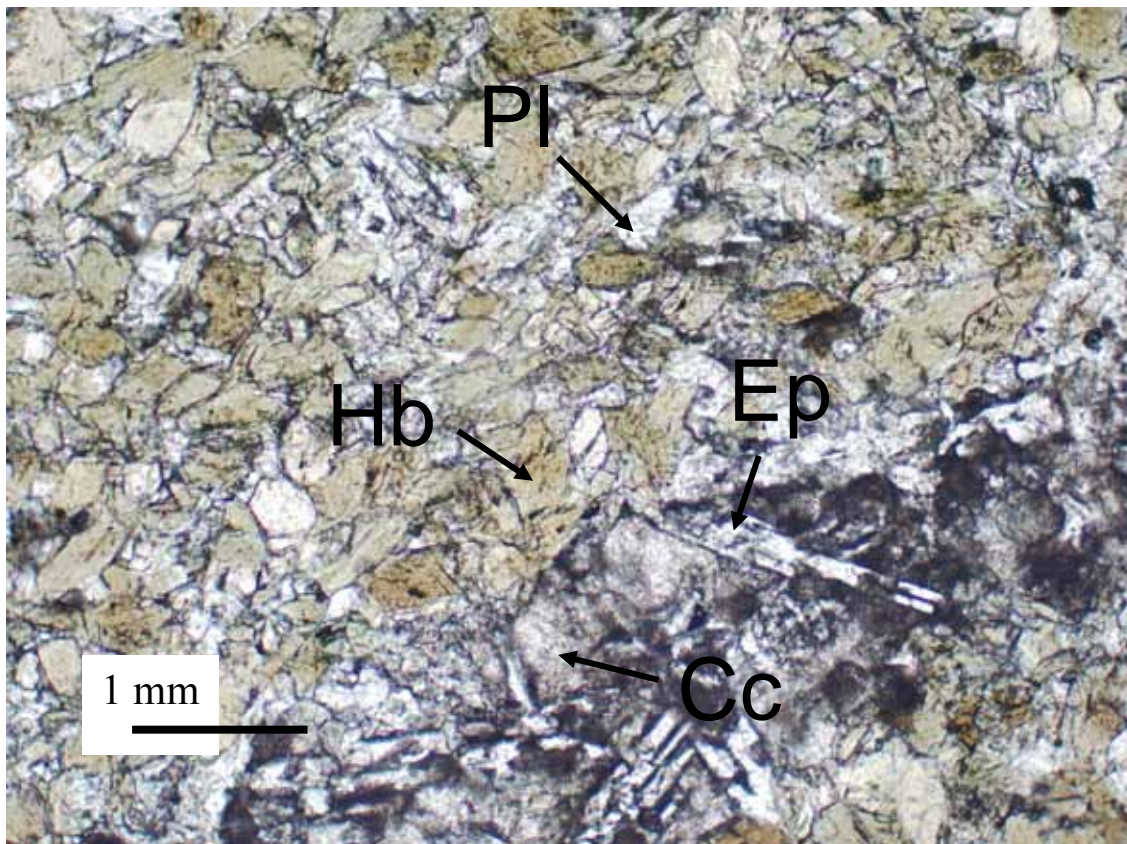


Fig.14. Photomicrograph of metabasalt from the inner contact metamorphic aureole at Stop 1. The mineralogy is dominated by hornblende (Hb) with minor plagioclase (Pl). There are veins of calcite (Cc) and epidote (Ep). PPL. (FH 06-01)

There are some loose blocks of dioritic pegmatite (FHI marginal rocks) by the small southern bridge. The contact between the FHI and the country rocks runs approximately along the stream to the north of the bridge.

Walking north along the western side of the stream the first exposures of the FHI marginal rocks are ~250 m north of the bridge (Fig.15). These consist of massive, medium-grained ferrodiorites. Un-metamorphosed FHI dioritic/gabbroic rocks weather to brownish gravel. Metabasaltic country rocks are exposed several meters to the west. There is no evidence of a chilled margin. The marginal dioritic rocks locally develop into a pegmatitic variety with large black hornblende crystals (brown in thin section), sodic plagioclase, magnetite, quartz and apatite (Fig.16).

Cross the stream at the southern end of a flat, marshy area (0623131 6980773). The smooth, water-worn outcrops of marginal rocks here contain faint, diffuse layering (strike ~166°) defined by 0.5 - 2 cm-thick trails of hornblende crystals. There are many hornblende oikocrysts. These features are best seen at low water level and in sunshine.



Fig.15. View to the north from just south of the bridge at Stop 1. The outcrops by the bridges and on the banks of the stream are of metabasaltic country rocks. Marginal diorites belonging to the Fongen-Hyllingen Intrusion outcrop ~250 m to the north along the stream.

We are here within the basal regression (Stage I) that is developed above the country rock floor in the Hyllingen Series. We are between profiles F and G in Fig.17. Rocks near the country rock contact are relatively evolved and gradually become more primitive upwards. The lowest rocks are un-layered (commonly quartz- and zircon-bearing apatite ferrodiorites). Faint layering begins to develop 100-200 m from the contact. The basal reversal is not very apparent in the field (and is poorly exposed here) but is clearly demonstrated by mineral compositions.

3.2.4. Significance of the outcrops

The FHI was intruded after at least one fold phase and accompanying regional metamorphism and subsequent emplacement of a suite of largely plagioclase-phyric mafic dykes (these can be seen at Stop 17), but before the main regional Caledonian deformation and metamorphism (the Scandian event). The FHI and part of its contact metamorphic aureole formed a large boudin-like feature during the Scandian event. Regional deformation is only locally

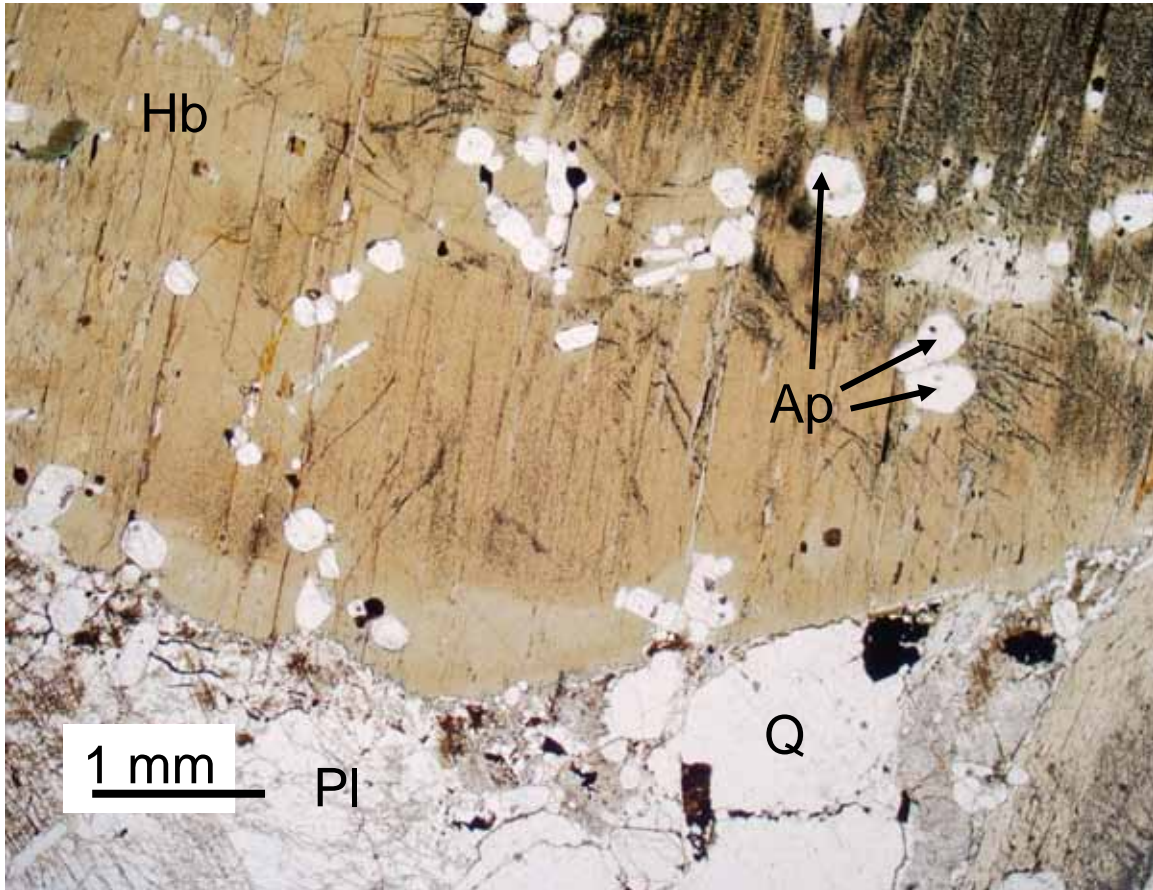


Fig.16. Photomicrograph of coarse grained dioritic from the Fongen-Hyllingen marginal facies near Stop 1. The large hornblende (Hb) contains ilmenite dust. The evolved composition of this rock from Stage I is evident from the presence of quartz (Q) and apatite (Ap). Pl = plagioclase. PPL. (FH 06-08).

developed in the Hyllingen part of intrusion in the form of shear zones. Within these the FHI lithologies have largely been transformed to foliated amphibolites. However, considerable portions of the FHI have been overprinted by amphibolite facies mineral assemblages. Primary igneous textures are commonly preserved. This metamorphism essentially involved hydration of the mafic minerals to various amphiboles, and the saussuritisation of plagioclase. The colour contrast between plagioclase-rich and mafic-rich layers is enhanced by this metamorphism.

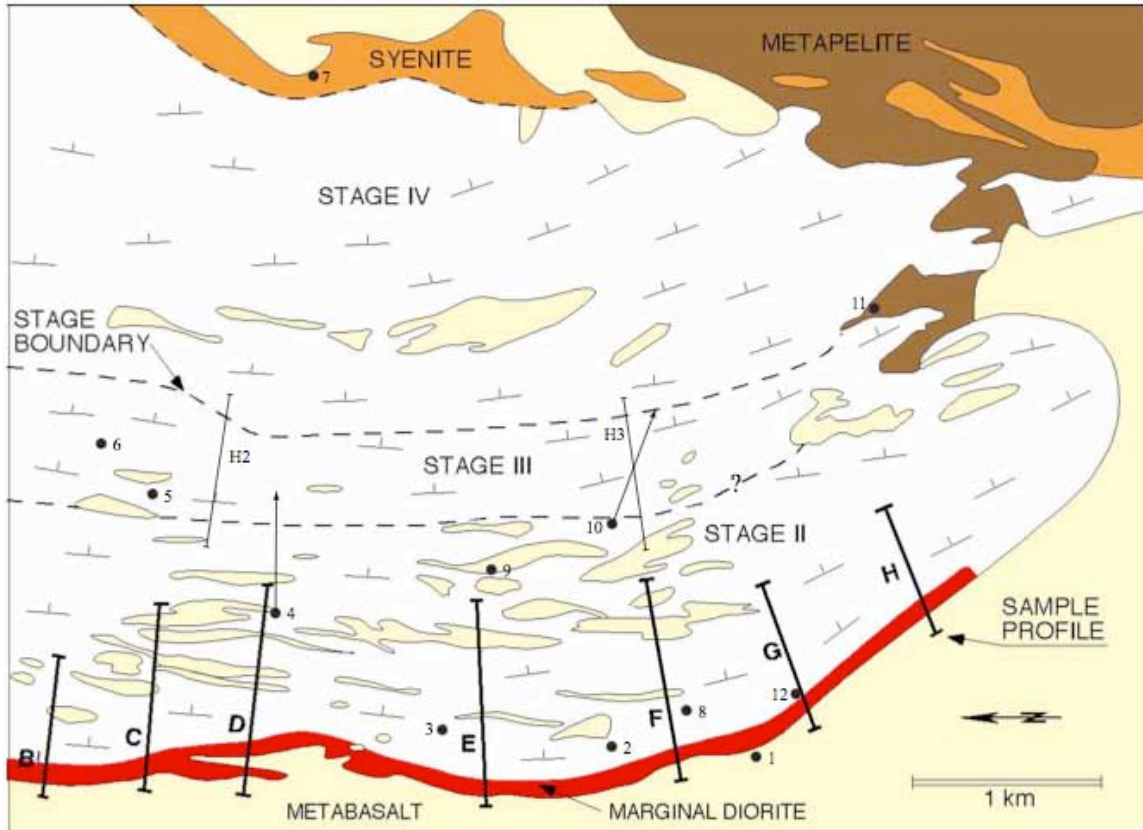


Fig.17. The southern part of the Hyllingen Series showing the locations of: a) profiles B' to H in Fig.18; b) profiles H2 and H3 in Fig.40; c) Stops 1 – 12.

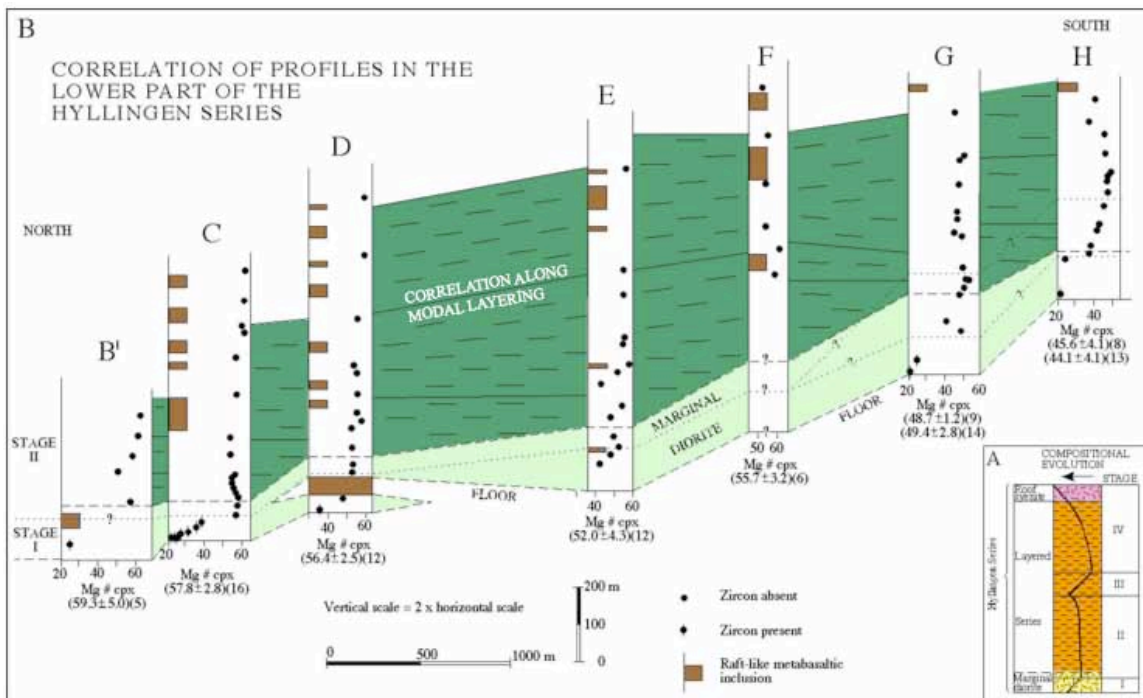


Fig.18. Subdivision of stratigraphic columns through the Hyllingen Series based on lithology and compositional evolution as shown by, for example, An% in plagioclase, Fo% in olivine and Mg# in pyroxenes. B. Correlation of profiles in the lower part of the Hyllingen Series showing modal layering, raft-like metabasaltic inclusions, presence of zircon, and Mg# in clinopyroxene. Stage I comprises a basal reversal. The Stage I/II boundary is located where Mg#cpx ceases to increase upwards. This boundary is not clear in profiles G and H where two possible interpretations are shown. Stage I is entirely located in un-layered diorites in the northern profiles i.e. modal layering first develops when the basal regression has ceased. Mg#cpx values remain more or less constant with stratigraphic height in the lower part of Stage II. The numbers in brackets below each profile are the average Mg#cpx values and standard deviations for the individual profiles. Two values are given for profiles G and H representing the upper and lower placings of the Stage I/II boundary respectively. It is important to observe that these compositions become quite systematically more evolved towards the south, from Mg#cpx_{~59} in profile B' to Mg#cpx_{~45} in profile H. The basal regression is also shown by other mineral compositions. For example, the profile C regression covers the ranges clinopyroxene Mg#cpx₂₀₋₅₇, plagioclase An₃₅₋₄₇, and olivine Fo₄₋₃₀, accompanied by the upward disappearance of zircon and apatite. Along the boundary between the layered series and the marginal diorite a thickness of ~600 m of layered rocks wedge out to the south over a distance of ~4 km, a discordance of ~7°.

The absence of a chilled margin reflects a combination of factors: a) the country rocks were relatively hot during the synorogenic emplacement of the layered intrusion; b) the mode of emplacement of the Hyllingen Series (laterally in an inflating wedge) meant that contact metamorphism continuously preceded the approach of magma; c) the first magma to come into contact with the floor was evolved, and therefore relatively cool.

The pronounced basal reversal that defines Stage I in the Hyllingen Series is a consequence of the mode of emplacement of the compositionally zoned magma. This will be discussed later.

3.3. Stop 2: Northwest of Gjetleken

3.3.1. Location

Coordinates: 0623123 6980997. Ålen 1:50000 map.

3.3.2. Introduction

This stop is at a small summit north of the stream crossing point and is close to the lowest occurrence of modal layering above the country rock contact (much better layering will be seen later; do not spend much time here).

3.3.3. Description

The weakly developed modal layering here strikes roughly north-south and dips ~50° E, consistent with the regional orientation of layering. Plagioclase lamination commonly results in the parting of FHI rocks along layer-boundaries. Hornblende oikocrysts here are commonly 1-3 cm across (locally up to 10 cm). The rocks contain a relatively evolved

assemblage with olivine, Ca-rich pyroxene, plagioclase, magnetite, apatite and brown hornblende (Fig.19).

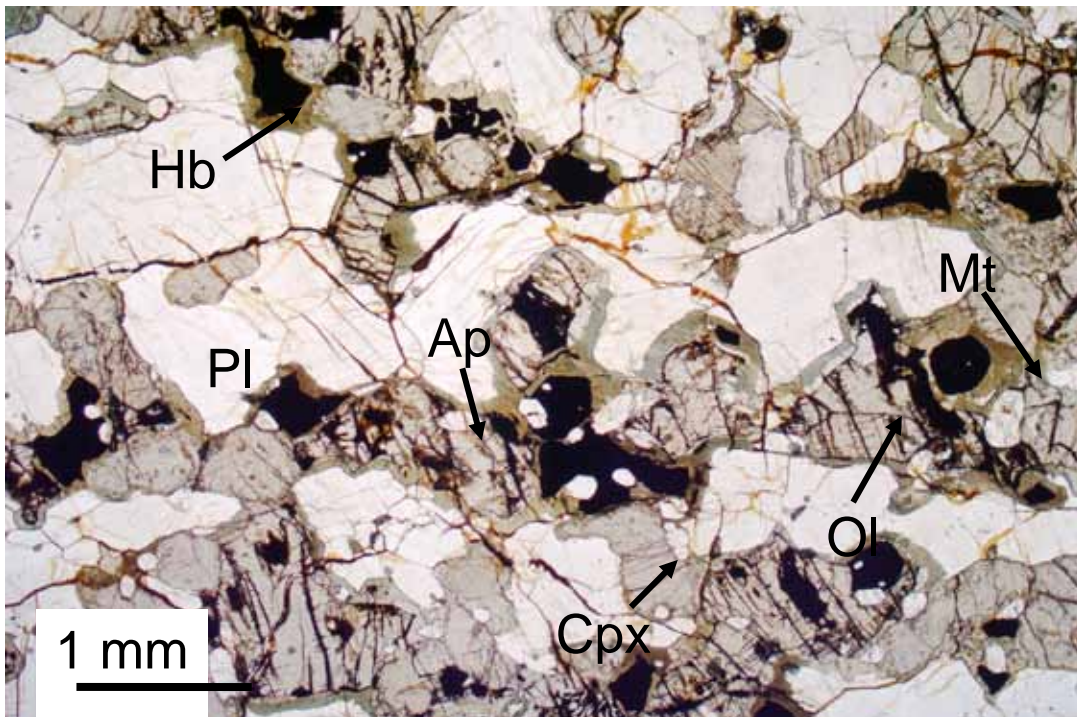


Fig.19. Photomicrograph of olivine diorite from Stop 2 near the base of Stage II in the Hyllingen Series. Olivine, plagioclase, Ca-rich pyroxene, magnetite and apatite are cumulus phases. Brown hornblende is intercumulus. The identified olivine grain has a narrow corona of orthopyroxene followed by green hornblende. PPL. (FH 06-2).

The summit of Hyllingen mountain (1205 m) can be seen to the NNE where the regional eastward dip (25°-30°) of the modal layering is clearly evident (Fig.20). Reddish-coloured rocks on outcrops about 1 km to the west of Stop 2 are at an abandoned copper mine at Rödhamaren within the Fundsjø Group metabasalts.

3.3.4. Significance of the outcrops

The modally layered ferrodiorites here are in the lower part of Stage II (Fig.18). The rocks become progressively more primitive upwards in Stage I because the rate of elevation of compositionally zoned magma was faster than the rate of crystallisation. The upper boundary of Stage I is defined where mineral compositions becomes essentially constant, reflecting a “steady state”- a balance between the rate of magma influx and the rate of crystallisation in Stage II. This will be discussed in greater depth later on.

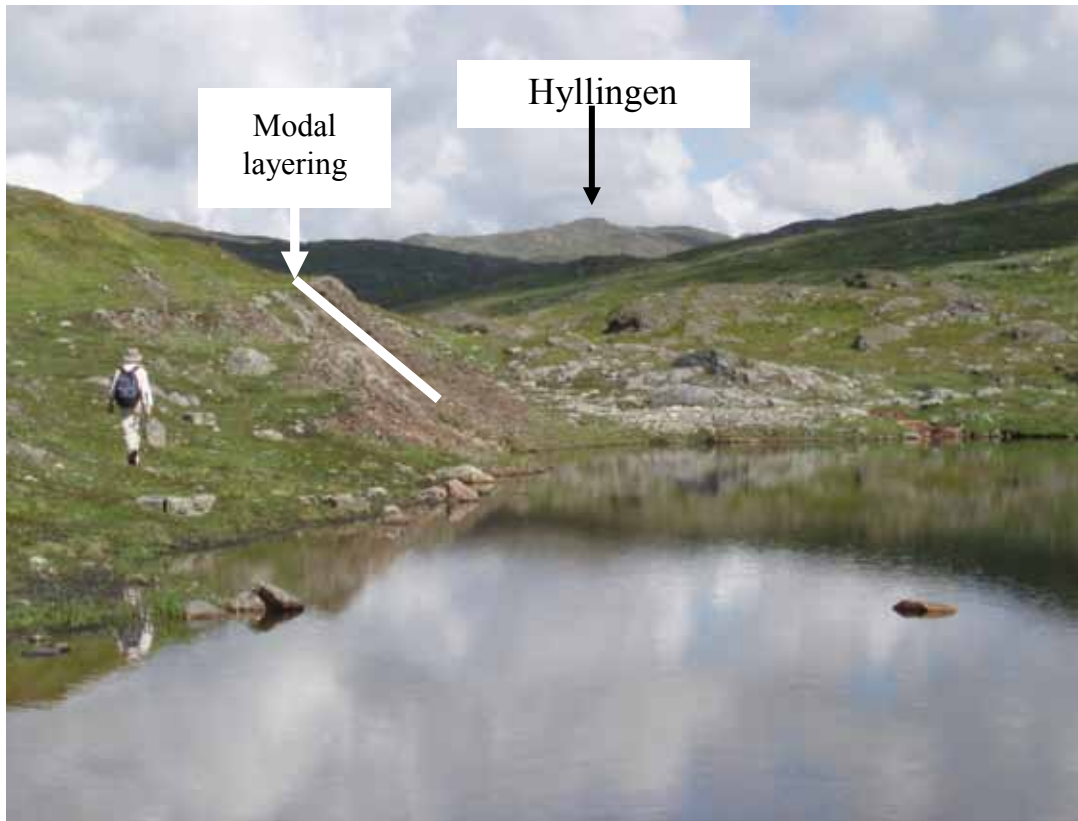


Fig.20. View to the north from near Stop 2. Modal layering (striking ~north-south and dipping to the east) in brown-weathering un-metamorphosed rocks is visible to the right of the person. The grey colour in the right centre is developed in metamorphosed equivalents (in amphibolite facies). The shallow eastward dip of the layering is apparent in the summit of Hyllingen (1205 m) in the distance (about 4 km away).

Hornblende oikocrysts are a widely developed feature of the FHI. In thin section they have a strong brown colour and poikilitically enclose the cumulus phases. Their presence reflects the hydrous nature of the parental magma to the FHI.

3.4. Stop 3: Southwest of Skjellåfjellet

3.4.1. Location

Coordinates: 0623594 6982649. Ålen 1:50000 map.

3.4.2. Introduction

This outcrop, on the eastern side of a small stream ~1 km north of Stop 2, illustrates the occurrence of different lithologies of country rock inclusions.

3.4.3. Description

There are two varieties of metabasaltic hornfels present here. The dominant type is a fine-grained dark grey, mostly equigranular metabasaltic hornfels (Fig.21). It contains, however, some coarser-grained patches and pyroxene-rich streaks. The texture is granoblastic with rounded grains of plagioclase and clinopyroxene. Some clinopyroxene porphyroblasts enclose granular plagioclases and there are sporadic porphyroblasts of brown hornblende. Some clusters of plagioclase grains may represent the remains of original plagioclase phenocrysts in the basaltic precursor.

The other type is medium grained and contains numerous, macroscopically obvious plagioclase grains (Fig.22). This is a contact metamorphosed plagioclase-phyric basalt of the type that occurs in dykes that cut across folded country rocks. It has been less thoroughly contact metamorphosed than the previous lithology. The relict plagioclase phenocrysts are only partially granular, there is relict igneous clinopyroxene and abundant brown hornblende.

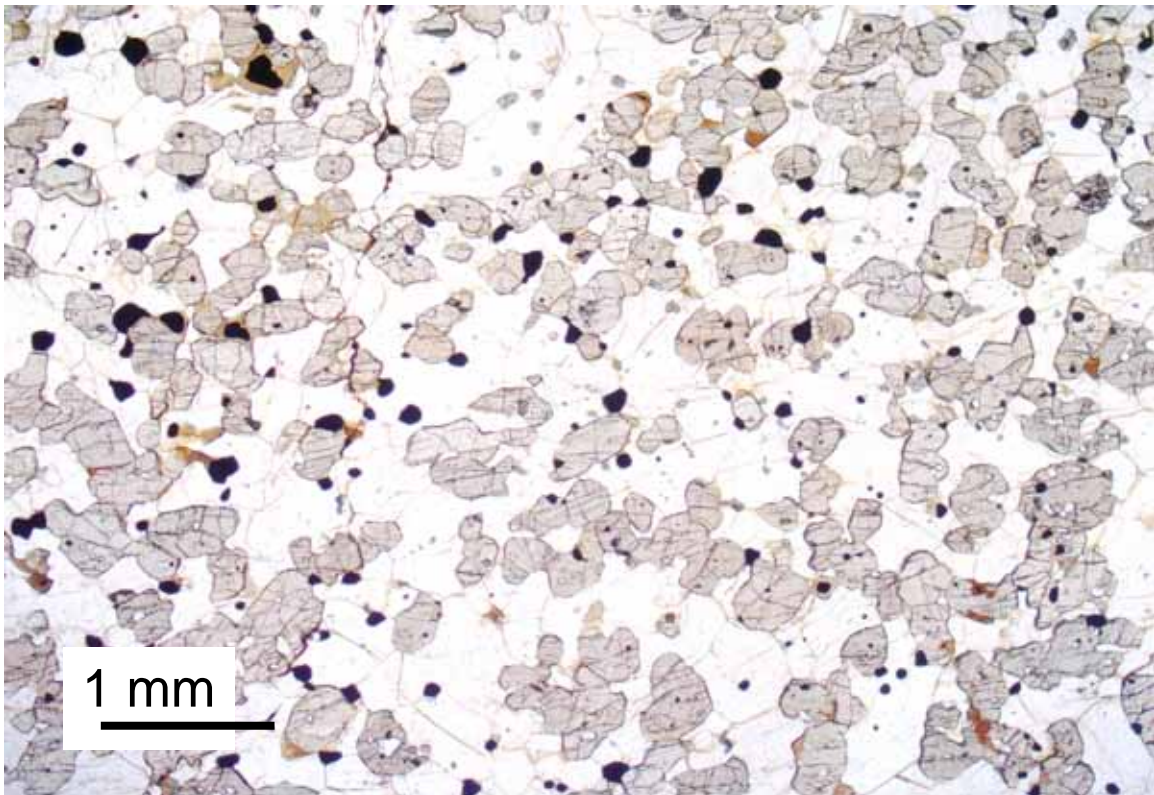


Fig.21. Metabasaltic hornfels inclusion at Stop 3 with a granoblastic texture consisting of small rounded grains of plagioclase, Ca-rich and Ca-poor pyroxene and minor FeTi-oxide. Pyroxene hornfels facies. PPL. (FH 06-3a)

3.4.4. Significance of the outcrops

Country rock inclusions are a major feature of the FHI. The vast majority are metabasaltic hornfels, but metapelitic hornfels are also locally abundant. They mostly show evidence of pyroxene hornfels facies contact metamorphism. Their lithologies match those of the adjacent country rocks. Their dimensions vary from cm-sized up to

huge rafts. The granoblastic texture of the metabasaltic hornfels at Stop 3 is typical for the FHI. We will return to the topic of inclusions many times and the appropriate aspect of their significance will be treated separately on each occasion.

3.5. Stop 4: Waterfall at westernmost of 5 lakes

3.5.1. Location

Coordinates: 0624030 6982949. Ålen 1:50000 map.

3.5.2. Introduction

This stop starts at the top of a prominent waterfall. Its lower reaches run over one of several elongate, plate-like metabasaltic hornfels inclusions in this area. The occurrence of large, plate-like inclusions in the FHI was first recognised in the vicinity of the lakes above the waterfall in 1982. This locality comprises a ~1 km long profile from west to east and is in the upper part of Stage II and the lower part of the compositional regression of Stage III.

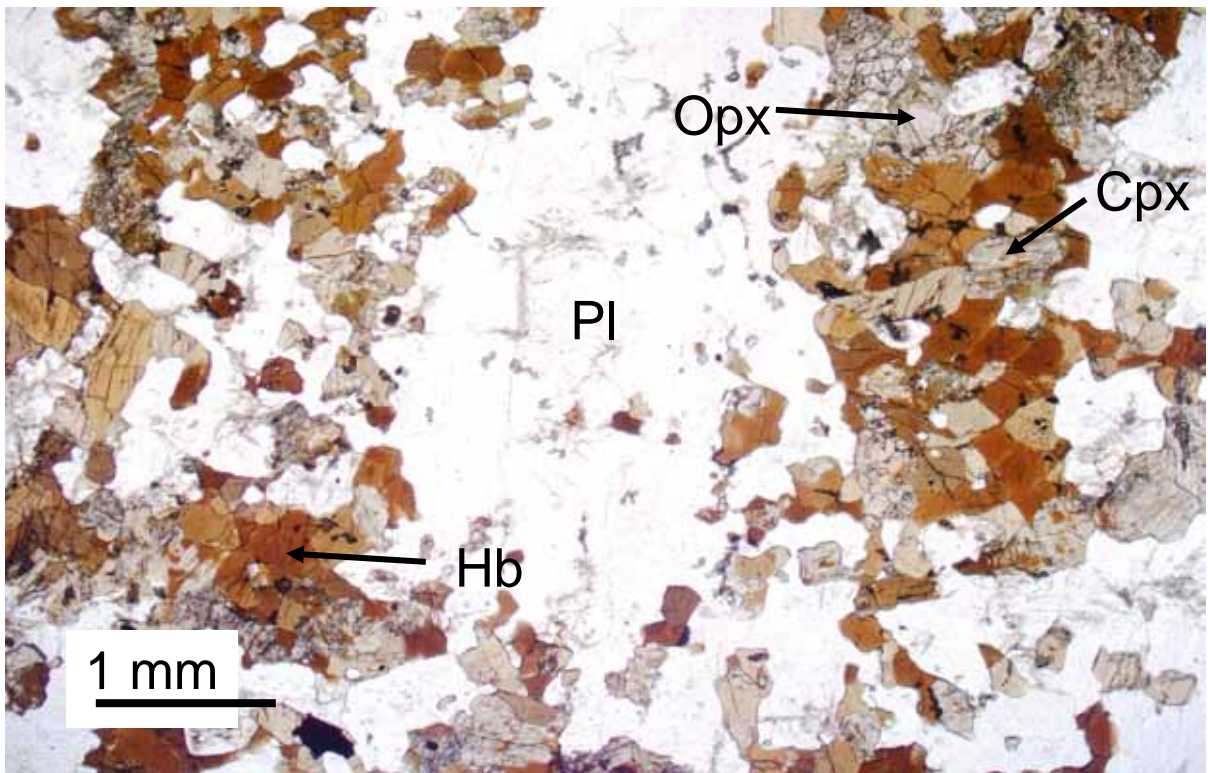


Fig.22. Contact metamorphosed plagioclase-pyrrhic basalt at Stop 3. The relict plagioclase phenocryst consists of several sub-grains. The main mafic minerals are Ca-rich and Ca-poor pyroxenes together with brown hornblende. PPL. (FH 06-3c)

3.5.3. Description

Modally layered rocks are well exposed in this area which is on the northern side of five large lakes. The strike is consistently close to north-south and the dip 40°-50°E. The compositional regression defining Stage III in the Hyllingen Series is developed in this

region. The modally layered rocks in most of Stage II have fairly constant mineral compositions (Fig.18), becoming gradually more evolved towards the top. The boundary between Stages II and III is defined where the minerals reach their most evolved compositions before gradually becoming more primitive. This is between the 3rd and 4th lakes from the west (Fig.13). The rocks here contain five cumulus phases: olivine (Fo₂₀), plagioclase (An₄₅), Ca-rich pyroxene (Mg#cp_{x44}), magnetite and apatite. It is evident that there is no obvious feature that marks the beginning of Stage III which has a total stratigraphic thickness of ~300 m here. Progressing eastwards towards the largest lake the rock become gradually and systematically more primitive. Cumulus apatite, and then cumulus magnetite progressively disappear, and the solid solution phases become more primitive. At the Stage III/IV boundary, near the northern extremity of the largest lake, mineral compositions in the olivine gabbros have reached Fo₅₇, An₅₈ and Mg#cp_{x71}. Stage III is traversed again in connection with Stop 10.

There is a very instructive exposure at the northern end of a small lake that forms an extension of a larger lake (0624714 6983128). Modal layering, trough-like features (Fig.23) and the development of amphibolite facies metamorphism (Fig.24) can be studied.



Fig.23. Several nested trough structures in olivine gabbro at Stop 4. Photograph taken looking north. Stratigraphic up is to the right.

Modal layering is a prominent feature here. The orange-brown weathering rocks are magnetite olivine gabbros in the lower central part of Stage III. This gabbroic unit with the characteristic weathering colour has been mapped along strike for ~6 km in the Hyllingen Series (Enclosure 1). Plagioclase-rich and mafic-rich (olivine + Ca-rich pyroxene + magnetite) layers are developed on a 2-10 cm-scale. Plagioclase lamination results in a prominent parting; there is no detectable lineation.

Some well-exposed trough-like features are developed on the top of a prominent outcrop. The troughs are ~1 m across and ~5 cm thick in their axial region. Some appear to be “nested” in underlying ones. The location of the trough axis migrates up-section.

There are several vein-like or dyke-like features here where olivine gabbro has been altered to metagabbro (Fig.24). The primary igneous texture is largely preserved but the mineral assemblage has clearly been altered. It is clear here that the metamorphism developed on either side of a crack along which fluids were introduced (Fig.24). The brownish colours of the un-metamorphosed layered rocks change to greyish tones. The mafic minerals are altered to amphiboles (mostly hornblende which is macroscopically black) and plagioclase becomes saussuritised.



Fig.24. Modally layered, brownish olivine gabbro is cut by a series of grey veins at Stop 4. These are fractures on either side of which the rock has been metamorphosed to an amphibolite facies mineral assemblage. This static metamorphism is locally widespread in the Hyllingen Series.

A common feature here and elsewhere in FHI is the presence of oikocrysts of calcic amphibole (Fig.26). These are brown in thin section and can readily be distinguished from amphiboles of metamorphic origin (Fig.27).



Fig.25. Alteration of brown-weathering gabbro to grey-weathering metagabbro is obviously related hydration on either side of a thin vein.

3.5.4. Significance of the outcrops

The main portion of Stage II crystallised over a period of time when the rate of magma influx balanced with the rate of crystallisation, resulting in a sequence of cumulates with essentially constant mineral compositions in any profile normal to the layering. When magma influx ceased (or slowed down) towards the top of Stage II (meaning also that the chamber ceased to expand (or slowed down)), rock compositions became more evolved upwards as a result of normal fractional crystallisation. Magma influx then resumed at a rate faster than that of crystallisation. This protracted event of influx resulted in the major compositional regression of Stage III.

Modal layering is an exceptionally well-developed feature of the FHI. The lateral compositional variations (see later) and other features of the Hyllingen Series can only be satisfactorily explained by the crystallisation of compositionally zoned magma along an inclined floor. Compositionally zoned magma is incompatible with large-scale convection. Field relations in the Hyllingen Series show that the magma chamber did not have steep walls. Under these circumstances it is difficult to escape from the conclusion that the cumulus minerals crystallised where they are now located; they cannot have been transported to their present locations. It therefore seems that *in situ* crystallisation was the dominant mechanism for formation of the Hyllingen Series.



Fig.26. Oikocrysts of calcic amphibole in gabbro near Stop 4.

The trough-like features are, however, difficult to explain in terms of *in situ* crystallisation alone. (Two much larger troughs will be seen at Stop 6). While large-scale convection cannot have taken place in the Hyllingen magma chamber, it is possible that small, local density currents could periodically have swept across the floor. There is little control as to the three-dimensional shape of the magma chamber. However, our interpretation of the method of formation of the discordant layering relations requires that the floor sloped inwards from the southern margin. It seems likely that the chamber had a saucer-shape, so that the floor sloped inwards from all the margins. The western margin of the Hyllingen magma chamber may well have been closer to Stop 4 than the southern margin (which is ~5 km away). Magmatic currents could have periodically swept down the sloping floor from the west, eroding small troughs and filling them with transported crystals. The troughs are filled by mafic minerals, implying that plagioclase grains may have been winnowed away. This, of course, is a type of crystal settling. We consider, however, that the dominant layer-forming process in the Hyllingen Series was *in situ* crystallisation. We have attempted to identify textural criteria to distinguish between these different types of layer-formation, but have not been successful. Evidence for current activity, including trough structures, is only sporadically developed in the Hyllingen Series. We can only speculate as to the cause of the magmatic currents. An earthquake is a possibility, but here one might expect there to be abundant evidence at a particular stratigraphic level. Alternatively, the impact of a block of roof rocks on the magma chamber floor may have initiated a magma current which flowed down towards the centre of the saucer-shaped chamber floor. Once a channel became established it

appears that it was re-used to form the nested troughs here and the repeated troughs at Stop 6.



Fig.27. Scan of thin section (2 x 3.4 cm) of olivine-bearing gabbro with a large, optically continuous, oikocryst of brown hornblende. Near Stop 4. PPL. (WF-183).

The local effect of amphibolite facies metamorphism at Stop 4 is evident. It is clearly related to mineral reactions on either side of a vein along which hydrous fluids were introduced. Igneous textures are commonly preserved. We use the term “metagabbro” for such rocks in which primary textures are largely preserved. When amphibolite facies metamorphism is accompanied by deformation the primary textures are commonly obliterated and we refer to these rocks as amphibolites (or foliated amphibolites). Modal layering is commonly emphasised in metagabbros compared with their un-metamorphosed equivalents because of the increase in colour contrast between the mafic-rich layers (which become dark grey to black) and plagioclase-rich layers (which become whiter).

3.6. Stop 5: ~1.5 km south of Hyllingen summit

3.6.1. Location

Coordinates: 0624766 6983646. Ålen 1:50000 map.

3.6.2. Introduction

This stop is at a strikingly white, bleached plagioclase-rich layer. The white colour is due to alteration to low-grade metamorphic minerals and is evidence of retrograde metamorphism.



Fig.28. Bleached plagioclase-rich layer at Stop 5.

3.6.3. Description

Some ~400 m north of Stop 4, a prominent white plagioclase-rich layer, ~70 cm thick, can be followed along strike for ~300 m (Fig.28). The two pyroxene magnetite gabbros above and below have been brecciated. The white “bleached” colour is due to the extensive alteration of plagioclase to clinozoisite ($\text{Ca}_2\text{Al}_3\text{Si}_3\text{O}_{12}(\text{OH})$) and prehnite ($\text{Ca}_2\text{Al}_2\text{Si}_3\text{O}_{10}(\text{OH})_2$).

3.6.4. Significance of the outcrops

There is widespread evidence for metamorphism of the FHI under amphibolite facies conditions after its crystallisation. There is also, however, local evidence for metamorphism in greenschist facies and prehnite-pumpellyite facies. Greenschist facies mineral assemblages are sporadically developed in connection with fractures and minor faults. Pale green chlorite (in veins up to a few mm-thick) replaces mafic phases along fractures in gabbro, metagabbro and foliated amphibolite. Plagioclase is strongly saussuritised in connection with this chloritisation.

The alteration of plagioclase to prehnite and clinozoisite is evidence of even lower grade metamorphism. In addition to this striking white plagioclase-rich layer, some fractures and minor faults are accompanied by pale green to white, fine-grained rocks that consist largely of prehnite and pumpellyite ($\text{Ca}_4\text{MgAl}_5\text{Si}_6\text{O}_{23}(\text{OH})_3 \cdot 2\text{H}_2\text{O}$) together with minor albite and quartz.

The amphibolite facies metamorphism took place at 5.5 ± 0.5 kb and $550 \pm 50^\circ\text{C}$; the greenschist facies event was at 4 ± 0.5 Kb and $425 \pm 50^\circ\text{C}$; and the prehnite-pumpellyite facies metamorphism at 2-3 kb and $200\text{-}250^\circ\text{C}$ (Fig.4). The amphibolite facies regional event is related to the main late Caledonian orogenic event (Scandian) in the Trondheim region after crystallisation of the FHI (~435 Ma) and before closure of the Rb-Sr system at 397 ± 8 Ma. The greenschist facies assemblages probably developed during nappe emplacement, whereas the prehnite-pumpellyite facies rocks could either represent retrograde metamorphism during late nappe emplacement or a local Late Devonian post-orogenic event.

3.7. Stop 6: ~1.2 km south of Hyllingen summit

3.7.1. Location

Coordinates: 0624951 6983816. Ålen 1:50000 map.

3.7.2. Introduction

Two large trough-like features are evidence for magmatic current activity.

3.7.3. Description

Two large troughs consisting mainly of ultramafic cumulates are developed just above the base of Stage IV. The modally layered host rocks are magnetite olivine gabbros; modal layering here strikes $\sim 28^\circ$ and dips $\sim 30^\circ\text{E}$. The lower trough has a strike-length of ~ 40 m and a maximum thickness of ~ 5 m. It consists of rounded olivines and magnetites poikilitically enclosed in clinopyroxene and brown hornblende oikocrysts (Fig.29). The

upper one (~100 m to the east; 0625042 6983793) is slightly larger (~55 m long; ~10 m thick) and richer in olivine. Here rounded olivines are poikilitically enclosed in oikocrysts of magnetite, clinopyroxene and brown hornblende.

The summit of Fongen mountain can be seen to the north, ~26 km away (Fig.30).

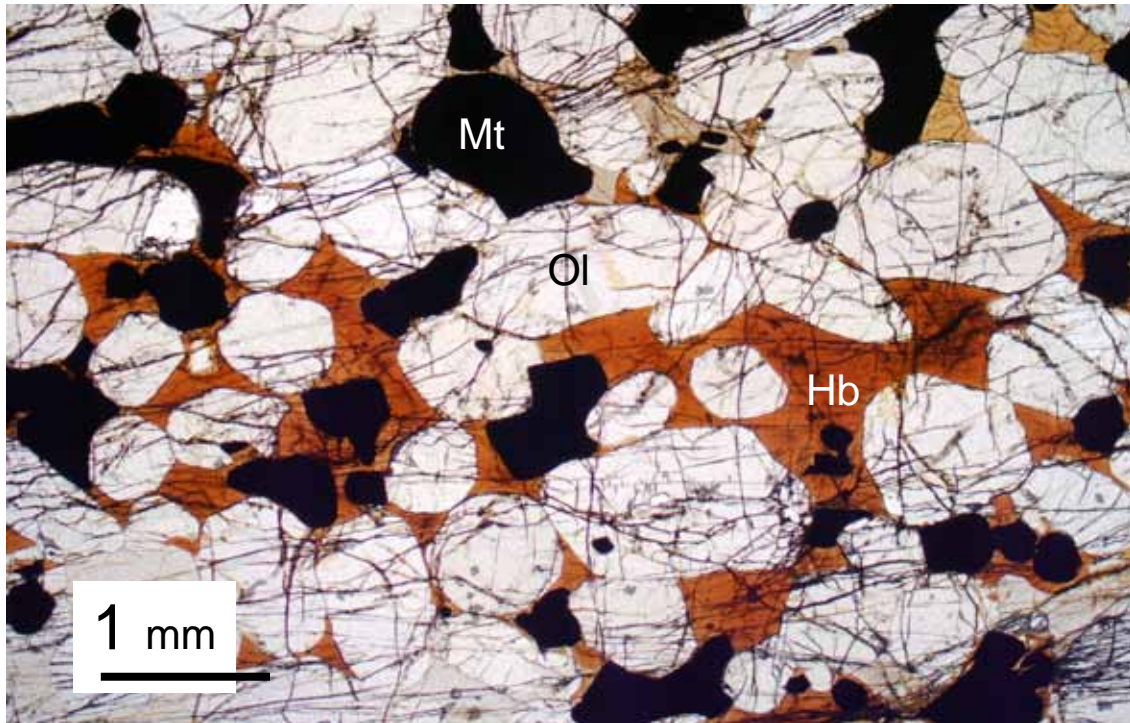


Fig.29. Rounded olivines and magnetite enclosed by brown hornblende in the lower of two large trough structures at Stop 6. PPL. (FH06-6).

3.7.4. Significance of the outcrops

The large troughs have essentially the same geometry and orientation as the much smaller ones at Stop 4 and were probably formed in a similar way. It is not clear whether these two large trough-like features cut down into the underlying cumulates or fill depressions because the underlying rocks are not well layered. Their ultramafic character is, however, striking in comparison with the mafic host rocks that have identical mineral compositions. Cumulus olivines in the troughs (and magnetites in the lower trough) are much more rounded than in the host cumulates (Fig.29). This could be a consequence of their transport in flowing magma before deposition in the trough where they rapidly became enclosed by the growth of oikocrysts.



Fig.30. View to the north from near Stop 6 looking along the strike of modal layering. The summit of Fongen (1441 m) is visible in the distance.

3.8. Stop 7: Southern Ysterhøgda

3.8.1. Location

Coordinates: 0627167 6982654 Ålen 1:50000 map.

3.8.2. Introduction

The roof contact is superbly exposed near the small hilltop at 1085 m above sea level (Fig.31). In earlier publications this locality is referred to as “Jensfjellet”. On the most recent topographic map, the name “Jensfjellet” has been moved about 3 km further north; the new name is Ysterhøgda.

3.8.3. Description

Approaching this locality from the Stage III/IV boundary the rocks become increasingly evolved with stratigraphic height. At the base of Stage IV in the vicinity of the large lake at 1088 m the mineral compositions in the olivine gabbros are Fo_{57} , An_{58} and $Mg\#_{cpx71}$. These minerals (and Ca-poor pyroxene) become progressively more evolved upwards and are joined in sequence by magnetite, calcic amphibole, apatite, biotite, zircon, quartz, K-feldspar and allanite. Calcic amphibole is a common intercumulus phase in the lower rocks; it becomes a cumulus phase after magnetite and before apatite in the Hyllingen Series. Extremely iron-rich olivine (commonly extensively replaced by magnetite and grunerite) and Ca-poor pyroxene disappear in the uppermost rocks. The latter mineral has exsolution features showing that it has inverted from pigeonite in the more evolved rocks. Apatite is also absent in the most evolved rocks. The last modal layering is observed

~500 west of the roof contact, near where alkali feldspar becomes a cumulus phase. There is an interval with rafts of metabasaltic inclusions in Stage IV, but otherwise there are far fewer inclusions than in Stage II.

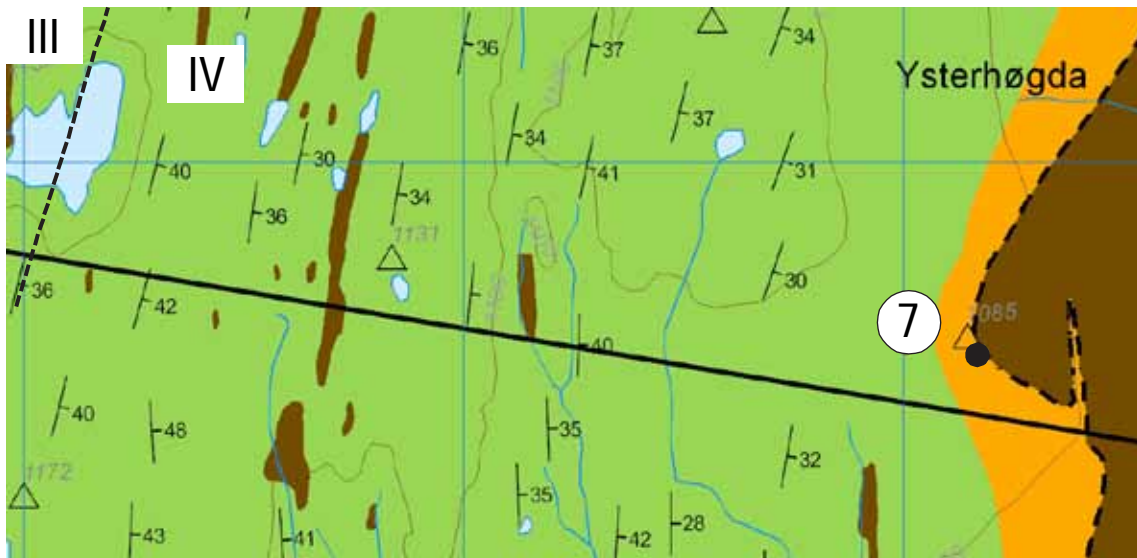


Fig.31. Location of Stop 7. This map has been extracted from Enclosure 1. The boundary between Stages III and IV is shown by a dotted line.

At the roof the quartz-bearing syenites (Figs.32 & 33) consist of albite (An_1), K-feldspar, minor quartz, hedenbergite ($Mg\#cpx_0$), ferroedenite (with $Mg\#_0$), zircon and allanite. The relatively uncommon mineral babingtonite ($Ca_2Fe^{2+}Fe^{3+}Si_5O_{14}(OH)$) has also been identified by Thaysen (1998). These quartz-bearing syenites are in direct contact with metabasaltic rocks that form the roof; the contact is very well exposed. The roof rocks consist of granular metabasalts that are in hornblende hornfels facies (Fig.34). They do not appear to have been significantly affected by the regional deformation or amphibolite facies metamorphism that followed crystallisation of the FHI.

3.8.4. Significance of the outcrops

Stage IV in the Hyllingen Series covers an extremely wide range of mineral assemblages and compositions. At the roof there is no evidence of a chilled margin or an upper border series; the rocks become progressively more evolved upwards through a thickness of ~1300 m in this profile and the most evolved rocks (with low temperature end-member mineral compositions) are in direct contact with the roof. Rocks become increasingly evolved upwards through Stage IV reflecting extreme fractional crystallisation. There are a few small reversals and “steady state” intervals, implying that there were some minor additions of magma during Stage IV, but fractional crystallisation was the dominant process. The fact that the most evolved rocks in the intrusion occur at the roof implies that the magma chamber was closed to the exit of magma, at least during its final stages of evolution, and probably throughout its life. It also implies that the magma was compositionally zoned throughout crystallisation of Stage IV. We will return to this issue later.



Fig.32. Sharp contact at the roof of the Fongen-Hyllingen layered intrusion between pink quartz-bearing syenites below and country rock metabasaltic hornfels above. The syenite is extremely evolved with low-temperature end-member mineral compositions.

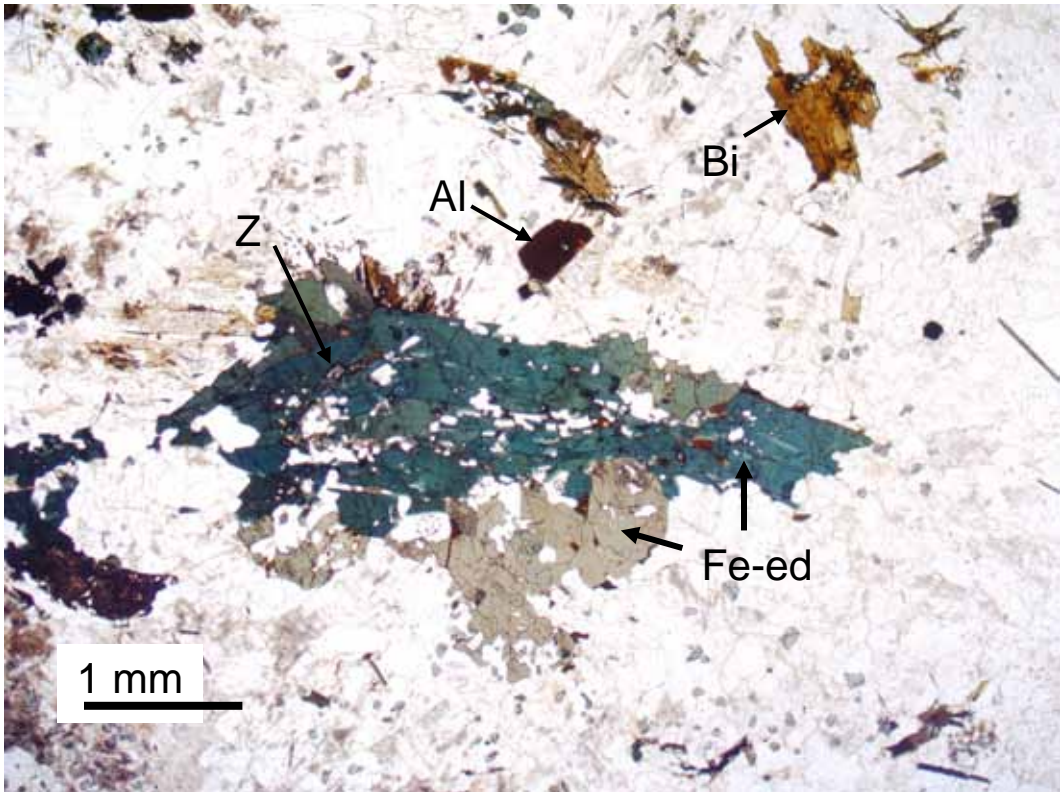


Fig.33. Quartz-bearing syenite from just below the roof at the top of the Hyllingen Series at Stop 7. The mafic minerals include ferroedenite (Fe-ed), allanite (Al), biotite (Bi), zircon (Z) and hedenbergite (not in photo). Felsic minerals are mainly albite and K-feldspar with minor quartz. PPL. (FH 06-16a).

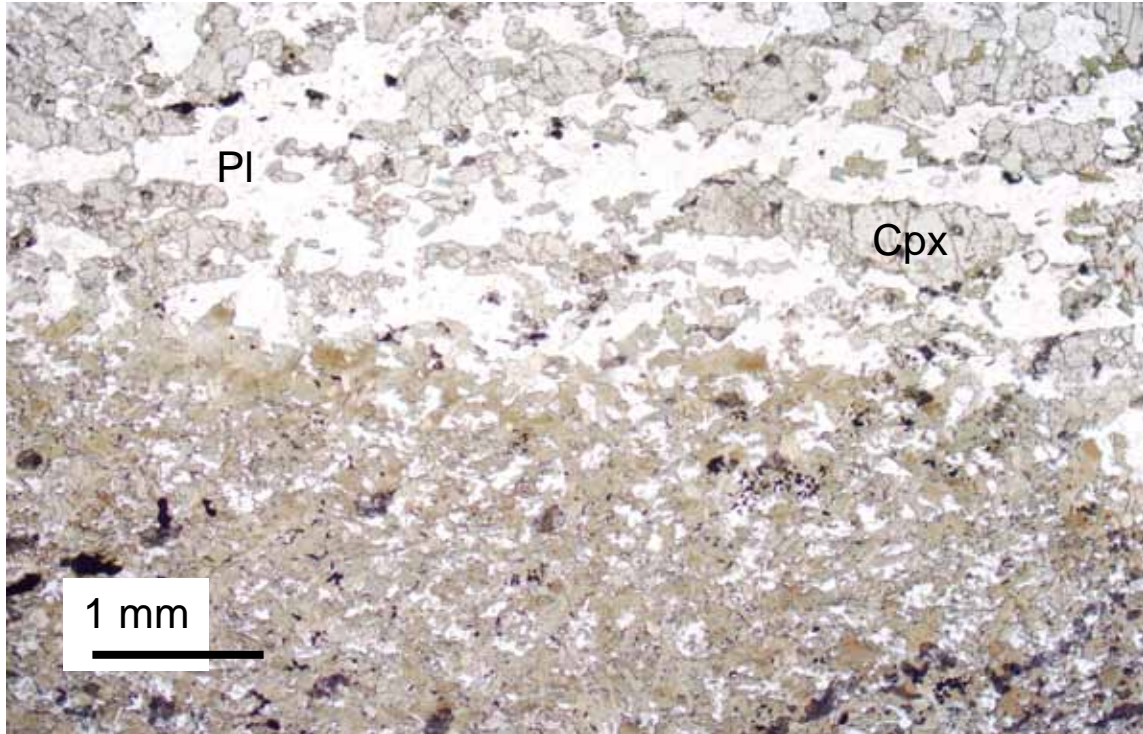


Fig.34. Metabasaltic country rock from ~1 m above the roof contact in the eastern Hyllingen area (Stop 7). The rock consists dominantly of granular hornblende and plagioclase (lower part of photo) with veins of coarser grained clinopyroxene and plagioclase (upper part). PPL. (FH 06-16b).

The evolved rocks in this area provided a Rr-Sr whole rock isochron age of 405 ± 9 Ma (Wilson & Pedersen, 1982); modified to 397 ± 8 Ma by Sørensen & Wilson (1995). This is much too young to represent the crystallisation age of these rocks, since the main Scandian regional metamorphic episode took place at 430-425 Ma. The 397 ± 8 Ma date has therefore been interpreted as representing a cooling age after the regional metamorphism since the Rb-Sr system must have remained open in these extremely evolved, relatively low-temperature, rocks for a long period of time. Zircons separated from these syenites gave a crystallisation age of $426^{+8/-2}$ Ma (Wilson et al., 1983). Nilsen et al. (2007) have recently obtained a U-Pb zircon age of 437.8 ± 2.3 Ma for the same rocks. Considered together, these two ages (which almost overlap within two standard deviations) imply that crystallisation took place at close to 435 Ma, just before the main Scandian orogenic event.

3.9. Introduction to Stops 8 - 12

The main focus of Stops 8 - 12 is on the lateral compositional variations in the Hyllingen Series and metabasaltic inclusions. We pass through Stage I (Stop 8) and most of Stage II

before reaching an abandoned small copper mine in a metabasaltic inclusion (Fig.35; Stop 9). After following this inclusion for several 100 m along strike, we pass through the compositional regression of Stage III (Stop 10). At the Stage III/IV boundary here the mineral compositions are more evolved than further north (e.g. near Stop 6). Progressing south along strike the rocks become increasingly evolved. Approaching the southern margin (Stop 11) the layered rocks are inter-fingered with country rock metapelitic and metabasaltic hornfels. Local contamination in the vicinity of metapelitic inclusions is apparent where the layered diorites contain garnet and/or biotite. The lower marginal rocks are examined on the return journey (Stop 12).

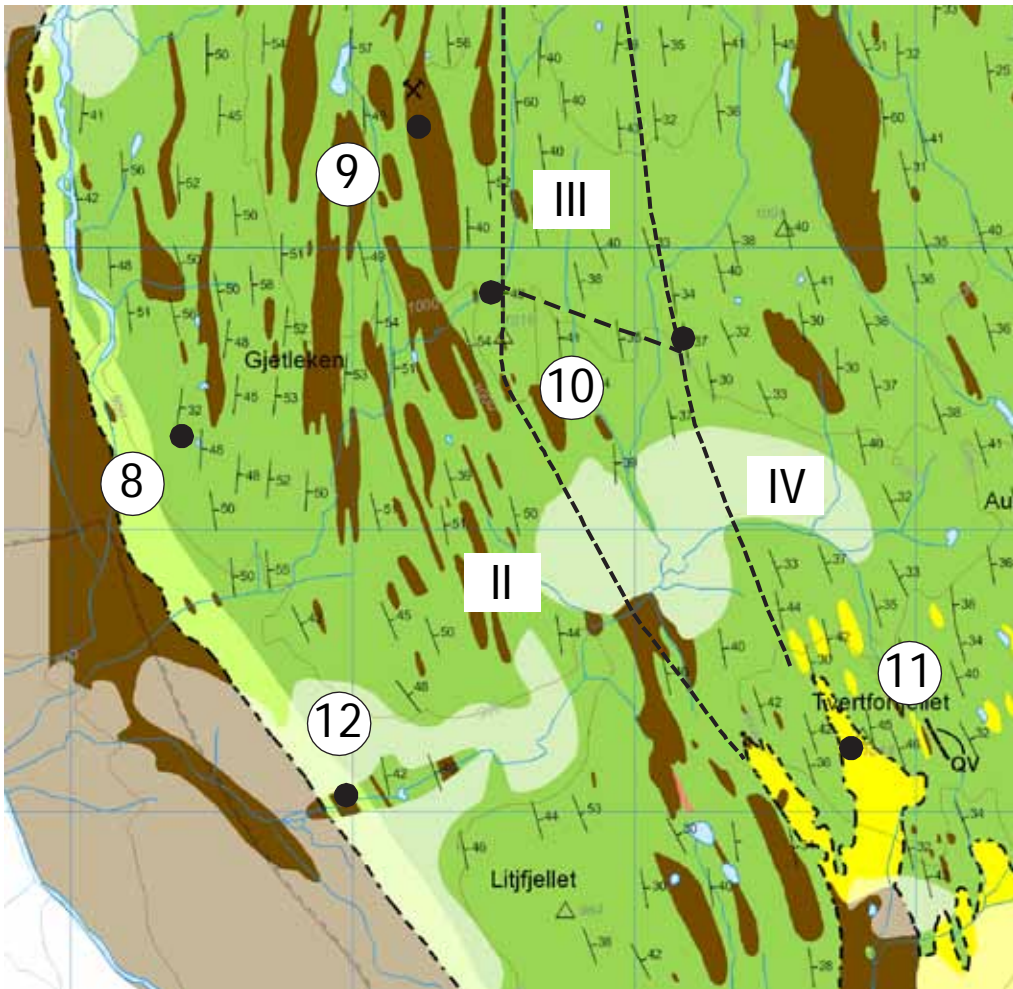


Fig.35. Locations of Stops 8-12. The boundaries between Stages II, III and IV are shown with dotted lines.

3.10. Stop 8: Top of Gjetleken

3.10.1. Location

Coordinates: 0623423 6980332. Ålen 1:50000 map.

3.10.2. Introduction

We are here near the Stage I/II boundary where the first occurrence of modal layering is developed. Partial metamorphism in amphibolite facies is quite widespread in the form of cummingtonite metagabbros.

3.10.3. Description

This stop is at the top (970 m) of the hill Gjetleken, north east of the bridge at Stop 1. Sporadic outcrops of un-layered, massive diorite on the western slope of Gjetleken belong to Stage I. Modal layering on a dm- to m-scale at the top of the hill strikes north-south and dips $\sim 50^\circ\text{E}$. Proceeding to the northeast the orientation of the layering is consistent and differential weathering of the layered sequence results in elongate north-south ridges. Close inspection of many outcrops reveals that some of the mafic cumulus grains have a dark rim where they are adjacent to plagioclase. This feature represents the partial alteration of Ca-poor pyroxene (or olivine) to cummingtonite/grunerite and a rim of hornblende against plagioclase. Such “cummingtonite metagabbros” with a corona of metamorphic hornblende are a characteristic feature of much of the partially metamorphosed parts of FHI (Figs.36 & 37). Another example of cummingtonite metagabbro is shown in Fig.50 (Stop 14).

Continuing northeast towards Stop 9 we traverse a ~ 70 m wide inclusion. This consists mostly of fine-grained grey- to rusty-weathering metabasaltic hornfels, but there are also plagioclase-phryic and metapelitic patches.



Fig.36. Modally layered metagabbro with a coronitic texture near Stop 8. Brown cores of cummingtonite (replacing Ca-poor pyroxene and/or olivine) are surrounded by black hornblende (green in thin section). See also Fig.37.

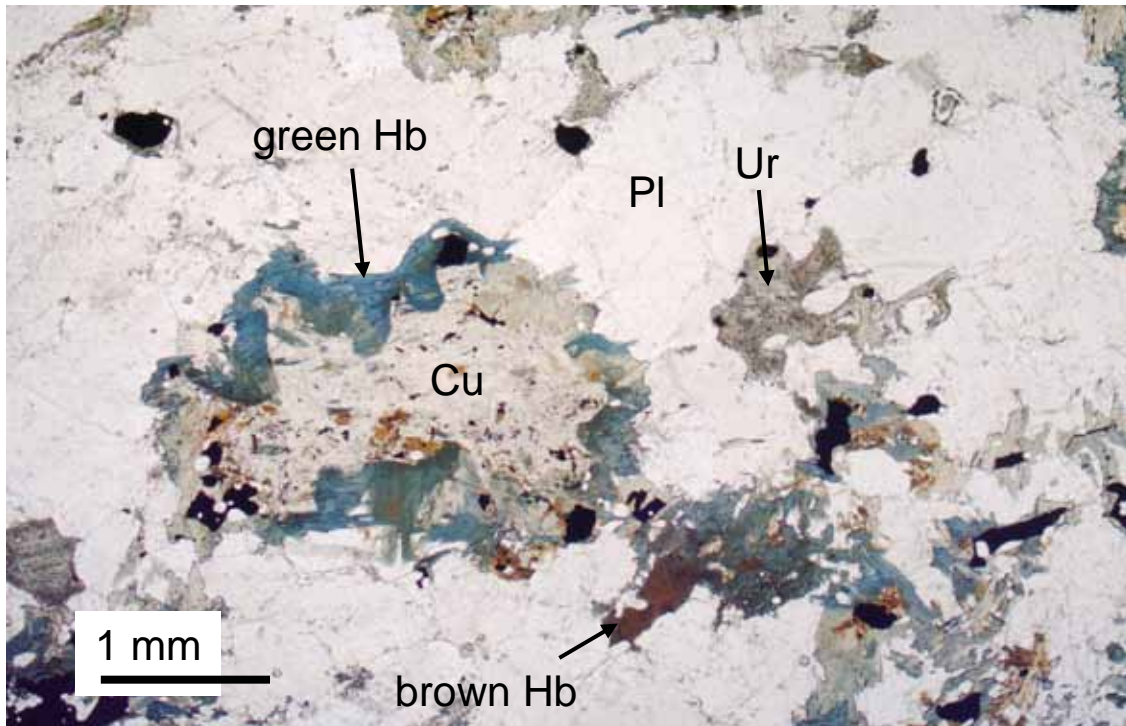


Fig.37. Cummingtonite metagabbro from near Stop 8. A Ca-poor pyroxene grain has been replaced by a granular aggregate of cummingtonite/grunerite (Cu) rimmed by greenish hornblende (green Hb) where the pyroxene was adjacent to plagioclase. This kind of corona structure is commonly developed in the FHI. Ca-rich pyroxene has been partially pseudomorphed to tremolite/actinolite (uralite; Ur). Primary igneous brown hornblende remains largely unaltered. There are many small apatite grains. This coronitic metagabbro contains four different amphiboles. PPL. (FH 92).

3.10.4. Significance of the outcrops

Stage II contains rocks in which mineral compositions remain fairly uniform with stratigraphic height. This reflects the fact that the rates of crystallisation and magma addition roughly balanced over a long interval. This stage contains numerous raft-like inclusions of metabasaltic hornfels. Partial amphibolite facies metamorphism, in which primary textures are largely preserved, is common.

3.11. Stop 9: ~1 km northeast of Gjetleken

3.11.1. Location

Coordinates: 0624213 6981550. Ålen 1:50000 map.

3.11.2. Introduction

This is the site of an abandoned small copper mine located in the northern end of a raft-like metabasaltic inclusion that extends several 100 m to the south.

3.11.3. Description

There are old copper mines in the vicinity of the FHI at Rødhammer (~ 1 km northwest of Stop 1) and Gressli (~ 2 km west southwest of Stop 13). Mining ceased at Rødhammer in 1824, and at Gressli in 1868. These two mines are in metabasaltic rocks of the Fundsjø Group and belong to the Røros family of copper mines; they are not genetically related to the layered intrusion. At Stop 9 there was copper-mineralisation in the metabasalt before it became included in the layered intrusion. The small mine was soon abandoned but the tip contains samples that are quite rich in chalcopyrite.



Fig.38. Rusty-weathering rocks at the tip near the entrance to the old copper mine at Stop 9.

The mine is in the northern end of a raft-like inclusion that is about 120 m wide in its central part and can be followed ~700 m to the south from the mine (Fig.35). The inclusion consists dominantly of fine- to medium-grained, grey to rusty weathering metabasalt. There are some intervals that are plagioclase-phyric. Continue to a small marshy lake ~400 m south of the mine.

3.11.4. Significance of the outcrops

The small abandoned copper mine represents the only attempt to mine economic mineral resources in the Fongen-Hyllingen Intrusion. Investigations for possible platinum group mineralisation were carried out in the 1980s, but the analytical results were discouraging.

There are many country rock inclusions in the FHI; the majority of these are of metabasaltic hornfels. Many of them are raft-like and the largest can be followed along strike for up to several 100 m. They are particularly abundant in Stage II which is believed to have developed during expansion of the magma chamber while the rate of magma influx roughly balanced the rate of crystallisation.

3.12. Stop 10: ~1 km east-northeast of Gjetleken

3.12.1. Location

Coordinates: Start: 0624571 6981144. Finish: 0625025 6981075. Ålen 1:50000 map.

3.12.2. Introduction

Stop 10 is a ~600 m long section through the compositional regression of Stage III.

3.12.3. Description

The boundary between Stages II and III is located near a south-flowing stream in a gully. Here minerals reach their most evolved compositions in this profile normal to the layering (Fo₁₅:An₄₃:Mg#cp_{x41}). Above this, mineral compositions gradually become more primitive through Stage III which is ~500 m thick here. This compositional regression is commonly not easy to appreciate in the field. Mineral compositions at the Stage III/IV boundary are the most primitive in this profile (Fo₅₂:An₅₅:Mg#cp_{x68}).

Mineral compositions at the Stage II/III and III/IV boundaries here are more evolved than those at these boundaries in the vicinity of Stop 4 (Fo₂₀:An₄₅:Mg#cp_{x44} and Fo₅₇:An₅₈:Mg#cp_{x71} respectively). Progressing southwards along strike towards Stop 11 (Fig.40), minerals continue to become more evolved.

3.12.4. Significance of the outcrops

The regression in mineral compositions through Stage III is accompanied by increasingly less-contaminated Sr-isotopic signatures (Fig.41; Sørensen & Wilson, 1995). In the vicinity of Stop 4 the initial ⁸⁷Sr/⁸⁶Sr ratio (Sr_i) decreases systematically from 0.7044 to 0.7035 from the base to top of Stage III. At Stop 10 this variation is from 0.7045 to 0.7040 (Fig.42). This implies that the magma already in the chamber just before the development of Stage III was somewhat contaminated, but had essentially the same degree of contamination throughout. The fact that mineral compositions become systematically more primitive upwards through Stage III at the same time as the magma becomes less contaminated cannot be explained by the gradual elevation of compositionally zoned magma alone. The resident magma must have become gradually more primitive by the addition of fresh magma. For this new, isotopically uncontaminated magma signature, to reach the crystallisation front high on the inward-sloping floor in the Hyllingen area cannot be achieved by the elevation of the compositionally zoned resident magma. Some kind of effective magma mixing is required. Sørensen & Wilson (1995) suggested that Stage III developed during long-lasting addition of magma by a fountaining process, allowing effective dilution of the resident melt by uncontaminated magma.



Fig.39. Looking north along the strike of modal layering from near Stop 10.

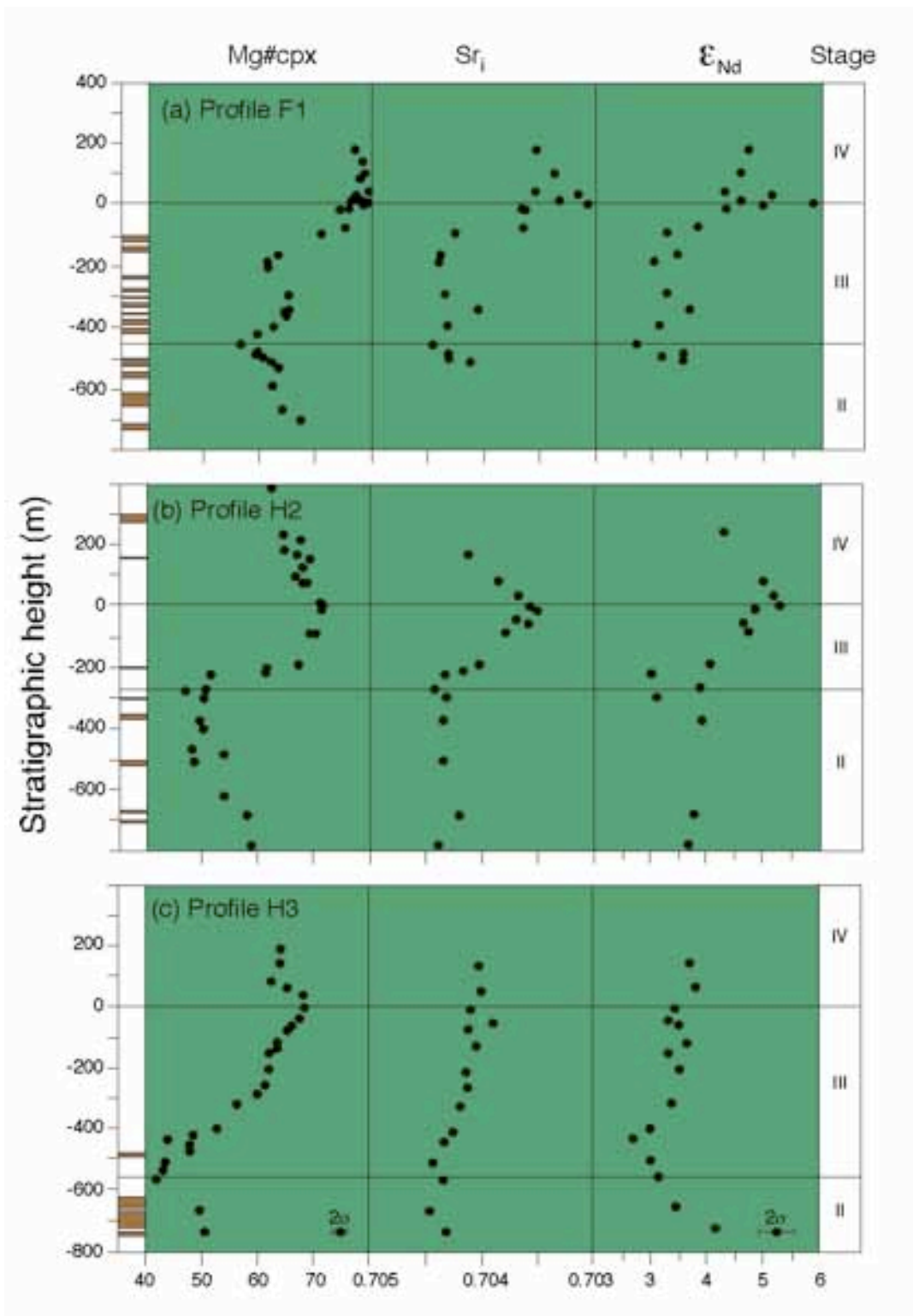


Fig.40. Compositional variation of Ca-rich pyroxene and Sr- and Nd-isotopic variations in Stage III in profiles F1 (in the northern Fongen area), H2 and H3. Locations of H2 and H3 are shown on Fig.17. Adapted from fig.7 in Sørensen & Wilson (1995) where the Nd-isotopes are discussed. Brown intervals to the left are metabasaltic inclusions.

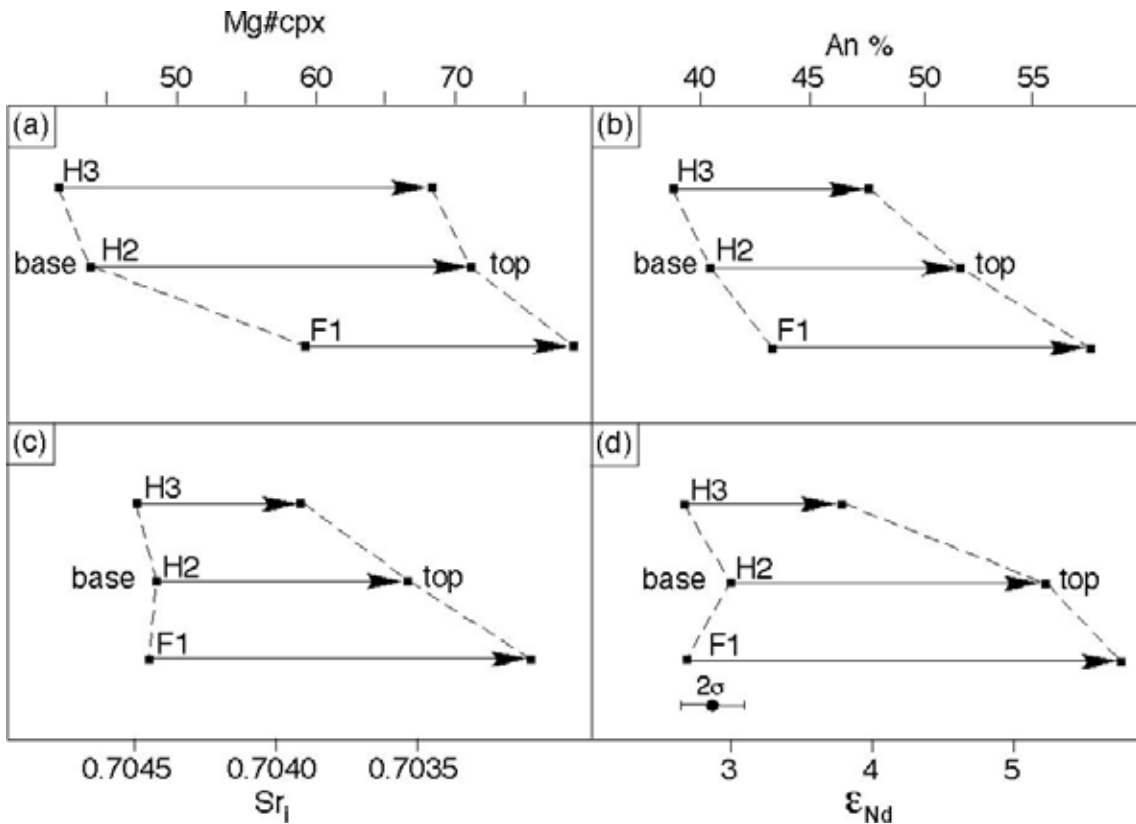


Fig.41. Comparison of Mg-number in Ca-rich pyroxene (cpx), plagioclase An%, Sr_i and ϵ_{Nd} at the base and top of Stage III in profiles F1 (northern Fongen), H2 (near Stop 4) and H3 (near Stop 10). Arrows point from data at the base to the top. So the length of the arrow shows the magnitude of the regression. Dashed lines connecting points from different profiles illustrate lateral compositional variations. Note that the scale for Sr_i has been reversed. Adapted from fig.8 in Sørensen & Wilson (1995) where the Nd-isotopes are discussed.

3.13. Stop 11: Tverfortfjellet

3.13.1. Location

Coordinates: 0625850 6979259 Ålen 1:50000 map.

3.13.2. Introduction

Tverfortfjellet is near the southern margin of the Hyllingen Series where layered rocks inter-finger with country rocks. The latter consist largely of metapelitic hornfels. It is noteworthy that the layering strikes towards the country rock margin. There is no evidence of steep walls or a chilled margin. Mineral compositions in the marginal layered rocks are very evolved; they become increasingly primitive along strike away from the margin. Local assimilation of metapelitic material is evident.

3.13.3. Description

Approaching Stop 11 from the north, along the strike of modal layering, the rocks continue to become more evolved. Mineral compositions at the Stage II/III boundary to the west of Stop 11 are Fo₆:An₃₄:Mg#cp_{x25}, whereas those at the Stage III/IV boundary at Stop 11 are Fo₁₃:An₄₂:Mg#cp_{x38}. Passing along strike from Stop 4 to Stop 11, a distance of ~3.5 km, these compositions have become systematically more evolved (Table 1).

Table 1. Lateral variations of mineral compositions along the strike of modal layering

Stop no.	Stage II/III boundary			Stage III/IV boundary		
	Olivine Fo%	Plag An%	Cpx Mg#	Olivine Fo%	Plag An%	Cpx Mg#
4	20	45	44	57	58	71
10	15	43	41	52	55	68
11	6	34	25	13	42	38

There are many metapelitic inclusions near Tverfortfjellet. Local contamination of the host rocks is evident by the presence of garnet and biotite in the FHI ferrodiorites (Fig.42). The metapelitic inclusions (Fig.42) are dominantly grey, medium- to fine-



Fig.42. Garnet-rich diorite resulting from the assimilation of metapelitic material near Stop 11.

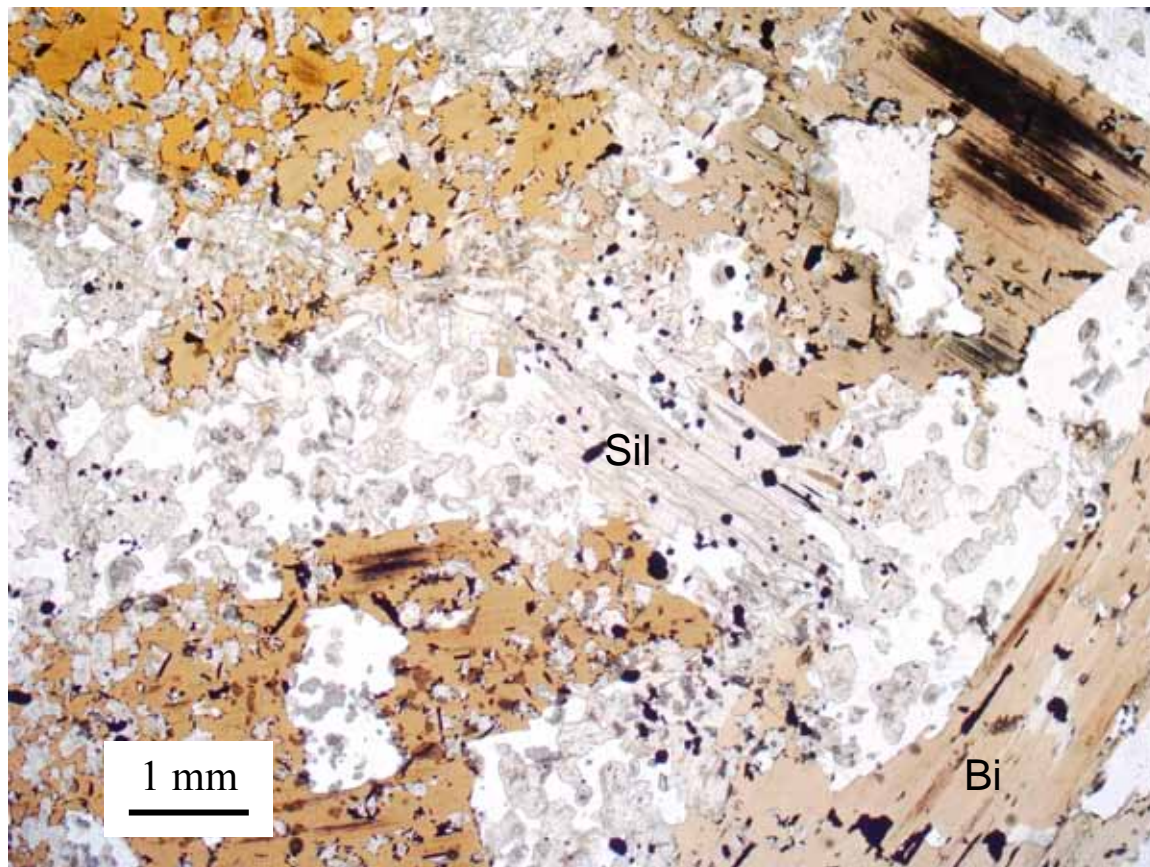


Fig.43. Metapelite hornfels from near Tverfortfjellet (Stop 11). Sillimanite (Sil) is partially altered to muscovite. Biotite (Bi) is abundant. The colourless groundmass consists largely of plagioclase and quartz. PPL. (FH 06-13).

grained massive rocks. Dark bands, rich in orthopyroxene and green spinel, represent original lithologically contrasting layers and locally display fold structures.

A prominent, white quartz vein can be seen ~200 m east of the top of Tverfortfjellet. This vein, which is remarkably free from accessory minerals, is up to ~15 m thick and can be followed for ~100 m along strike. This is a unique feature in the FHI and is believed to reflect hydrothermal activity, re-depositing some of the quartz available in the metapelite inclusions.

3.13.4. Significance of the outcrops

The presence of folded metapelite hornfels inclusions implies that emplacement of the FHI post-dated at least one episode of regional deformation. Local contamination is developed around some of these inclusions, but it does not extend more than a few meters into the enclosing layered rocks (Wilson et al., 1987).

Assuming that modal layering represents the crystallisation front implies that these mineral compositions crystallised at the same time on the magma chamber floor. This means that significantly more primitive magma was crystallising at, for example, Stop 4 while much more evolved magma was crystallising closer to the magma chamber margin

(near Stop 11). The presence of systematically more evolved compositions along strike means that the along-strike change in magma composition was gradual. This precludes (a) chamber-wide magma convection and (b) the transport of minerals from elsewhere. The model proposed by Wilson & Larsen (1985) involves the crystallisation of compositionally zoned magma along an inclined floor; *in situ* crystallisation is also implied.

3.14. Stop 12: Synste Skjellåa

3.14.1. Location

Coordinates: 0623874 6979024. Ålen 1:50000 map.

3.14.2. Introduction

This series of exposures is close to the basal contact of the Hyllingen Series with metabasaltic country rocks.

3.14.3. Description

There is a series of small waterfalls near Stop 12. Approaching from the east, indistinct modal layering is developed in ferrodiorites just above the uppermost waterfall. The layering strikes $\sim 150^\circ$ and dips $\sim 35^\circ$ E. Hornblende oikocrysts are locally prevalent. These ferrodiorites are in contact with fine-grained aphyric metabasaltic hornfels at the uppermost waterfall. The metabasalts are cut by two (~ 10 and ~ 20 cm wide) felsic dykes consisting of very fine-grained trondhjemite. The dykes are close to vertical and strike at $\sim 110^\circ$. The metabasaltic hornfels continues downstream for ~ 100 m where it is cut by several 1-10 cm-wide veins of dioritic pegmatite. The metabasalt is locally plagioclase-phyric. The lowermost exposures are of metabasalt, but it is not clear whether these represent *in situ* country rocks or inclusions.

3.14.4. Significance of the outcrops

The absence of chilled marginal rocks is again apparent, together with their evolved nature. While it is not certain that the lowermost exposed rocks represent country rocks and not inclusions, we are clearly very close to the basal contact of the layered intrusion here. However, it is important to be aware of the fact that we are high up on the side of the funnel-shaped magma chamber, not far from its “leading edge” at the southern margin of the Hyllingen Series (Figs.10 & 11).

3.15. Introduction to Stops 13 - 16

Stops 13 – 16 are located in the central, narrow part of FHI where deformation and metamorphism are extensively developed.

3.16. Stop 13: Road 705 at Gressli

3.16.1. Location

Coordinates: 0625895 6993913. Tydal 1:50000 map.

3.16.2. Introduction

This locality is on the main road (705; near Gressli) above the dam across the Nea river (Fig.44). It illustrates extensive metamorphism and deformation of the FHI (Figs.45-48).

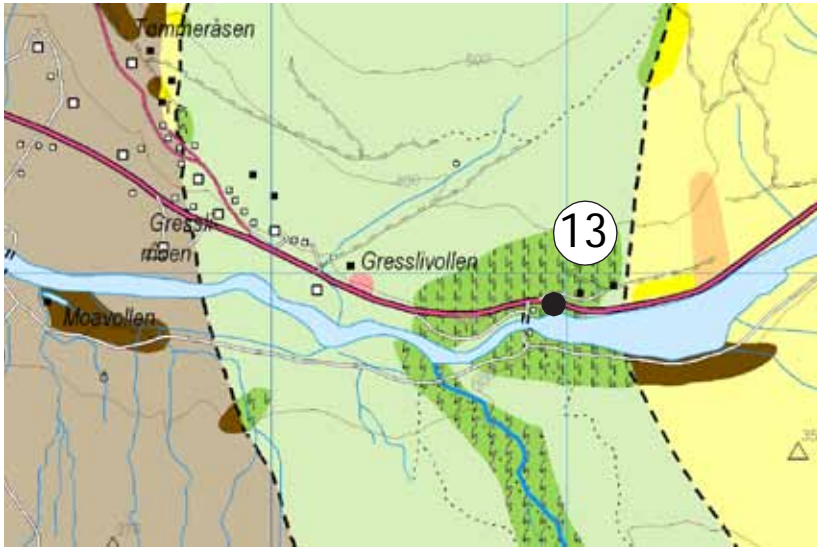


Fig.44. Location of Stop 13.

3.16.3. Description

Modal layering in metagabbro strikes north-south and dips $\sim 25^\circ$ W just to west of a track with a telegraph pole. The layering is dragged into a shear zone to the west (Fig.45). Within the shear zone the layered metagabbros have been transformed into foliated amphibolites with veins and patches of hornblende-bearing tonalitic and granitic pegmatites.

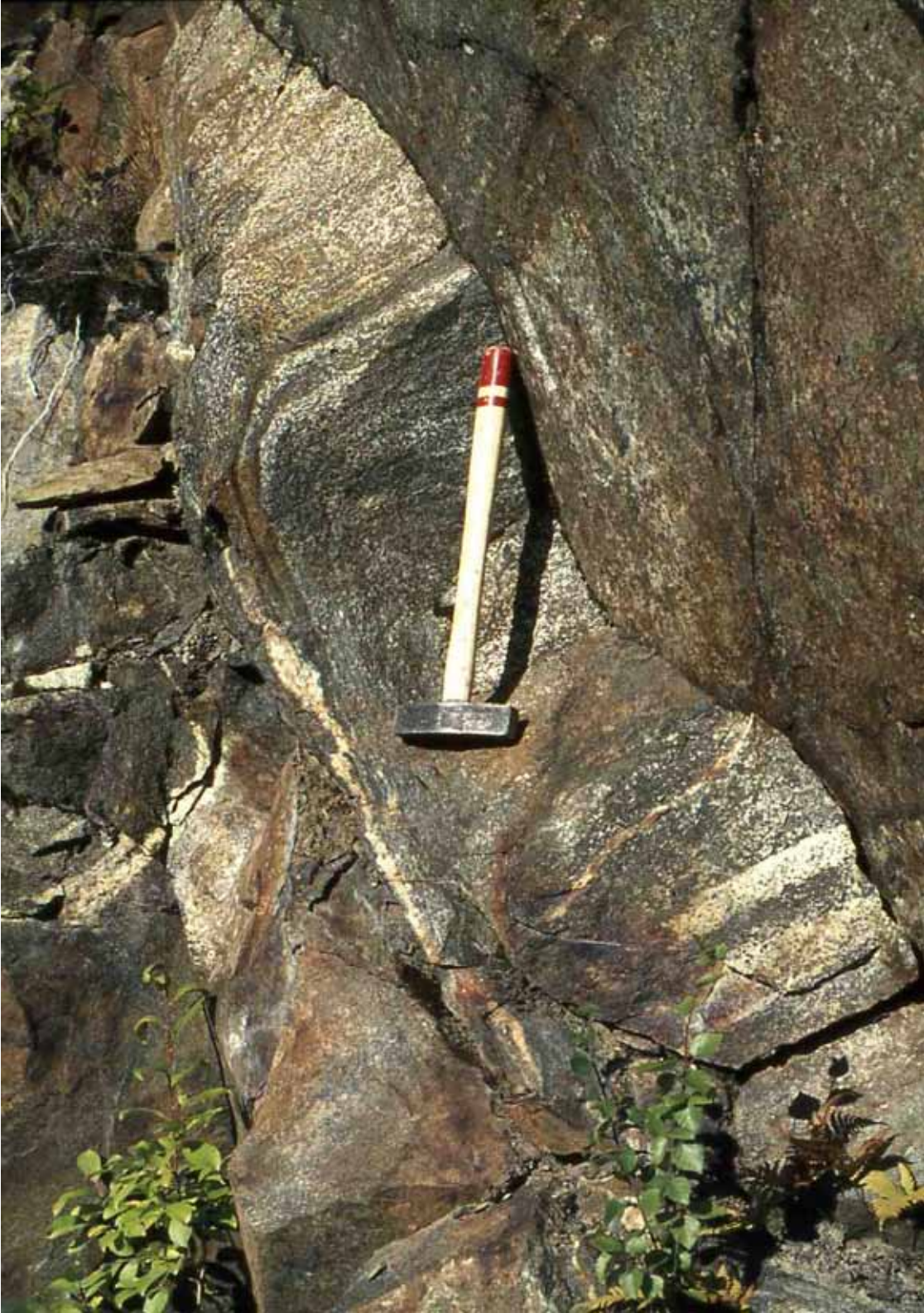


Fig.45. Layered metagabbro on the right is dragged into a shear zone at Stop 13. Within the shear zone the rocks are foliated amphibolites with tonalitic and granitic veins.



Fig.46. Foliated amphibolite at Stop 13 cut by tonalitic and granitic veins, some of which are pegmatitic. The arrowhead is in a near-vertical fine-grained felsic dyke that cuts across all other lithologies. The hammer shaft to the left of the arrowhead is 40 cm long.

Some 150 m to the east along the road a large outcrop (Fig.46) exposes unfoliated (Fig.47) and foliated amphibolites (Fig.48). Some faint remnants of modal layering are locally preserved, but it is far from obvious that these rocks were originally layered gabbros. Some of the finer grained portions may originally have been metabasaltic inclusions. There are numerous veins of undeformed and deformed hornblende-bearing pegmatites. The foliated amphibolites are cut by several 30-80 cm wide, very fine-grained, felsic (trondhjemitic) dykes (Fig.46).

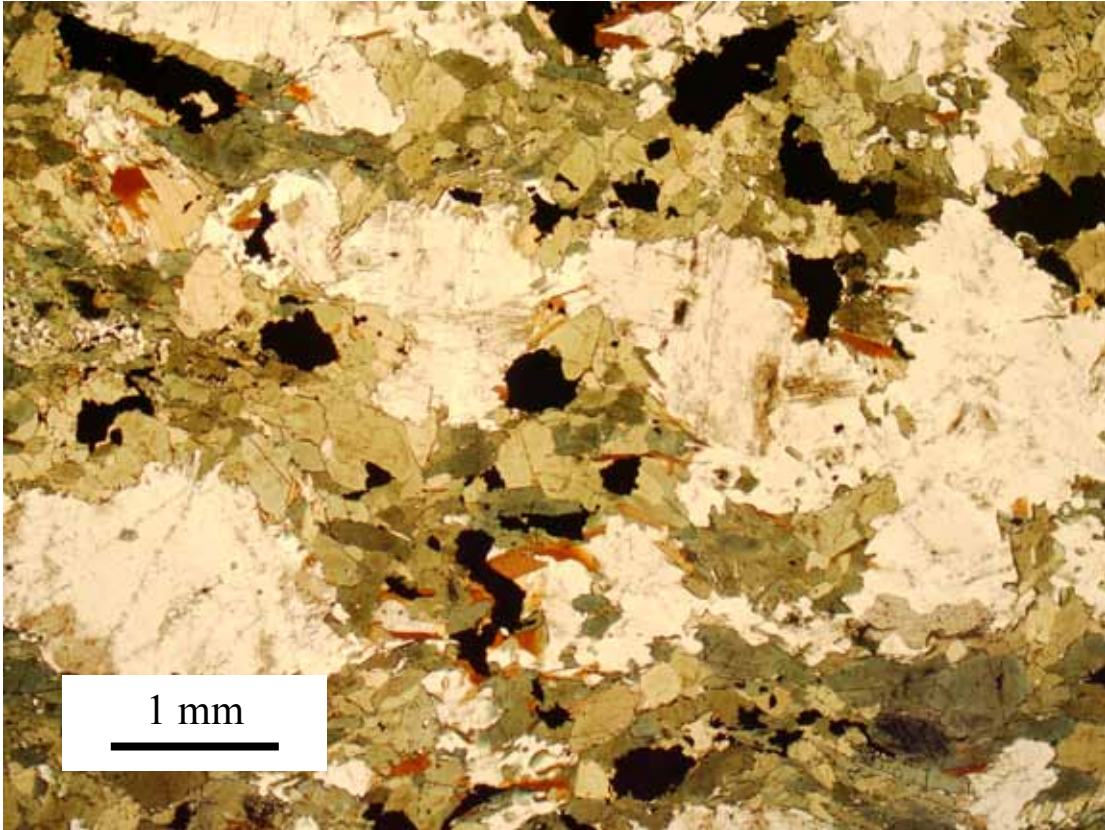


Fig.47. Microphotograph of amphibolite from Stop 13 (Fig.46). Original igneous plagioclases retain some of their integrity whereas the mafic minerals now consist of green hornblende, ilmenite and minor biotite. PPL. (FH07-6a).

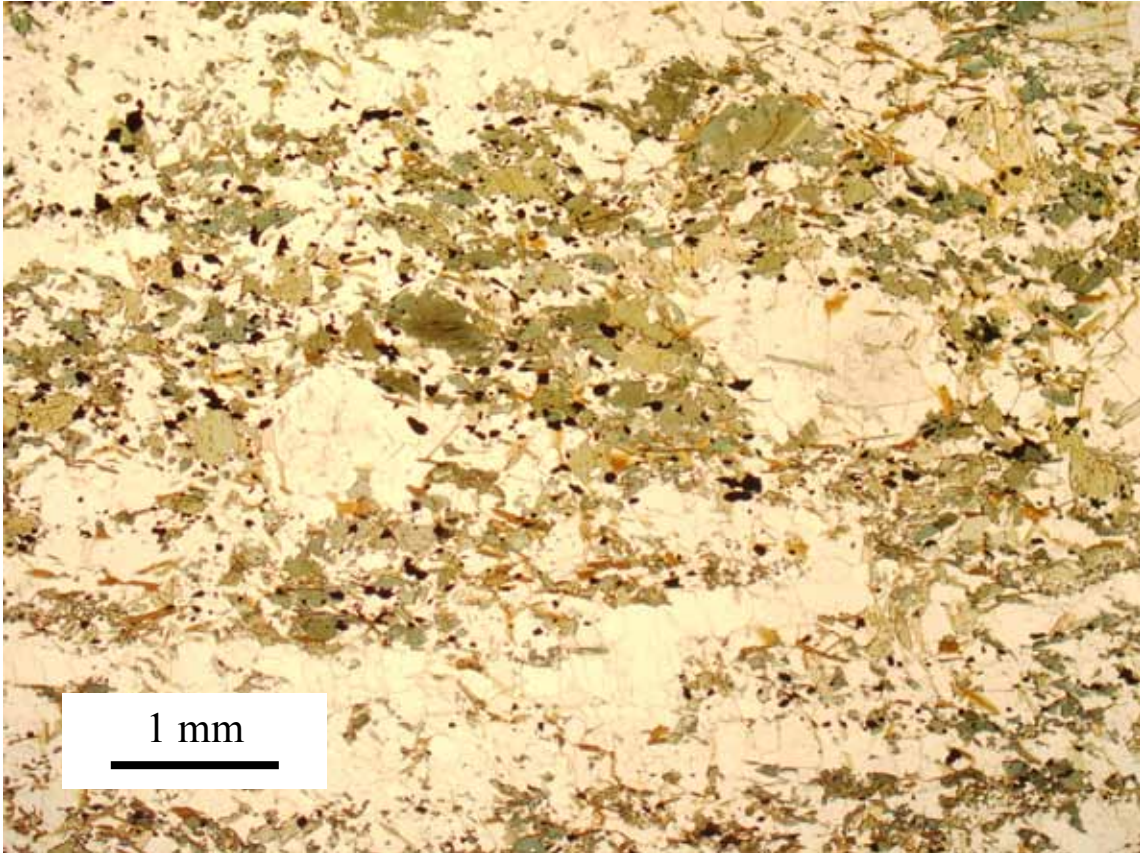


Fig.48. Microphotograph of foliated amphibolite from the outcrop shown in Fig.47 at Stop 13. The texture is much finer grained than in Fig.47 and the foliation (E-W in the picture) is obvious. The mineral assemblage is the same as that in Fig.47. PPL. (FH07-6b).

3.16.4. Significance of the outcrops

We are within the narrowest part of the FHI (Enclosure 1) where deformation and amphibolite facies metamorphism are most extensively developed. In a regional context, modal layering in this part of the intrusion strikes ~NS and youngs to the east. This is not consistent with observations at this locality. Large blocks of layered rocks have been rotated during deformation and the formation of large shear zones.

The broadly granitic pegmatites are a product of partial melting during upper amphibolite facies metamorphism (possibly accompanied by metasomatism involving K-rich fluids). Several fine grained felsic (trondhjemitic) dykes cut the FHI, most significantly in the Melshogna area (Enclosure 1) where they weather out and form linear clefts in the landscape. They are younger than the deformation and metamorphism and are genetically unrelated to the FHI.

3.17. Stop 14: Gresslivola

3.17.1. Location

Coordinates: 0625169 699744. Tydal 1:50000 map.

3.17.2. Introduction

This series of exposures is within one of the most strongly deformed and metamorphosed parts of the intrusion.

3.17.3. Description

The outcrops in the Gresslivola area consist of grey metagabbro and foliated amphibolite. Near the summit of Gresslivola (Fig.49) the original igneous texture can still be recognised in the metagabbros, despite extensive metamorphism of the mafic minerals to amphiboles. Corona textures are commonly developed where original cumulus orthopyroxene grains have been replaced by cummingtonite which is surrounded by dark green to black hornblende (Fig.50). In the foliated amphibolites the igneous texture has generally been entirely obliterated. Sporadically preserved modal layering is close to vertical in the metagabbros, roughly parallel to the superimposed foliation. There are many quartz veins and small granitic pegmatites. There are local exposures of cm-thick dark brown layers that strike ~north-south. These are olivine-rich layers, now largely altered to serpentine, that belong to the lower part of Stage IV (Fig.51).

The southern slopes of Melshogna dominate the view to the north from the summit of Gresslivola. The western country rock contact is close to the tree line. The Melshogna sequence, now dominantly metagabbros and foliated amphibolites, youngs to the east. Several large sheets of granitic pegmatite form the light-coloured outcrops. A notably straight, ~2 m-wide, ~NE-striking depression can be followed for several kilometres towards the summit of Ruten (Enclosure 1); this is the course of a felsic dyke of fine-grained trondhjemite. Several of these dykes cut the FHI, but they are most common in the Melshogna area. They are notoriously poorly exposed and generally weather out to form gullies in the landscape.

3.17.4. Significance of the outcrops

The narrowest, central part of the FHI is the most strongly deformed and metamorphosed section. It is important in that it links the Fongen Series in the north with the Hyllingen Series to the south (Fig.12 and Enclosure 1). While the deformation and metamorphism make direct correlation difficult in the field, the similarity in strike and dip of modal layering in the Fongen and Hyllingen Series, the concentration of country rock inclusions in the lower part of the layered sequence (Stage II) and, most importantly, the compositional reversal of Stage III in both the northern and southern parts, strongly favour the correlation shown in Fig.12 and Enclosure 1. The sporadic occurrence of ~north-south striking, metamorphosed olivine-rich layers in the eastern Gresslivola area, that resemble those in the lower part of Stage IV in the Ruten area (Enclosure 1), support this correlation.

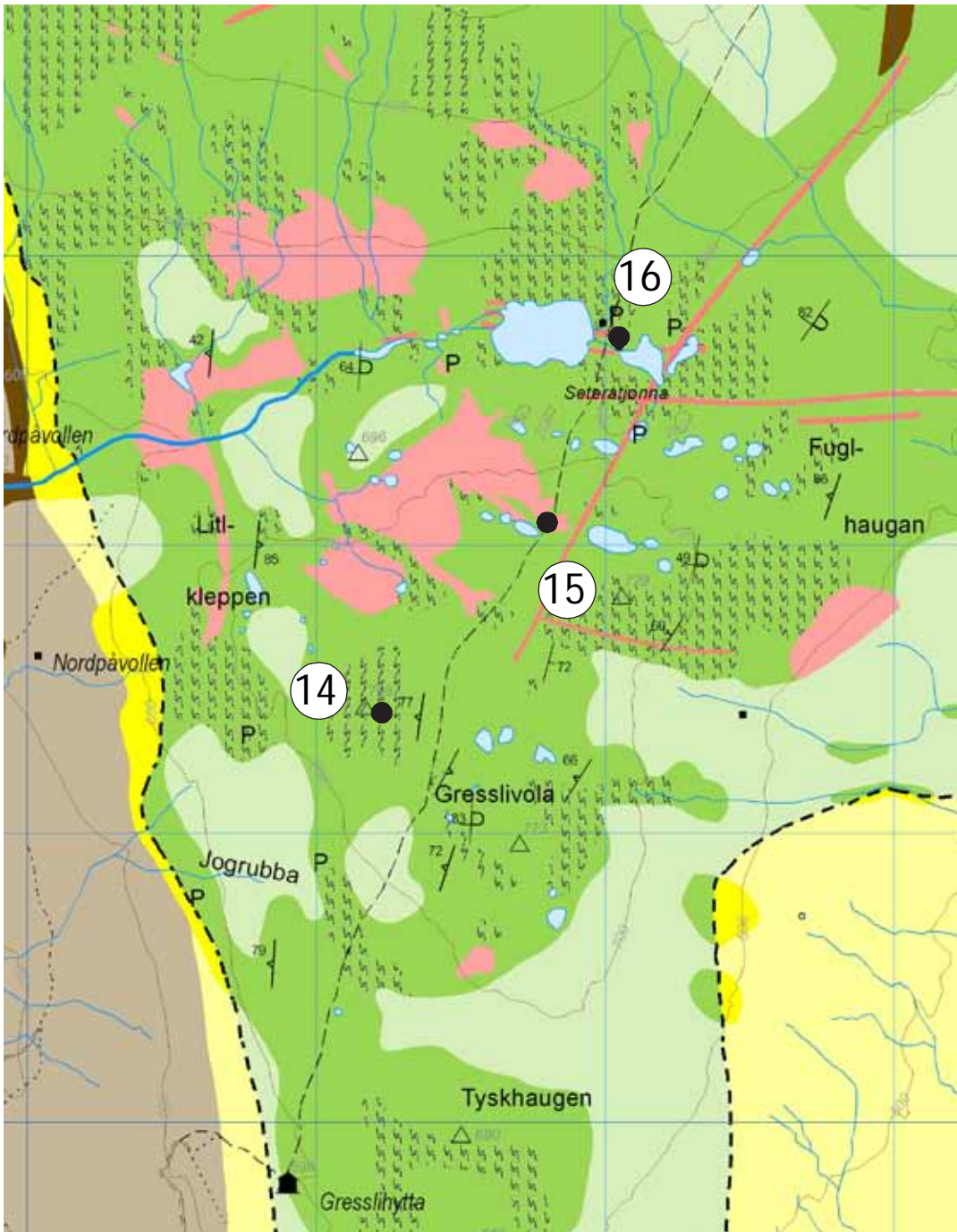


Fig.49. Locations of Stops 14 to 16 in the Gresslivola area. This map has been extracted from Enclosure 1.



Fig.50. Microphotographs of cummingtonite metagabbro in plane polarised light (above) and cross-polarised light (below). (Sample FH07-7 from the Gresslivola area).



Fig.51. Serpentinised, brownish, olivine-rich layer (to right of hammer) in grey metagabbro striking towards the summit of Melshogna to the north. The olivine-rich layer has been slightly offset by a minor fault.

3.18. Stop 15: NNE of Gresslivola

3.18.1. Location

Coordinates: 0625784 6998147. Tydal 1:50000 map.

The path with red-painted markers goes from the Trondheim Turistforening hut at Gressli (Gresslihytta; Figs.12 & 49)) to Schulzhytta, ~15 km to the north.

3.18.2. Introduction

Large bodies of granitic pegmatite form dominant features here. They are exclusively associated with the more strongly metamorphosed and deformed parts of the intrusion.

3.18.3. Description

At Stop 15 the path crosses the eastern end of a large, flat-lying sheet of granitic pegmatite. This pegmatite is dominated by white alkali feldspar and quartz with many thin, randomly orientated flakes of biotite (Fig.52). These flakes can be up to 20 cm long, but are usually in the range of 1-5 cm. Tourmaline and garnet are sporadically developed accessory phases. The pegmatitic body to which this outcrop belongs forms extensive, white, smooth rock surfaces to the west and northwest. This irregularly shaped body

covers an area of $\sim 250 \text{ m}^2$ and is one of several large granitic pegmatite sheets in the vicinity.



Fig.52. Stop 15. Granitic pegmatite with large, thin flakes of biotite.

3.18.4. Significance of the outcrops

Small veins of granitic pegmatite are developed locally throughout the layered intrusion, but large bodies, like those developed here, are restricted to the most strongly deformed and metamorphosed parts. The margins of these large pegmatites have locally been deformed in shear zones, but most outcrops retain a coarse-grained, pegmatitic texture with no evidence of recrystallization. They were therefore probably intruded during the waning stages of the extensive amphibolite facies metamorphism and associated deformation that affected parts of the layered intrusion. The source of the abundant SiO_2 and K_2O in these bodies is not obvious. The host gabbroic/dioritic rocks cannot produce much of these components. It seems likely that an external source of hydrothermal fluids was involved.

3.19. Stop 16: Sæteråtjørna

3.19.1. Location

Coordinates: 0626001 6998697. Tydal 1:50000 map.

3.19.2. Introduction

Well-exposed metagabbro and foliated amphibolite can be studied here.

3.19.3. Description

The outcrops in the area between the two lakes show the development of foliated amphibolite in shear zones (Fig.53). In most cases it is far from obvious that the gabbroic precursor was layered, but some blocks do preserve relict modal layering (Fig.54).



Fig.53. Stop 16. Foliated amphibolite within a shear zone. An agmatitic structure is developed in which blocks and streaks of grey amphibolite are separated by veins of tonalite and granite.

3.19.4. Significance of the outcrops

The outcrops indicate that the amphibolite facies metamorphism was accompanied by partial melting of the gabbroic/dioritic precursor to give the agmatitic structure. This required the addition of water to the system to give the hydrous conditions necessary for anatexis.



Fig.54. Stop 16. Relict modal layering is preserved in this block of metagabbro that is enclosed by strongly foliated felsic rocks.

3.20. Introduction to Stops 17 - 24

In the ground above ~1200 m there is a very high degree of exposure. Most of the area is covered by snow for many months of the year so that vegetation (including lichen) is generally very sparse. Many of the outcrops are truly excellent and illustrate important features in a very clear manner. The broad ridge northeast of Fongen is readily accessible. Good exposures are so abundant that it is superfluous to identify specific stops except where these are of special importance. In this area it is easy to become detached from a group as individuals may want to spend more time looking at a particular feature.

Stop 17 is in the inner part of the contact metamorphic aureole to FHI. Stops 18 - 24 are within the FHI. The features to be seen include a very impressive angular discordance (Stop 18) and a series of slump structures caused by the impact of large xenoliths on the magma chamber floor (Stop 19). Some of the metapelitic hornfels inclusions retain earlier features in the form of isoclinal folds. Modally layered olivine gabbros are superbly exposed in a gully at Stop 20 where detailed investigations of the layering have been performed. The section between Stops 21 and 22 is entirely within a huge metabasaltic inclusion. This metabasalt shows a wide variety of contact metamorphic features, including local recrystallisation to layered gabbros and evidence of partial melting. The view from the top of Fongen (1441 m) is excellent (Stop 22). A small “impact structure” is well exposed at Stop 23 on the descent. Stop 24 is at a well-exposed shear zone that

cross-cuts modally layered gabbros. These outcrops are accessible from the Trondheim Turistforening hut Ramsjøhytta (Fig.55).

3.21. Stop 17: Ramskar

3.21.1. Location

Coordinates: 0633705 7010141. Tydal 1:50000 map.

3.21.2. Introduction

Fongen mountain dominates the view to the west of lake Ramsjø (Fig.55). Ramskar is the name of the pass between the summits of Ramfjellet to the north and Fongen to the south. The path between the Trondheim Turist Forening (TTF) tourist huts Schulzhytta (to the west) and Ramsjøhytta (east) goes through the pass.

We are here in the inner part of the contact metamorphic aureole around the FHI. The rocks are dominantly metapelites which were folded and intruded by a swarm of basaltic dykes (many of which are plagioclase-phyric) prior to emplacement of the layered intrusion. Olesen et al. (1973) recognised cordierite, sillimanite and andalusite zones, all with additional almandine, in the contact aureole in this area. Regional metamorphism in amphibolite facies took place after intrusion of the FHI, but the rocks here have not been severely affected by this overprinting. Ramskar is one of the best locations to study the FHI contact aureole (Fig.56).



Fig.55. View of Fongen from the east across Ramsjø lake. The summit (1441 m) is ~5 km away. The Trondheim Turistforening tourist hut “Ramsjøhytta” is on the left. The pass “Ramskaret” is just off the photo to the right. Stops 18 – 23 are on the ridge to the right of the summit. Stop 22 is at the summit. The summit of Fongskaftet is behind the large hut to the left of Fongen. The overall ~20-30° southerly dip of the layering in this area can be discerned below Fongen summit.

3.21.3. Description

Proceeding northwest along the path from Ramsjøhytta the first outcrops in the Ramskar area are of folded metapelites that form rounded grey to brown outcrops. Garnet is generally present and whitish sillimanite prisms are locally visible. The metabasaltic dykes form angular, grey outcrops; some of them are plagioclase-phyric (Fig.57). Most of these dykes are several meters wide. Their mineralogy is difficult to determine in the field but here they contain contact metamorphic pyroxene in addition to hornblende and plagioclase. Approaching the layered intrusion (up hill to the south) the metapelites become brecciated and veined by anatectic granite where they have been subjected to partial melting.

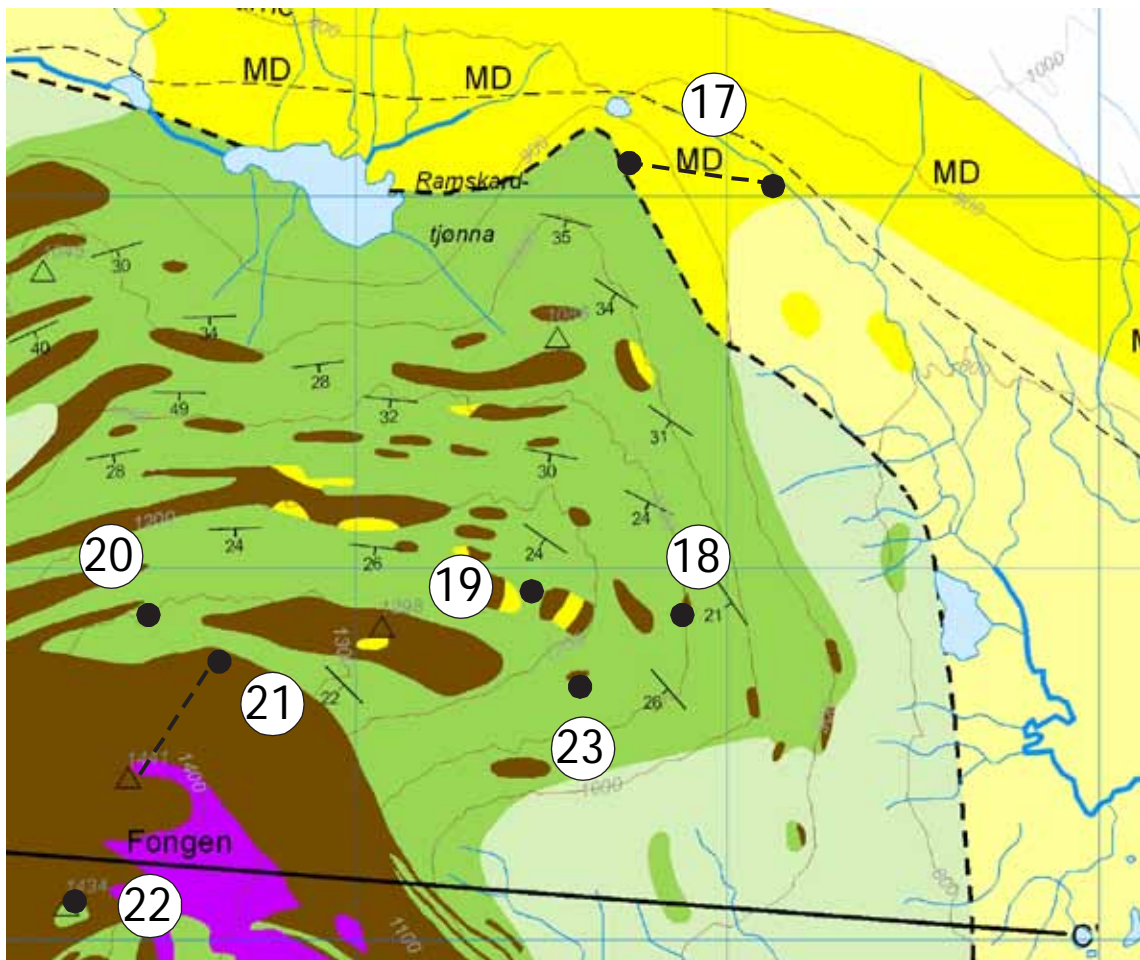


Fig.56. Locations of Stops 17 to 23.



Fig.57. Plagioclase-phyric metabasaltic dyke in the Ramskar area (Stop 17).

The contact between the metapelitic country rocks and marginal rocks of the FHI is located on the slope SW of the pass, but is not well exposed. There are isolated outcrops of metapelitic hornfels showing evidence of partial melting below outcrops of medium-grained diorite.



Fig.58. Brecciated metapelite hornfels with granitic veins from the inner contact metamorphic aureole at Stop 17.

3.21.4. Significance of the outcrops

Mineral assemblages in the contact metamorphic aureole provide information as to the depth of emplacement of the FHI. Olesen et al. (1973) suggested that emplacement took place at 5-6 kb, but since then the triple point in the Al_2SiO_5 system has been relocated in PT space (e.g. Bucher & Frey, 1994). The presence of a wide andalusite contact metamorphic zone implies that this mineral formed well within its stability field i.e. below 4 kb (Fig.59). We now believe that contact metamorphism took place at ~3.5 kb, implying a depth of intrusion of 11-12 km. Subsequent regional overprinting in amphibolite facies involved a pressure increase (kyanite is developed in metapelites; Olesen et al., 1973) and, as described elsewhere (Stop 5), later low grade metamorphism is also recorded locally.

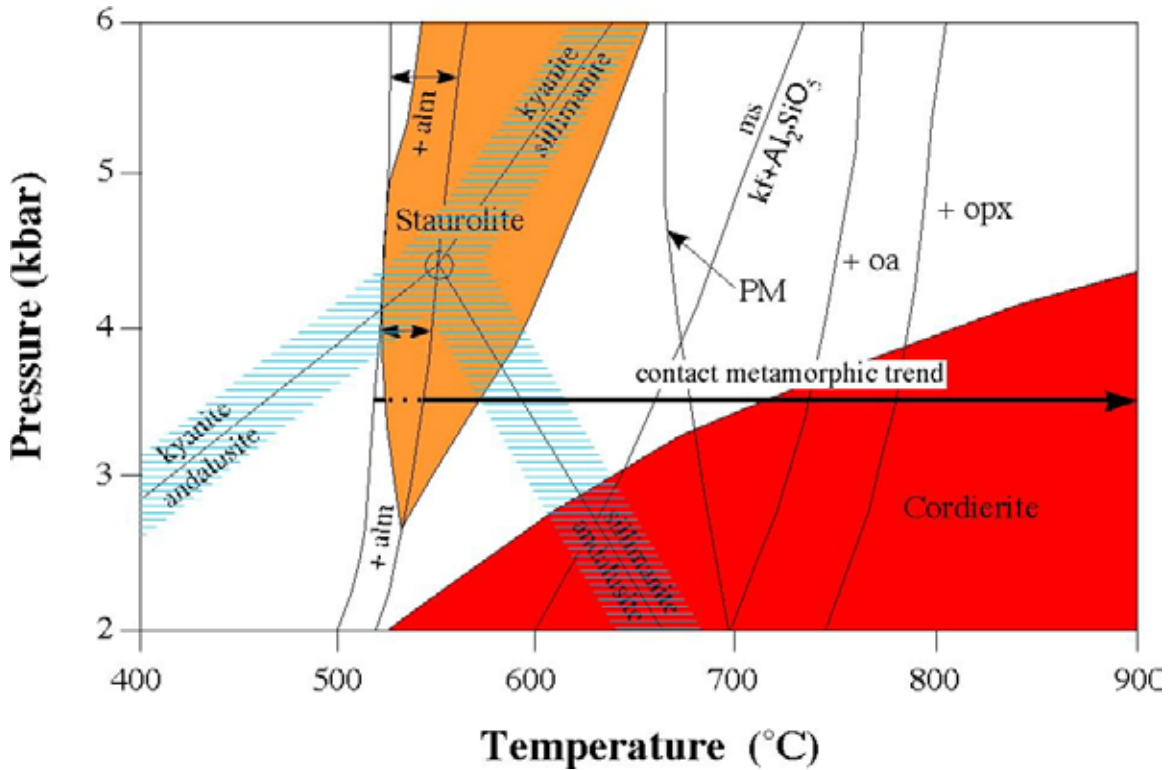


Fig.59. PT diagram for contact metamorphism in metapelites around the Fongen-Hyllingen layered intrusion. The Al_2SiO_5 phase boundaries (with some degree of uncertainty in blue lines), first occurrence of almandine (+ alm; by a variety of mineral reactions), staurolite stability field, first occurrence of orthoclase (kf) (by the reaction muscovite = K-feldspar + Al_2SiO_5) and the onset of partial melting (PM) are from fig.7.8 in Bucher & Frey (1994). The cordierite stability field has been expanded towards higher pressures than shown in fig.8 in Bucher & Frey (1994) as would be appropriate for slightly more magnesian compositions than used by these authors. The + oa (= orthoamphibole-in) and + opx (orthopyroxene-in) curves have been moved to temperatures intermediate between those shown in figs.7.8 and 7.13 in Bucher & Frey (1994). The contact metamorphism took place below ~4 kb because of the presence of a wide andalusite zone, but the lower limit is hard to constrain. A pressure of 3.5 ± 0.5 kb seems a reasonable estimate. It must be borne in mind that the FHI has a thickness of ~6 km.

3.22. Stop 18: Angular discordance

3.22.1. Location

Coordinates: 633838 7008731 Tydal 1:50000 map.

3.22.2. Introduction

This locality exposes a superb angular discordance in layered metagabbro (Fig.60). This is strong evidence for the erosive action of magmatic currents.

3.22.3. Description

The rocks here are two pyroxene gabbros which have been overprinted by amphibolite facies metamorphism but have retained their igneous texture. Modal layering strikes $\sim 110^\circ$ and dips $25\text{-}30^\circ\text{N}$. Many of the layers below the unconformity show modal grading, with relatively sharp, mafic-rich bases and gradually increasing proportions of plagioclase upwards. There are several “load” structures at the boundaries between plagioclase-rich and mafic-rich layers (Fig.61). The angular discordance wedges out a thickness of several meters of layered rocks. The apparent angle of discordance is up to $\sim 20^\circ$, reducing to a true angle of $\sim 10^\circ$. Mineral compositions above and below the discordance are indistinguishable. We have not been able to trace this feature along strike in either direction.



Fig.60. Angular unconformity in layered metagabbro at Stop 18. Up is to the left.



Fig.61. Load features at the top of a plagioclase-rich layer just below the unconformity in Fig.60. Up is to the left.

3.22.4. Significance of the outcrop

It is difficult to envisage a process that does not involve mechanical erosion to remove the missing layers. It seems likely that magmatic currents scoured down into partially consolidated layered cumulates. Material was removed as single crystals or possibly also as rock fragments. The more or less planar, eroded surface subsequently became the crystallisation front and crystallisation resumed shortly thereafter.

There are several unanswered questions in connection with such a process.

- a) What caused the current activity?
- b) What happened to the removed material?

The current activity could have been initiated by an earthquake or by the impact of a large xenolith of roof rocks on the magma chamber floor. We will see other evidence of the latter process elsewhere.

It seems unlikely that the magma responsible for removing the material was able to dissolve it, since the rocks above and below are mineralogically and compositionally identical (i.e. had the same parental magma composition). It seems most likely that the removed material was deposited elsewhere when the current activity waned. We have not, however, been able to unequivocally identify such material in the cumulates.

3.23. Stop 19: Fongen: the eastern ridge

3.23.1. Location

Coordinates: 0633777 7008865 to 0633095 7008836. Tydal 1:50.000 map.

3.23.2. Introduction

There are many interesting features on this ridge east of Fongen mountain where exposures are excellent. Individual localities have not been selected because the choice is overwhelming.

3.23.3. Description

The main features to be observed are:

- a) Strongly disturbed modal layering (Figs.62 & 63).
- b) Inclusions of metabasaltic hornfels, both aphyric and plagioclase-phyric. Brown olivine porphyroblasts are common (Fig.64). Relict basaltic dykes, whose chilled margins have survived the contact metamorphism, can be found (Fig.65).
- c) Inclusions of metapelitic hornfels show isoclinal folding (Fig.66). The metapelites weather to a pale-grey colour with dark bands and streaks showing the folded nature of the original bedding.
- d) The country rock inclusions here are up to several tens of meters across. Individual inclusions consist of mixed lithologies.



Fig.62. Strongly disturbed modal layering caused by the impact of a large inclusion on the magma chamber floor.



Fig.63. Modal layering truncated by disturbed layered rocks. This is again caused by the impact on the floor of an inclusion falling from the roof.



Fig.64. Metabasaltic hornfels inclusion with dendritic olivine porphyroblasts. The olivines are altered to amphibole along a vein just above the pen.



Fig.65. Chilled contact between a basaltic dyke (left) and metabasalt in an inclusion. Both are now in pyroxene hornfels facies.



Fig.66. Fold structures in an inclusion of metapelitic hornfels. The light layers consist largely of plagioclase and quartz and the dark layers of orthopyroxene and green spinel.

3.23.4. Significance of the outcrops

The dramatic slump structures shown by the modal layering in this area were caused by the impact of large roof xenoliths on the crystallisation front. The lithologies of the inclusions (metapelites and metabasalts) match those of the country rocks. It is very clear that the metapelites were folded before they became contact metamorphosed, so that emplacement of the Fongen-Hyllingen magma chamber took place after at least one major fold phase. We are here in Stage II of the layered intrusion. This is characterised by numerous inclusions, many which are raft-like. Mineral compositions are fairly constant through considerable thickness of cumulates. This is believed to reflect that crystallisation took place during magma influx i.e. during magma chamber expansion. The rate of influx more or less more or less balanced with the rate of crystallisation. The new magma was emplaced at the base of the saucer-shaped chamber and elevated the resident magma column.

3.24. Stop 20: Modal layering profile

3.24.1. Location

Coordinates: 0632454 708816. Tydal 1:50.000 map.

3.24.2. Introduction

This is a superb section through modally layered cumulates (Fig.67). The dominant brownish weathering colour reflects the fact that there is only minor metamorphic overprinting.

3.24.3. Description

A 6.5 m-thick profile through this layered sequence has been studied in detail by Josephsen (2003); most of the description below has been taken from this thesis. A total of 73 layers have been identified whose thickness varies from 1-38 cm with an average thickness of 9.3 cm (Fig.68). Layer boundaries are macroscopically sharp. Individual layers can be followed for up to 100 m along strike. About 59% of the layers appear to be macroscopically isomodal; the remainder are modally graded. There are ~30% “inversely-graded” layers (with plagioclase-rich bases and mafic-rich tops) and ~11% “normally-graded” layers (with mafic-rich bases and plagioclase-rich tops). Inverse grading is therefore three times more common than normal grading. 7 of the 8 normally graded layers lie below an isomodal layer. 15 of the 22 inversely graded layers occur in reversely graded sequences with 3 consecutive inversely graded layers. The grain-size is usually in the range 1-3 mm. No size grading has been noted but the grain size can vary considerably from layer to layer. Plagioclase-rich layers are generally the coarsest as a result of post-magmatic recrystallisation. Modal lamination (dominantly shown by plagioclase, but locally also by Ca-rich pyroxene) is generally moderately well developed. No lineation has been observed.



Fig.67. The modally layered sequence at Stop 20 has been studied in detail by Josephsen (2003). The section in Fig.68 is marked.

A total of 73 thin sections have been studied from 48 samples, some of which cover more than one layer. The thin sections were cut normal to the layering. Modal compositions were determined by point counting ~1000 points per thin section. Olivine, plagioclase, Ca-rich pyroxene, Ca-poor pyroxene and magnetite occur as cumulus phases whereas brown hornblende has intercumulus status. Modal compositions vary enormously through the profile, from ultramafic to anorthositic. The bulk weighted modal composition of the entire profile in volume percent is plagioclase 57%, pyroxenes 27%, FeTi-oxide 11%, olivine 3% and Ca-amphibole 2%. It was not possible to reliably distinguish between the two pyroxenes in many samples, but it is clear that Ca-rich pyroxene dominates over Ca-poor pyroxene. We estimate that there is (in the bulk composition) ~20% Ca-rich and ~7% Ca-poor pyroxene. These modal estimates are supported by CIPW normative compositions of some whole rocks from the profile.

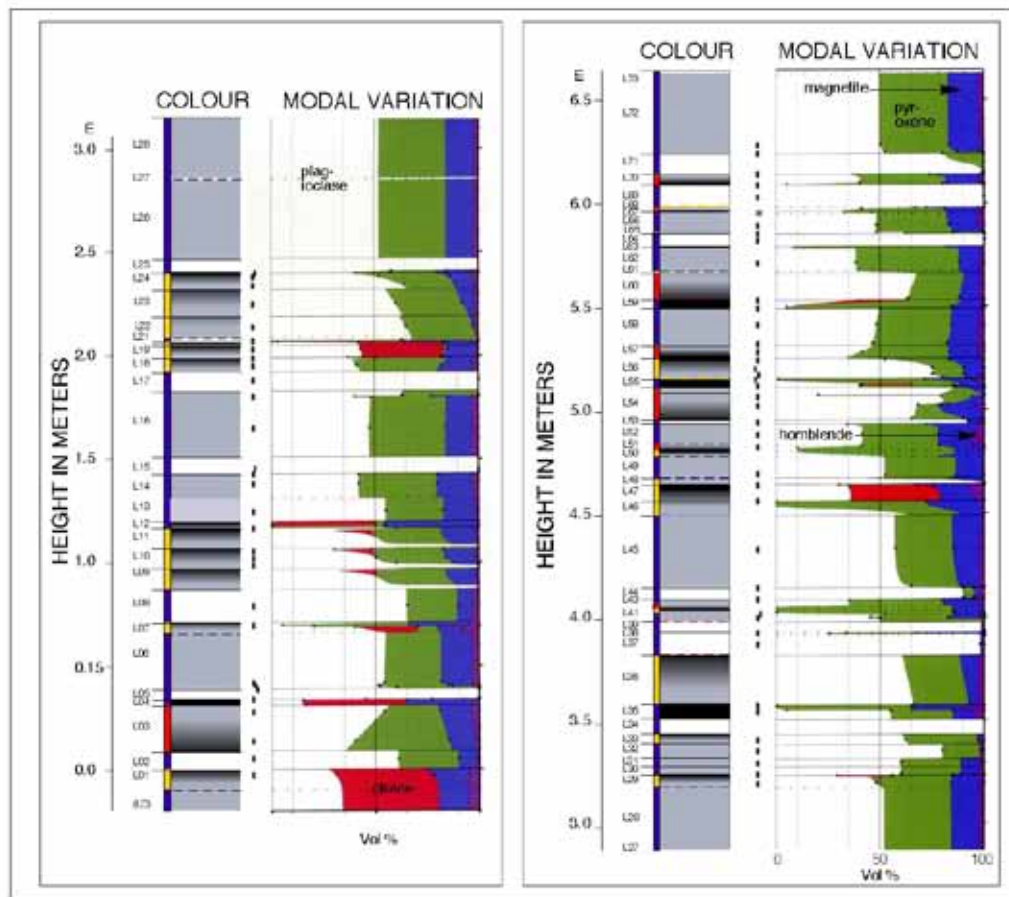


Fig.68. Detailed stratigraphic log through a 6.5 m-thick profile normal to the layering at Stop 20. The lower ~3 m of the profile are on the left and the upper ~3.5 m on the right. From left to right: Stratigraphic height relative to the top of a striking olivine-rich layer (Fig.67); layer number (L1-L73); indication of the type of layer – isomodal (blue), normally graded (red) or inversely graded (yellow); illustration of the lithological variation of the profile in grey tones; location of thin sections for point counting; modal variation.

Mineral compositions are fairly constant throughout the profile. Average compositions (based on 3 core analyses in each of 3 grains in each of 15 selected samples) are as follows: olivine Fo₅₁₋₄₈, plagioclase An_{50.5-47.5}, Ca-rich pyroxene Mg_#_{cpx65.5-63.5}, Ca-poor pyroxene Mg_#_{opx59.5-58}. There are no significant compositional jumps or breaks in the profile.

It is interesting to plot the relative proportions of plagioclase, Ca-rich pyroxene and olivine in the bulk composition for the 6.8 m-thick profile (71:25:4) in the Fo-An-Di phase diagram (Fig.69). It has a much more plagioclase-rich composition than the An-Di cotectic for 1 atm. This phase diagram is, however, for high-temperature end-member

mineral compositions under dry conditions at low pressure. The point at which plagioclase, olivine and Ca-rich pyroxene crystallised together in equilibrium must have been close to the bulk composition. The bulk compositions for smaller intervals ($1/2$, $1/4$, $1/8$, $1/16$) of the profile have also been plotted. It emerges that the bulk compositions of both $1/2$ and $1/4$ of the profile lie quite close to the total bulk, whereas intervals thinner than this begin to scatter rather widely. This implies that the process responsible for the formation of the layering in this profile returned to its starting point after ~ 2 m (rounded up from 1.6 m representing $1/4$ of profile) of layered cumulates had formed. This in turn implies that the layer-forming mechanism was, over the long term, essentially a constant process that oscillated over a frequency during which ~ 2 m of cumulates crystallised. This conclusion may not, of course, be valid for the entire Fongen-Hyllingen intrusion but provides a valuable estimate.

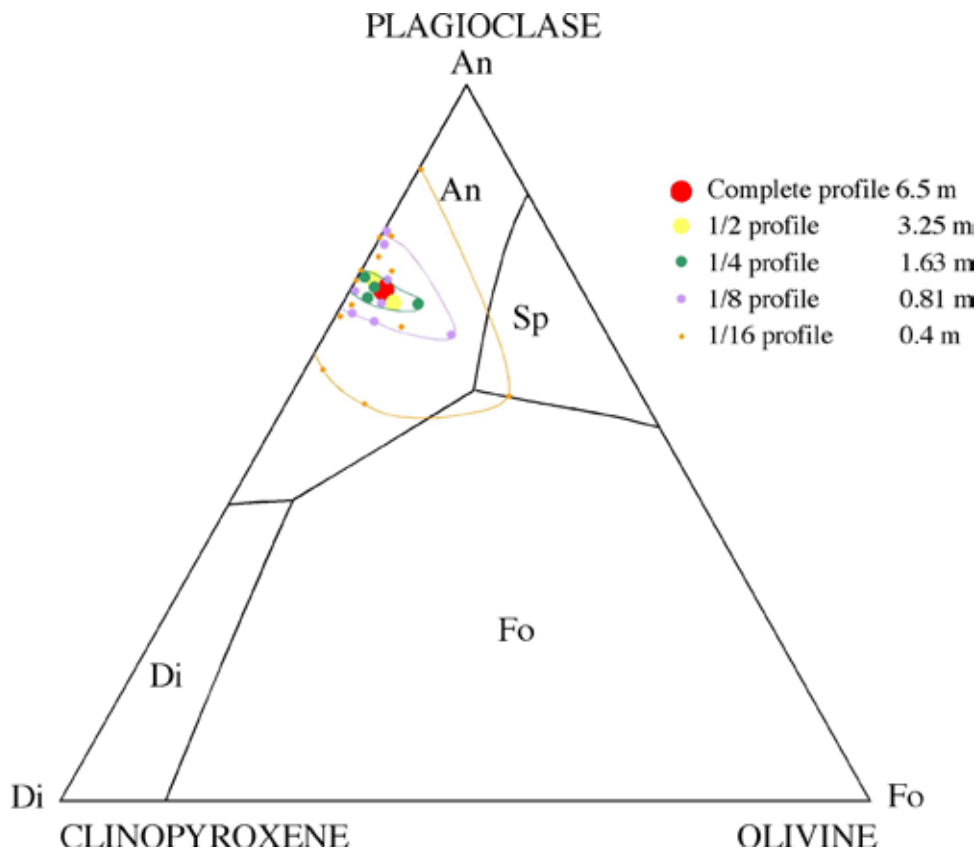


Fig.69. Fo-An-Di phase diagram at 1 atmosphere from Morse (1980). The bulk modal compositions of different intervals are plotted together with some relevant contours.

3.24.4. Significance of the outcrops

As has been discussed elsewhere, the discordant relations between modal and cryptic layering in the Hyllingen Series imply that crystallisation took place *in situ*. The most likely process is oscillatory nucleation in slightly undercooled (or slightly supersaturated) magma, as described by Maaløe (1978). Results from this profile suggest that this

oscillation returned to its starting point after ~2 m of cumulates had crystallised on the magma chamber floor. Any ~2 m thick interval in Fig.67 contains, on average, ~22 layers that vary in composition from anorthositic to ultramafic. The oscillatory process that formed the layers does not, on first sight of the outcrop, appear to be systematic, but this study reveals that the overall sequence is repeated after a thickness of ~2 m of modally layered rocks had crystallised.

3.25. Stop 21: The “summit inclusion”

3.25.1. Location

Coordinates: 0632704 7008758 to top of Fongen mountain. Tydal 1:50.000 map.

3.25.2. Introduction

This is a section up through a huge metabasaltic inclusion - the summit inclusion. The section starts at the base of the inclusion and proceeds to its upper boundary near the top of the mountain. It has a thickness of ~160 m in this section through which there are many textural varieties developed as a result of contact metamorphism. Most of the material presented below is taken from Holm (2003).

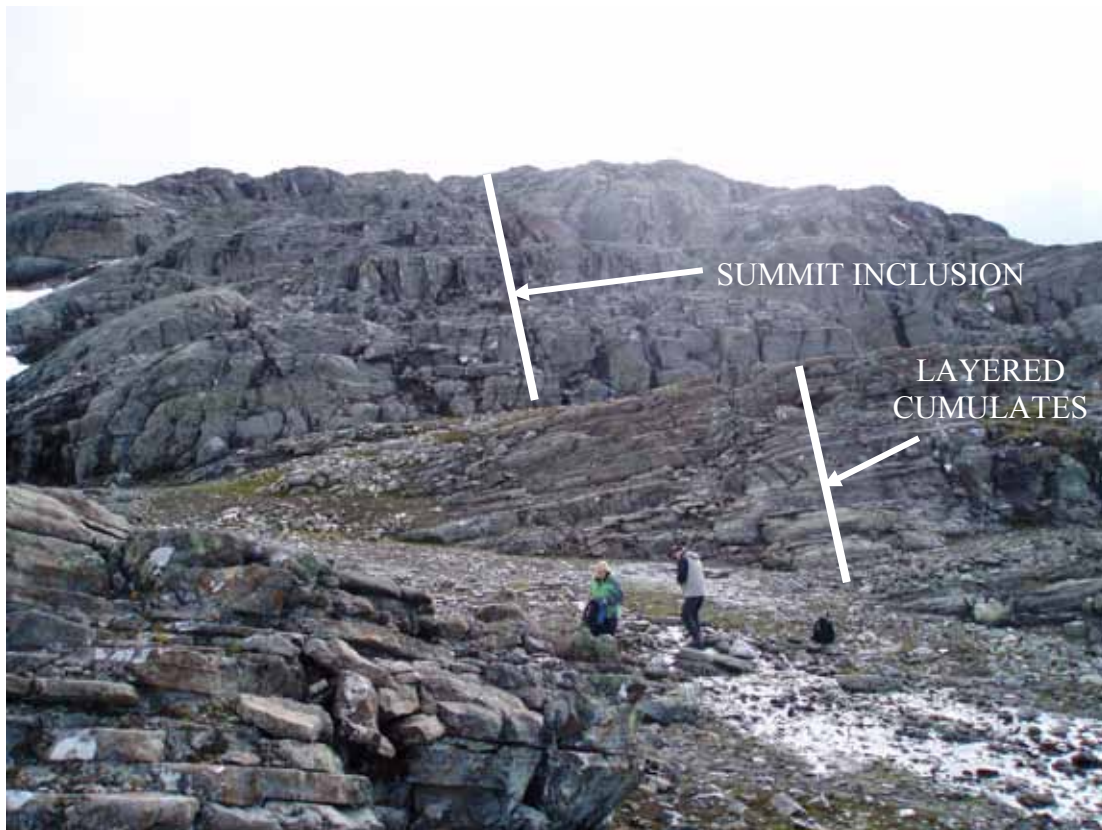


Fig.70. The basal contact of the summit inclusion is concordant with modal layering in the underlying cumulates. Stop 21.

3.25.3. Description

The basal contact of the summit inclusion (0632704 7008758) at ~1280 m above sea level is concordant with modal layering in the underlying gabbros (Figs.70 & 71). It continues to the top of the mountain at ~1440 m. The summit inclusion develops a wide variety of textural types (Fig.72).

- (a) Homogeneous metabasalt consists of granular metabasaltic pyroxene hornfels (plagioclase + Ca-rich pyroxene + Ca-poor pyroxene \pm Ca-amphibole \pm olivine \pm FeTi-oxide).
- (b) Homogeneous metabasalt with ultramafic segregations.
- (c) Metabasalt with diffuse, laterally impersistent modal layering. Locally with ultramafic segregations.



Fig.71. Stop 21. Modally layered cumulates to the left are overlain concordantly by the summit inclusion.

- (d) Layered metabasalt with some hornblende-rich layers, coarse-grained gabbroic patches and ultramafic segregations.
- (e) Metabasalt with gabbroic streaks, locally with ultramafic segregations (Fig.73).
- (f) Medium- to coarse-grained modally layered metabasalt (i.e. layered gabbro) (Fig.74).
- (g) “Globular” metabasalt with rounded blocks of granular metabasalt in a gabbroic matrix (Fig.75).

This is not a strict subdivision. Some of the types grade into each other.

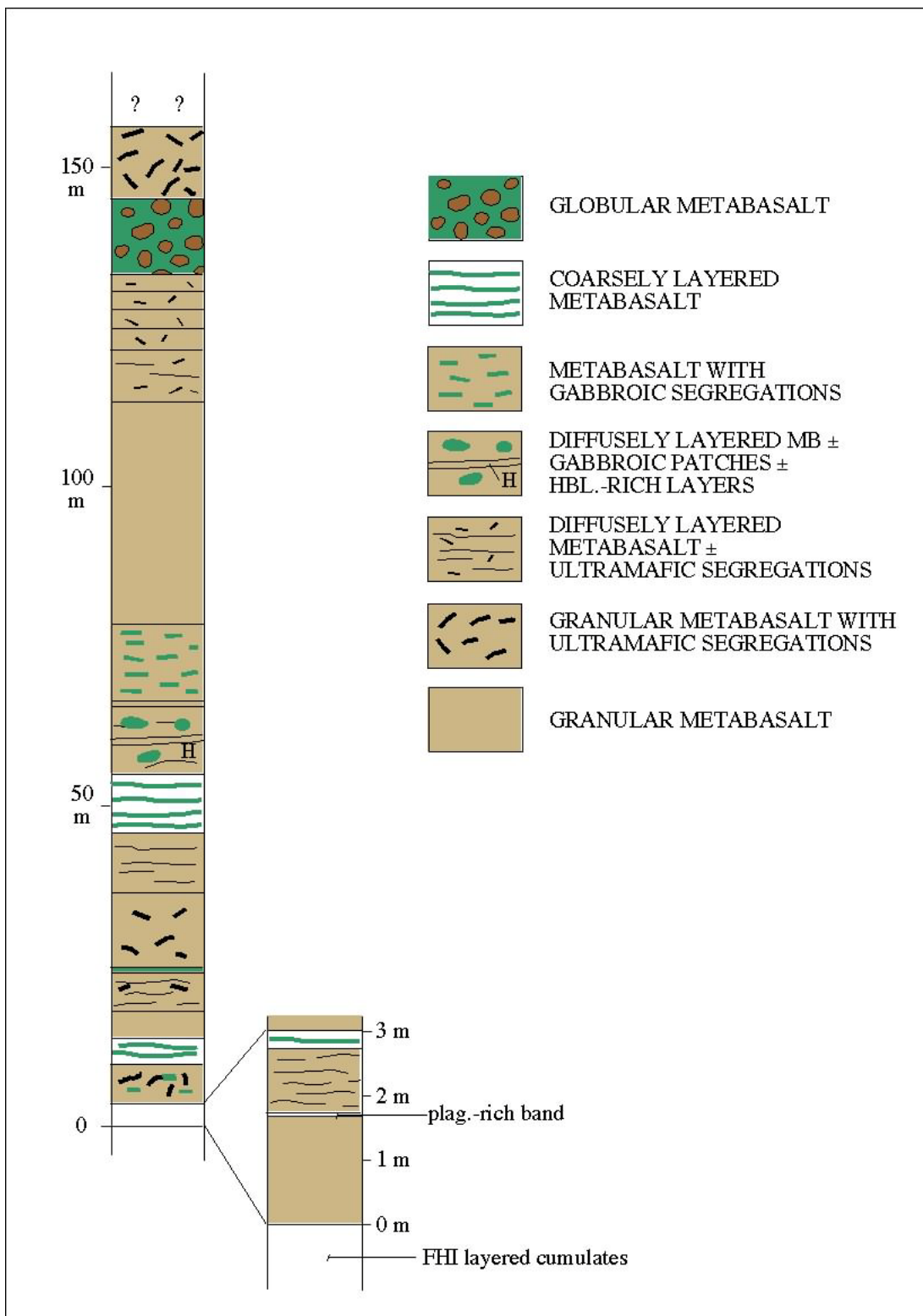


Fig.72. Vertical section through the summit inclusion.



Fig.73. Metabasaltic hornfels with gabbroic streaks in the summit inclusion.



Fig.74. Layered gabbroic interval in the summit inclusion.



Fig.75. Globular metabasaltic hornfels in a gabbroic matrix in the summit inclusion.

Some of the outcrops in this section are cut by numerous thin veins, along which the rock has been transformed to an amphibolite facies mineral assemblage. These veins have a greyish colour and stand out because they are more resistant to weathering than the enveloping rocks. Parts of the summit inclusion have been subjected to more pervasive amphibolite facies metamorphism.

We have studied the summit inclusion in an attempt to find evidence for the nature of the protolith (e.g. internal contacts between original lava flows; relict phenocrysts or amygdales; pillow structures) but have been unsuccessful. Any original features must have been erased by thorough recrystallisation during contact metamorphism.

There does not appear to be any systematic development of textural varieties with vertical height in the summit inclusion in Fig.72. Relatively homogeneous, granular metabasalt occurs near the base and in the middle of the inclusion; modally layered intervals occur from ~10-14 m above the base and in the lower central part (at ~47 - 55 m). Globular-textured metabasalt is restricted to the interval between 133 and 145 m.

Mineralogy and petrography

Thin section studies confirm the macroscopic impression that there is a continuum from fine-grained granoblastic basaltic hornfels textures (Fig.76) to coarse-grained gabbroic textures (Fig.77). Poikiloblasts enclosing granular matrix minerals are widely developed

in the granular metabasaltic hornfels and may consist of plagioclase, Ca-rich pyroxene, Ca-amphibole or olivine with a diameter up to 4 mm. The ultramafic segregations consist dominantly of two pyroxenes and FeTi-oxide. The most coarse-grained textures occur in plagioclase-rich or mafic-rich varieties in the modally layered intervals. Some plagioclase grains in the gabbroic rocks enclose a zone of small, granular pyroxene grains (Fig.78), and some clinopyroxenes enclose small, granular plagioclase grains (Fig.78). These are taken as evidence that the rock has passed through a granular texture and has subsequently almost completely recrystallised to a coarse-grained texture. Complete recrystallisation results in elimination of these relict textures. The globular-textured rocks have sharp boundaries between the fine-grained, granular spherical bodies and coarse-grained gabbro.

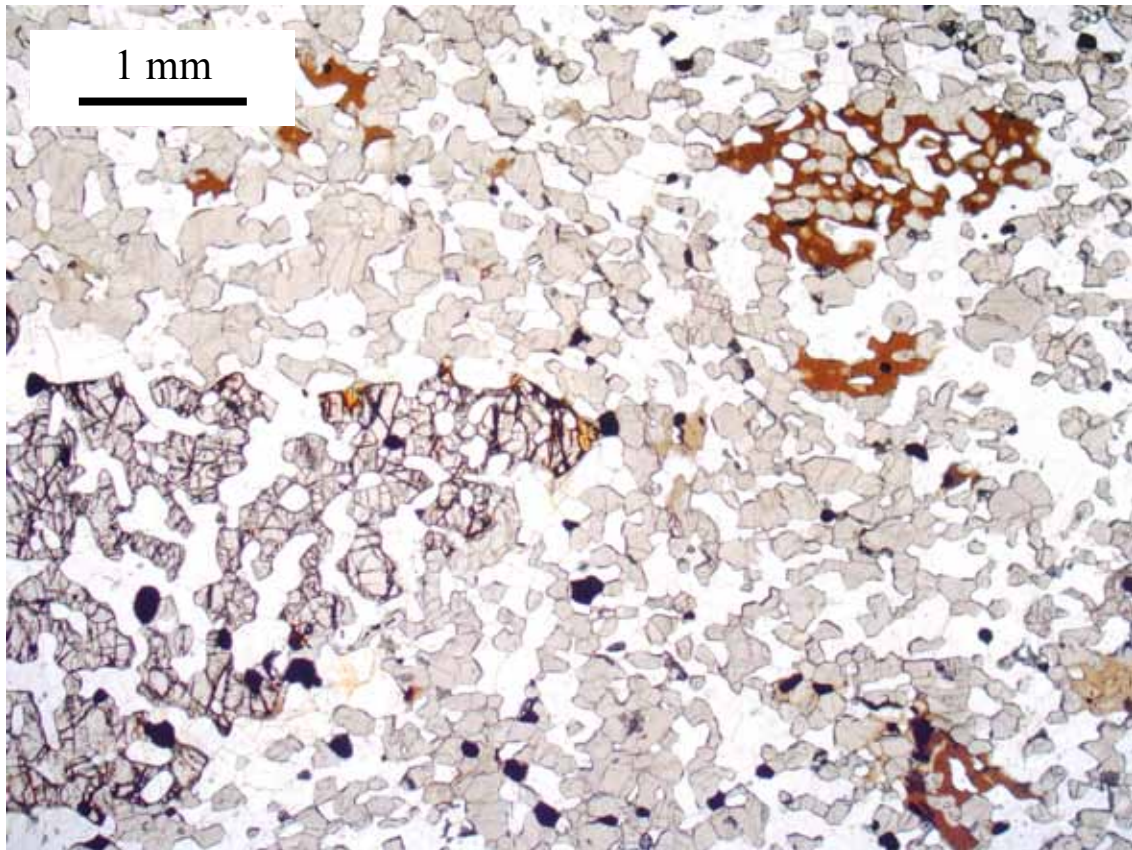


Fig.76. Granoblastic metabasaltic hornfels with porphyroblasts of olivine and brown hornblende.



Fig.77. Scans of thin sections (2 x 3.5 cm). Left: Contact between globular metabasaltic hornfels and gabbroic matrix. Sample from outcrop in Fig.75. Right: Metabasaltic hornfels with gabbroic streaks. Sample from outcrop in Fig.73.

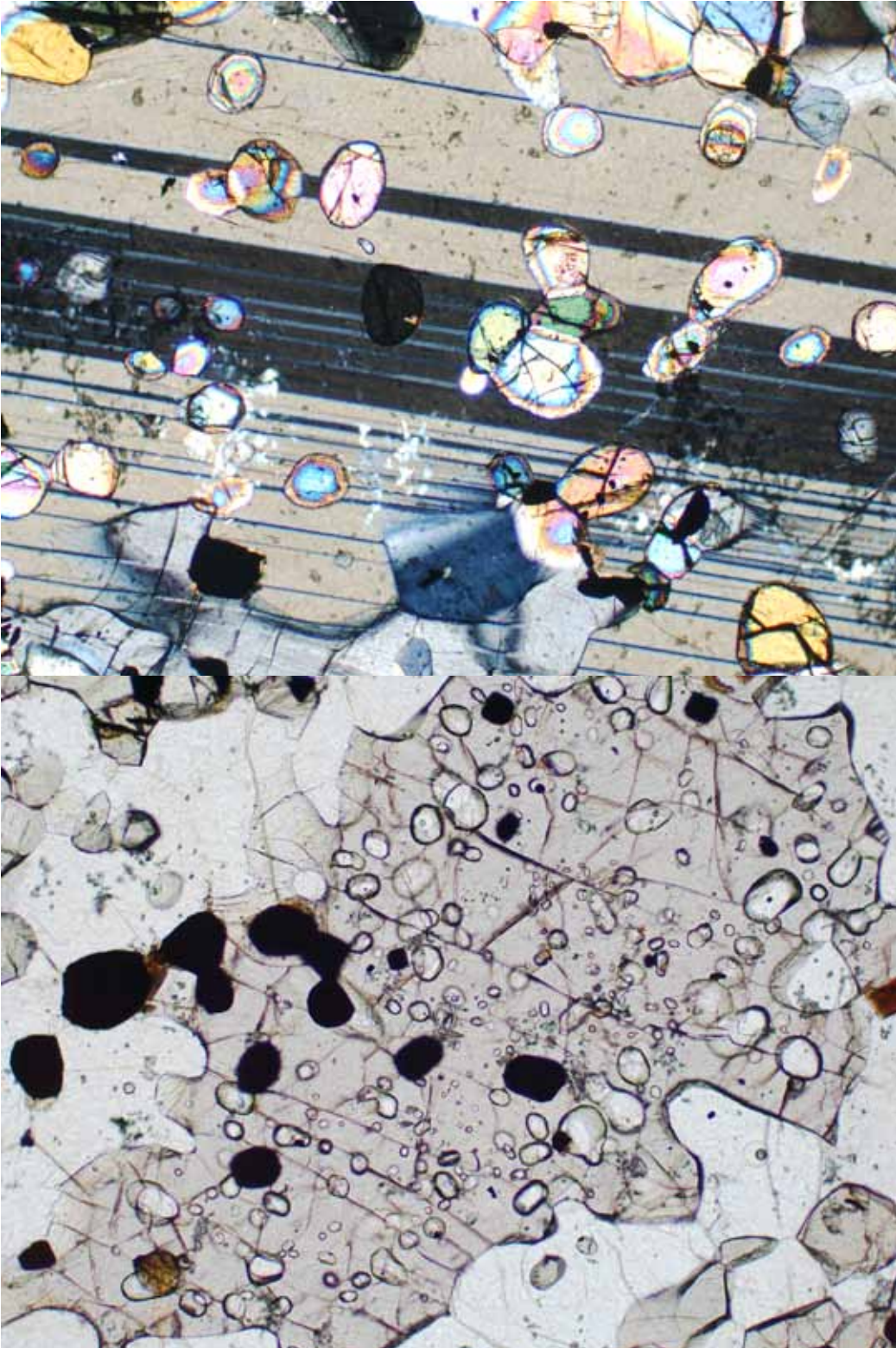


Fig.78. Plagioclase grain enclosing granules of clinopyroxene (top; CPL) and a clinopyroxene grain enclosing small granules of plagioclase (bottom; PPL). Fields of view ~2 x 3 mm. (DH13).

Mineral chemistry

Mineral compositions of 20 samples from the main textural varieties of the summit inclusion lie within fairly close ranges (Fig.79). Plagioclase is in the labradorite range (An_{64-52}); it does not show optical zoning and its composition does not vary systematically with height in the summit inclusion or textural type. Olivine, which is present in 7 of the analysed samples, is in the range Fo_{63-53} . Ca-rich pyroxene compositions cluster quite tightly in the augite field in the pyroxene quadrilateral with an average composition of $Ca_{43}Mg_{39}Fe_{18}$, whereas Ca-poor pyroxenes lie in the range $Mg\#_{px_{69-60}}$. It is noteworthy that these mineral compositions are, on average, slightly more primitive than those from the layered cumulates that immediately underlie the summit inclusion (Fig.79).

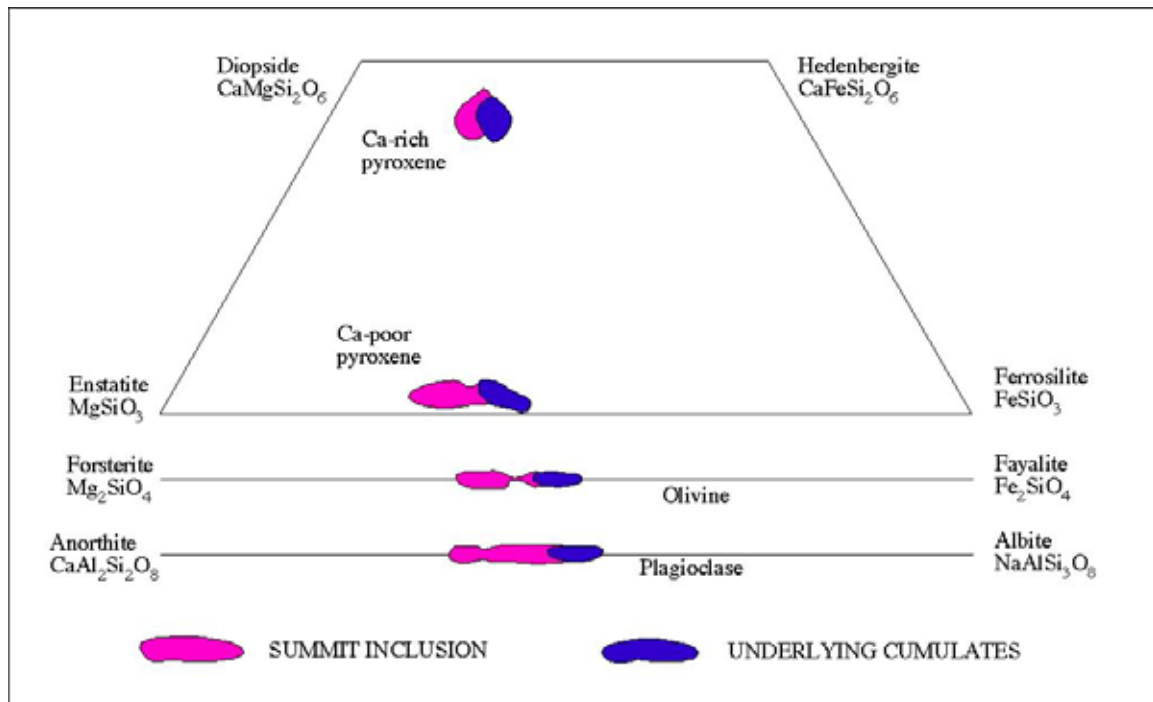


Fig.79. Compositions of pyroxenes, olivine and plagioclase in the summit inclusion. The compositions of the same minerals in FHI cumulates immediately under the inclusion are shown for comparison.

Whole rock chemistry

The whole rock chemical compositions of 14 samples of relatively homogeneous rocks from the summit inclusion have been determined, partly to assess the nature of the protolith. All samples plot in the basaltic field in a TAS diagram with distinct tholeiitic affinity (Fig.80). It is noteworthy that the believed composition of the FHI parental magma is somewhat more evolved than that of the metabasalt of the summit inclusion. The majority of the 14 samples have CIPW-normative diopside, olivine and hypersthene, classifying them as olivine tholeiites. The metabasaltic country rocks in the vicinity of the FHI belong to the Fundsjø Group. These basaltic rocks have been studied in the Meråker-Verdalen area, about 50 km NNW of FHI, by Grenne & Lagerblad (1985). Unfortunately, all the Fundsjø Group rocks have a metamorphic overprint which is in amphibolite facies in the Meråker area. The whole rock composition of the summit inclusion is broadly

similar to these amphibolites and there is no reason to involve a different protolith than Fundsjø Group metabasalts for the summit inclusion.

3.25.4. Significance of the outcrops

It is evident that the summit inclusion has been subjected to extremely thorough contact metamorphism, locally involving partial melting (to produce, for example, the globular textures). This required a considerable amount of heat. The composition of the parental magma to the FHI is believed to have been more evolved than that of the summit inclusion metabasalts with, for example, an Mg# of ~48 (Abu El-Rus et al., 2007). This is much less than the Mg# of the basaltic precursor to the summit inclusion (~62; Holm (2003)). It seems unlikely that the parental magma to the FHI could have produced the extreme contact metamorphic effects observed in the summit inclusion if it consisted of dry basalt.

The FHI was emplaced at ~3.5 kb. At this pressure the dry solidus for basalt lies at ~1120°C, whereas the wet solidus is at 700-750°C (Shelley, 1993). It is therefore likely that the basaltic precursor to the summit inclusion had been hydrated during the regional metamorphism that preceded emplacement of the FHI. All of the Fundsjø Group country rocks surrounding the FHI have, however, been overprinted by amphibolite facies metamorphism which is commonly accompanied by penetrative deformation, during the Scandian orogenic event. The metamorphic state of these rocks before emplacement of the FHI is therefore difficult to establish.

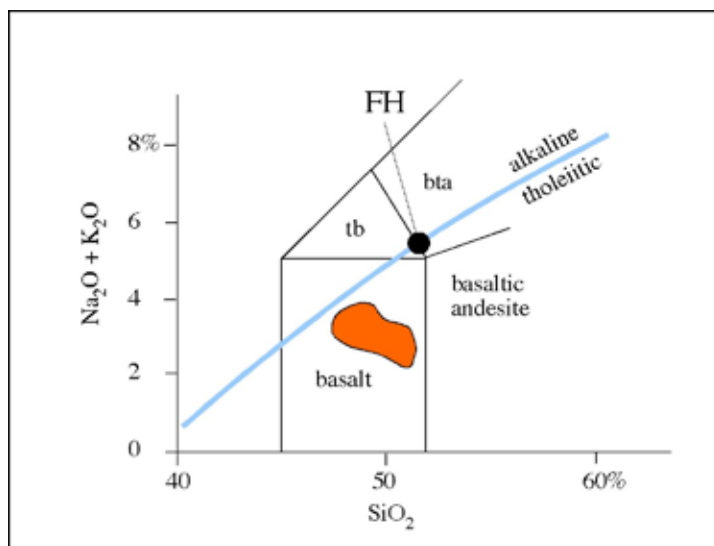


Fig.80. Total alkali vs silica plot for 14 essentially homogeneous samples from the summit inclusion (orange area). They all lie in the basalt field and are more primitive than the composition of the FHI parental magma (FH from Abu El-Rus et al., 2007).

The heat source for the contact metamorphism of the summit inclusion was the FHI magma. The layered features in the summit inclusion are concordant with its basal contact and with modal layering in the underlying cumulates. It seems likely that the features developed parallel with isotherms that migrated through the inclusion. At some

time this huge inclusion probably formed the magma chamber roof. The complicated distribution of raft-like inclusions and layered cumulates in the FHI (particularly in Stage II) is believed to have resulted from the magma penetrating into the roof rocks as sill-like bodies (Fig.81; Habekost & Wilson, 1989). The summit inclusion was therefore heated by magma both from below and above (Fig.82). Contact metamorphism progressed inwards from both contacts as heat and fluids migrated into the inclusion.

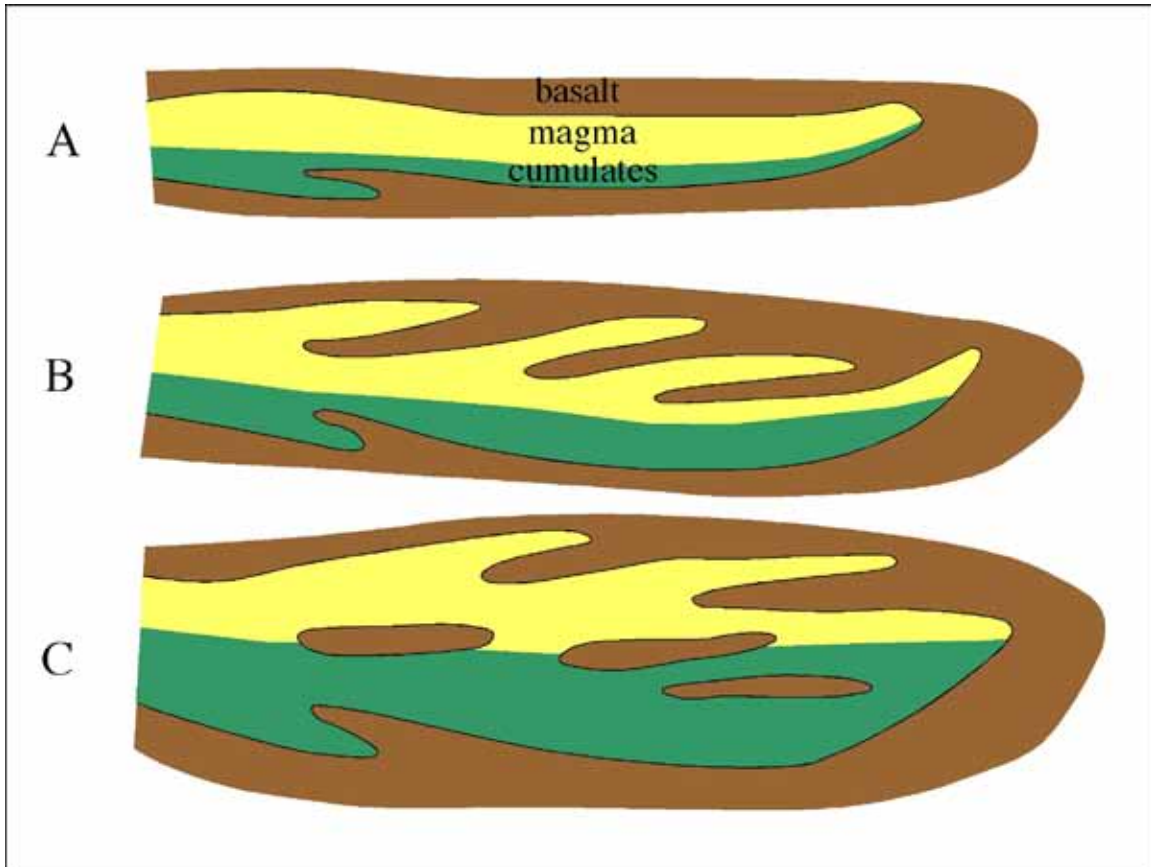


Fig.81. Simplified model for generation of metabasaltic inclusions in the FHI. Intrusion of a wedge-shaped, sill-like body into Fundsjø Group metabasalts. Continued influx and magma chamber expansion results in the magma penetrating the roof. During continued influx some of the sill-like bodies at the roof merge. Raft-like portions of the roof become totally engulfed in magma. The raft-like inclusions may remain interlinked in three dimensions. The crystallisation front moves upwards throughout this process.

Recrystallisation to granoblastic metabasaltic pyroxene hornfels was the initial stage. This was accompanied by the local concentration of mafic phases into patches and streaks to form ultramafic segregations, sometimes together with self-organisation into diffuse mafic-rich and plagioclase-rich layers. Some local coarsening in grain-size resulted in the formation of patches of hornblende gabbro. Local very hornblende-rich layers also developed. The widespread presence of hornblende poikiloblasts also bears witness to the role of hydrous fluids in these processes.

Significant widespread coarsening in grain-size first developed in elongate streaks, parallel with the layering and basal contact of the summit inclusion. Continued coarsening was accompanied by more or less extensive segregation into plagioclase-rich and mafic-rich layers. This involved diffusive recrystallisation – a type of Oswald ripening. The layered gabbros that result from this extreme form of self-organisation in response to contact metamorphism of basaltic inclusions are not easy to distinguish from those formed in the Fongen-Hyllingen magma chamber. It seems likely that some of the rocks that we have mapped as “modally layered cumulates” belonging to the FHI are in fact the result of the extreme contact metamorphism of basaltic inclusions.

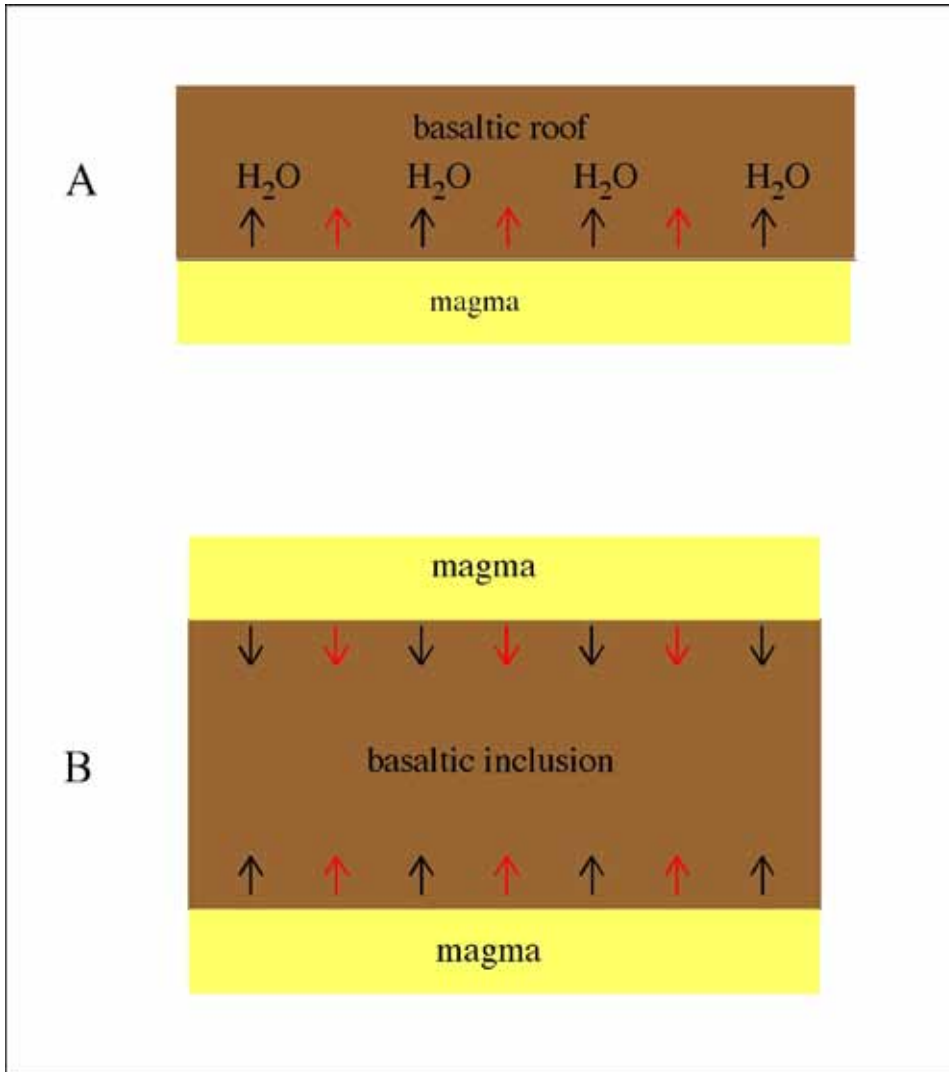


Fig.82. Model for genesis of the extreme textural variations in the summit inclusion involving the flux of heat (red arrows) and fluids. The summit inclusion initially formed part of the roof and was only heated from below (during stage A in Fig.81). As magma penetrated above the inclusion it became heated from both sides (during stages B & C in Fig.81). The boundaries between the different textural types and the orientation of layering in the summit inclusion are parallel with its contacts and probably developed along isothermal surfaces.

The globular-textured metabasalts in which “blobs” of granular metabasalt are enclosed in a gabbroic/dioritic matrix appear to have involved disaggregation. They superficially resemble pillow-like structures formed as a result of magma mixing. It seems likely that they were formed as a result of partial melting of the metabasalts in which the “blobs” represent the unmelted fraction and the gabbroic/dioritic matrix represents the crystalline result of the melt that remained more or less in place.

Comparative examples involving the extreme contact metamorphism of basaltic precursors have been described from the Kap Edvard Holm Complex, East Greenland (Brandriss & Bird, 1999; Brandriss et al., 1996), the Basistoppen Sill, East Greenland (Naslund, 1986) and the Miki Fjord Macrodyke, East Greenland (Bird et al., 1985; Leshner et al., 1992).

3.26. Stop 22: Fongen summit

3.26.1. Location

Coordinates: 0632239 7008122. Tydal 1:50.000 map.

3.26.2. Introduction

This is the top of Fongen mountain. There are two cairns at about the same height on the summit plateau. The northern one (1441 m) is the highest but the southern one (1434 m) is the most impressive and the views are best from here.

3.26.3. Description

The northern cairn is still within the summit inclusion that here consists of granular metabasaltic hornfels. There are both metabasalts and metapelites exposed on the plateau. The main cairn is on layered gabbros above the summit inclusion (Fig.83). Some 10 m to the SW of the main cairn, modally layered gabbros are draped over the top of a small metabasaltic hornfels inclusion.



Fig.83. Stop 22. The author at the main cairn on the top of Fongen (1434 m). The view is to the east.

To the east the view is towards Sweden. The border passes through the summit of the highest mountain (Storsylen; 1762 m) which is ~32 km away. To the west the view is towards Trondheim which is hidden by hills. The large lake in the distance is at Selbu, ~35 km away. The size and shape of the FHI can be appreciated to the south. The summit of Fongskaftet (Stage II) is closest, followed by Ruten (in Stage IV). The long, rounded ridge of Melshogna (Stage II) is obvious to the SW. The Hyllingen part of the intrusion is farther south; the summit of Hyllingen (1205 m) is ~23 km away, beyond the wooded valley occupied by the Nea river and the main road 705 from Tydal to Selbu.

3.27. Stop 23: Impact structure

3.27.1. Location

Coordinates: 633633 7008702. Tydal 1:50.000 map.

3.27.2. Introduction

A well-developed deformation structure, caused by the impact of a metabasaltic block on the crystallisation front, is exposed on the western side of a broad gully.

3.27.3. Description

Well-developed modal layering in this area strikes approximately north-south and dips $\sim 30^\circ$ W. The more or less planar surface on which the impact structure is exposed has a dominantly grey to black colour, reflecting its metagabbroic nature. The planar surface is probably parallel with a joint, along which migrating fluids caused hydration under amphibolite facies conditions in the rocks on either side. Olivine and plagioclase compositions in this vicinity are Fo ~ 55 and An ~ 52 , accompanied by clinopyroxene + magnetite \pm orthopyroxene. The outcrops here are dissected by many thin veins, along which the rock has been bleached. These detract from the aesthetic value of the outcrops; try to ignore them!

There are two xenoliths of metabasaltic hornfels at different levels (Figs.84 & 85). The lower one (A) has a curved, plate-like shape whereas the upper one (C) is more equidimensional. The feature of most interest is the effect of xenolith A on the adjacent layering which has been disrupted and thrown into overfolds. The layering is continuous throughout the folds. It is not difficult to assess what happened in a general way.

Xenolith A became detached from the magma chamber roof and sank through the magma with sufficient velocity to disrupt the partially consolidated crystal mush on the floor to a depth of ~ 120 cm and to compress a further ~ 80 cm of the underlying layered cumulates. The displaced material formed a cloud of crystals in the vicinity of the disrupted floor. Layers on either side of the impact remained more or less coherent and were thrown outwards as overfolds. Some fragments of these layers became detached and are now located in the "crater" area, together with the mass of disrupted individual crystals. Layer B shows no evidence of discontinuity above the structure which suggests that any excess material thrown out by the impact was removed, leaving a planar surface. This may imply that magmatic currents were able to winnow the crystals away and deposit them elsewhere, but alternatively the displaced material could have resettled in a more compact manner, leaving a smooth interface between the disturbed crystal pile and the magma. After deposition of a ~ 2.5 cm-thick mafic-rich layer (B), xenolith C hit the floor with a velocity sufficient to indent the layering to a depth of ~ 20 cm. The mafic-rich layer D is draped over xenolith C and subsequent layers bear no evidence of the buried structures.

3.27.4. Significance of the outcrops

It is evident that small fragments of the roof periodically became detached and were able to sink through the magma and cause impact structures on the magma chamber floor.



Fig.84. Stop 23. Impact structure formed by a metabasaltic inclusion. A sketch of the structure as seen normal to the layering is shown in Fig.85 which identifies inclusion A. The small inclusion C is near the hammer at the top of the photograph.

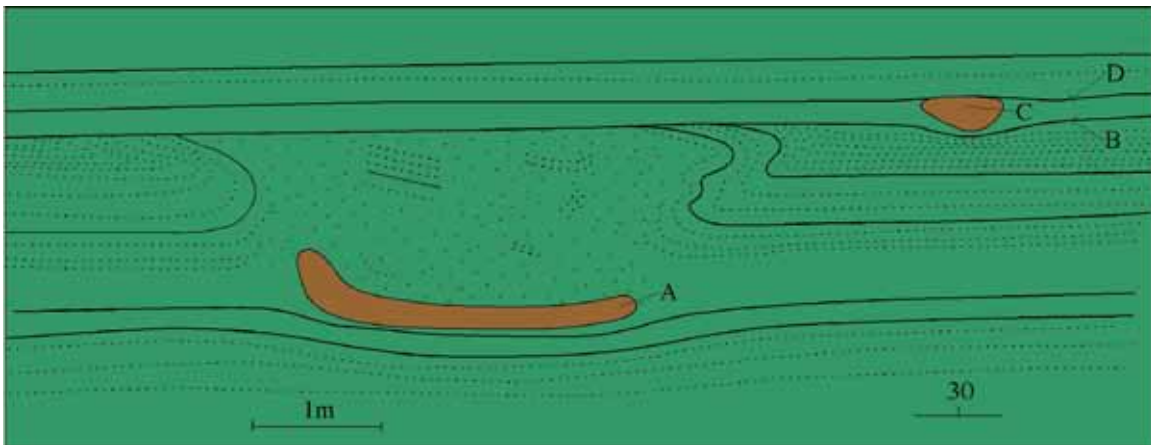


Fig.85. Stop 23. Sketch of the impact structure in Fig.84.

3.28. Stop 24: Shear Zone west of Ramsjø lake

3.28.1. Location

Coordinates: 0633589 7007452. Tydal 1:50000 map.



Fig.86. Location of Stop 24. Two different views of the elongate EW metabasaltic inclusion at 1098 m are shown in Figs.87 & 89.

3.28.2. Introduction

The exposure here is of a very impressive shear zone that cuts sharply through layered gabbros.

3.28.3. Description

We are here within Stage II in the Fongen Series. The relatively un-metamorphosed layered rocks have brownish colours. Where they have been overprinted by amphibolite facies metamorphism to give grey tones, the colour contrast between the mafic-rich (dark grey to black) and plagioclase-rich (pale grey to white) lithologies increases and modal layering becomes more obvious. The shear zone in Fig.88 has an extremely sharp contact with the layered rocks. Within the shear zone the layered gabbros have been transformed to foliated amphibolites with a few felsic segregations. The foliated amphibolites are similar to those seen at Stops 13 and 16.

From here the view to the SW includes a prominent ridge formed by a large metabasaltic hornfels inclusion (Fig.87).

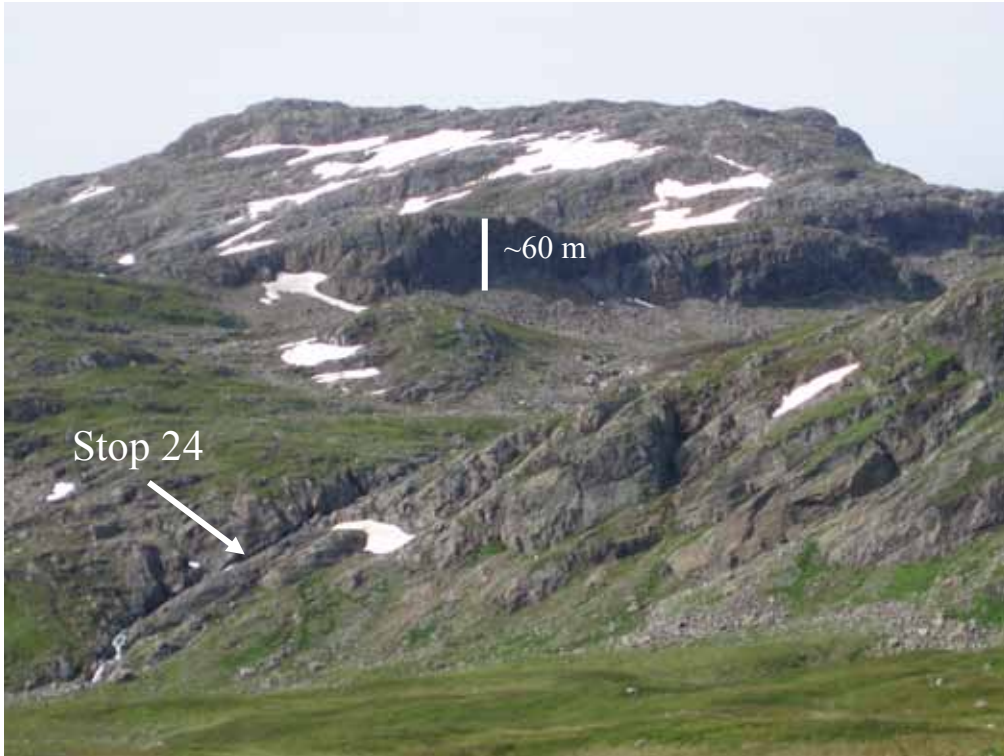


Fig.87. View of Fongskaftet from the NE showing the location of the shear zone at Stop 24 illustrated in Fig.88 and a ridge formed of a metabasaltic inclusion (~60 m high). A view of this ridge from above is shown in Fig.89.



Fig.88. Stop 24. Shear zone cutting through layered gabbro.



Fig.89. The elongate east-west metabasaltic inclusion (the highest point of which is at 1098 m) in Fig.86 forms a striking ridge which is ~700 m long. The ridge seen from a different angle is shown in Fig.87.

3.29. Introduction to Stops 25 – 27

These stops are in the extreme northwestern part of the Fongen-Hyllingen complex and are most accessible from Schulzhytta (Fig.12). Stop 25 is on the path from Schulzhytta to Gresslihytta, whereas Stops 26 and 27 are on the path between Schulzhytta and Ramsjøhytta. Stop 25 is at an impressive dioritic pegmatite with large, prismatic, branching hornblende crystals. Stops 26 and 27 are within the Treknattan Intrusion which is a small, mafic to ultramafic body that is emplaced within the FHI.

3.30. Stop 25: Ramåa (NW of Litlefongen)

3.30.1. Location

Coordinates: 0627653 700866. Tydal 1:50000 map.

3.30.2. Introduction

A hornblende plagioclase pegmatite is locally developed along the western margin of the FHI. This is the largest and best-exposed example.

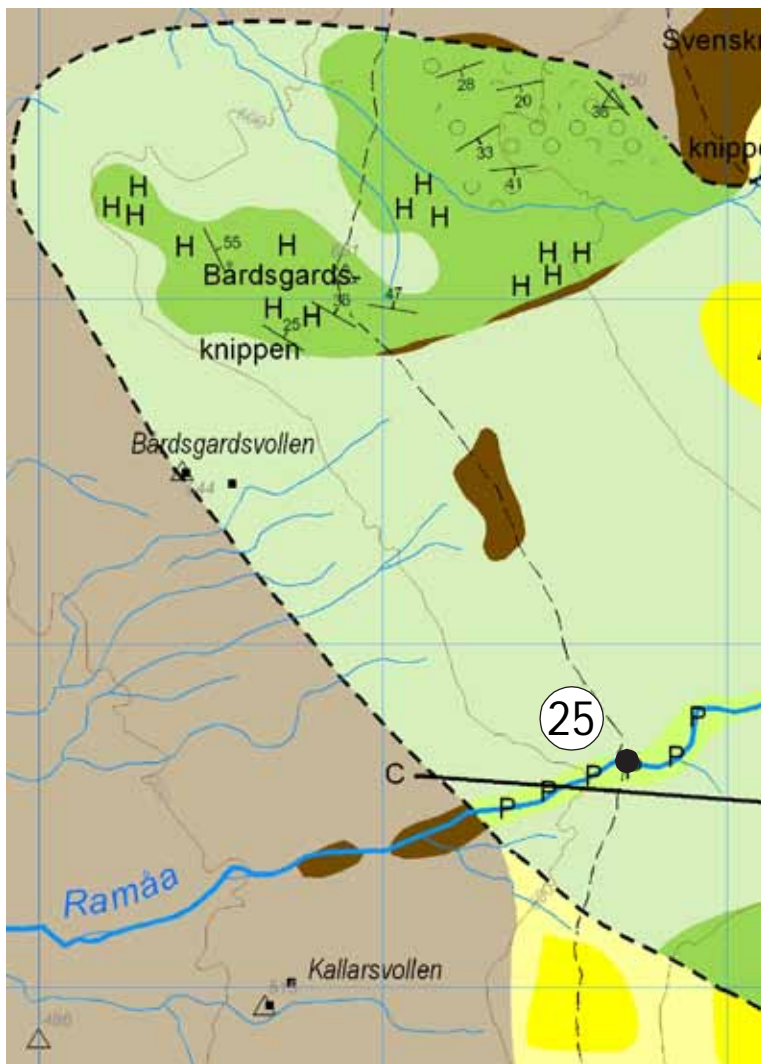


Fig.90. Location of Stop 25.

3.30.3. Description

Where the marked path crosses river Ramåa (Fig.90), the riverbed consists of polished outcrops of hornblende plagioclase pegmatite (Fig.91). These pegmatitic rocks extend from the country rock contact for ~1 km upstream. Their extent to the north and south is unknown because of poor exposure.



Fig.91. Hornblende plagioclase pegmatite at Stop 25. Relatively fine-grained (A) or coarse-grained, massive (B) bands rich in hornblende are roughly perpendicular to prismatic hornblendes. Some of the elongate hornblendes branch from right to left, implying that they grew in that direction.

Prismatic, black hornblende crystals, up to ~40 cm in length, are separated by white plagioclases. A coarse layering structure is defined by hornblende-rich bands that are roughly perpendicular to prismatic hornblende crystals (Fig.91). Some of the hornblendes have a skeletal structure (Fig.92). Inclusions of metabasalt are locally present in the pegmatite.

In thin section the large hornblendes have beige-brown pleochroism and a dusting of tiny, exsolved ilmenite grains. Some of them have cores of cummingtonite or uralitised Ca-rich pyroxene. Green hornblende and chlorite are locally present along the margins of the

large prismatic brownish hornblende grains. The plagioclase, which has locally been replaced by clinozoisite, is accompanied by accessory magnetite, apatite and quartz.

Ca. 1.5 km to the northwest the path to Schulzhytta crosses outcrops of hornblende-rich metagabbro (Fig.93). The alteration of gabbro to metagabbro can be studied where brown gabbro is cross-cut by veins of grey metagabbro. Near the highest point (661 m) the metagabbro contains numerous rust-coloured inclusions that are generally elongated in a NW-SE direction. There is no convincing modal layering developed in this area.



Fig.92. A skeletal structure is sometimes developed in hornblende crystals in the hornblende plagioclase pegmatite at Stop 25.

3.30.4. Significance of the outcrops

The prismatic hornblende crystals appear to have grown from right to left in Fig.91, in the direction in which they branch. The branching and skeletal features indicate rapid growth. The presence of pyroxene cores to some of the hornblendes implies that pyroxene crystals nucleated initially to be overtaken by hornblende when pH_2O increased. The overall pattern in Fig.91 suggests that nucleation took place in a rhythmic fashion, bands of hornblende and plagioclase forming the crystallization front on which prismatic crystals subsequently nucleated and grew.

The hornblende plagioclase pegmatite in the Ramåa area is lithologically similar to that encountered at Stop 1. Both are developed near the western margin of FHI. At Stop 1 in

the Hyllingen Series the pegmatite belongs to the evolved rocks in the basal reversal of Stage I (Fig.18). The western margin of the Fongen Series has not been studied in the same detail as that in the Hyllingen Series, partly because of poor exposure and metamorphic overprinting. The presence of this pegmatite, however, implies that compositionally evolved rocks occur along at least part of the western margin of the Fongen Series. This in turn would imply that there is a basal reversal below Stage II in the Fongen Series, so that Stage I in Fig.11E is probably also present in the northern part of FHI.



Fig.93. Brownish olivine gabbro showing alteration to grey metagabbro ca. 1.5 km northwest of Stop 25.

The alteration of gabbro to metagabbro (Fig.93) took place along veins where water penetrated the rock under amphibolite facies conditions. Igneous textures are commonly preserved in these metagabbros, despite the extensive replacement of mafic minerals by amphiboles.

3.31. Stop 26: North of Ramåa (A)

3.31.1. Location

Coordinates: 0629210 7010058. Tydal 1:50000 map.

Just south of the path linking the Trondheim Turistforening huts Gresslihytta and Schulzhytta.

3.31.2. Introduction

The northern part of the FHI is cut by a small (~3 km²) mafic – ultramafic body called the Treknattan Intrusion. This body is elongate from NW to SE (Enclosure 1). The most accessible outcrops of the Treknattan Intrusion are in this area to the north of river Ramåa. The information for Stops 26 and 27 is mostly taken from Sørensen & Wilson (1996).

3.31.3. Description

Approaching this locality along the path from the west (Fig.94), the first outcrops of the Treknattan Intrusion are of orange- to brown-weathering troctolite. The troctolite has been extensively overprinted by amphibolite facies metamorphic assemblages in the form of grey-weathering outcrops. The metamorphism involved hydration and locally occurs as broad “veins”, similar to that illustrated in Fig.93.

Stop no. 26, just south of the path, is of olivine cumulates (Fig.95). There are two main varieties of olivine cumulates; type A is very olivine-rich (with minor intercumulus plagioclase, clinopyroxene and hornblende); type B contains more intercumulus plagioclase. There are sub-rounded blocks of type B in type A and vice versa. The blocks range in size from 5 – 100 cm across. Olivine in these rocks has a composition of Fo_{~86} and is accompanied by Cr-spinel. This composition is much more magnesian than the most primitive olivines from the FHI (Fo₇₃).

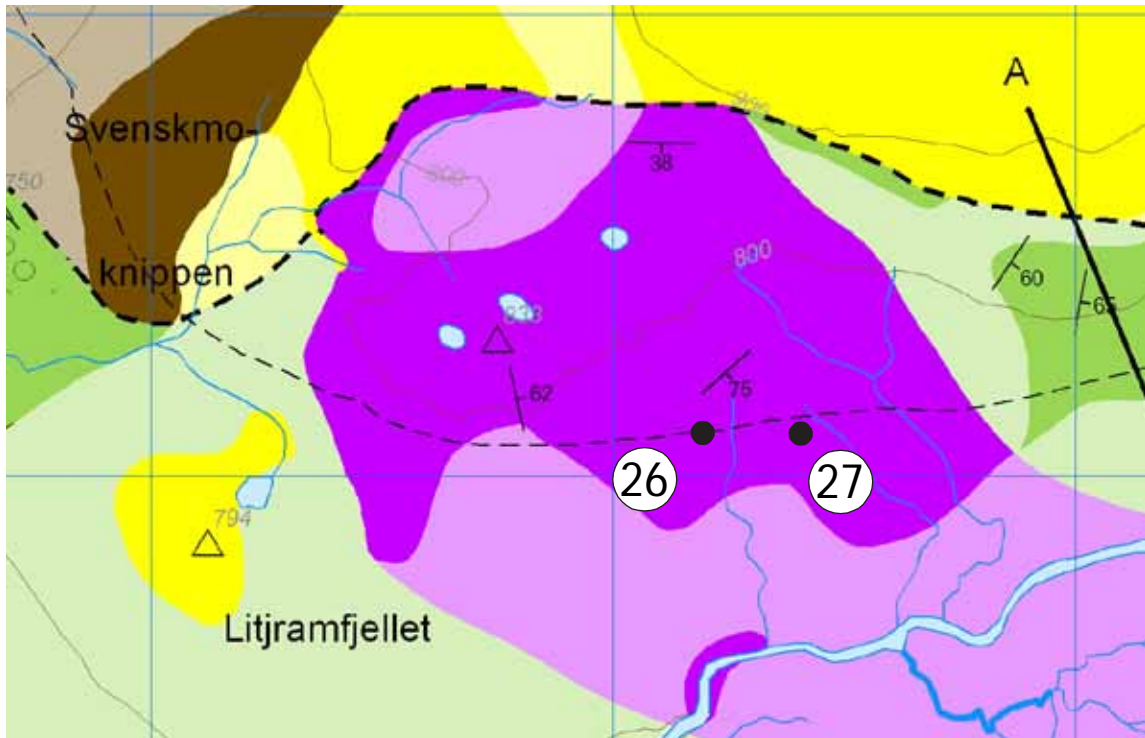


Fig.94. Location of Stops 26 and 27 in the Treknattan Intrusion.

3.31.4. Significance of the outcrops

The primitive rocks north of the river Ramåa were previously believed to represent the lowest part of the layered series of the FHI (Wilson et al., 1981). Mapping by in the Treknattan area by Knudsen (1990), however, revealed that olivine-rich rocks cross-cut layered cumulates that belonged to the FHI. Later work by Sørensen (1990, 1994) established the detailed form and compositional variation of this small body that was first referred to as the “Treknattan Intrusion” by Knudsen (1990).

Cumulus olivine compositions in the Treknattan Intrusion vary from Fo₈₈ to Fo₆₉, whereas cumulus plagioclases vary from An₇₇ to An₆₅. As shown by Sørensen & Wilson



Fig.95. Olivine cumulates of the Treknattan intrusion at Stop 26. Sub-rounded blocks of greyish-brown, plagioclase-rich olivine cumulates are enclosed in brown olivine cumulates with less intercumulus plagioclase. In the picture this is most obvious to the right of the hammer.

(1996), there are several compositional reversals in the constructed stratigraphic sequence through the Treknattan Intrusion, reflecting repeated magma replenishment. The blocks of “cumulates within cumulates” at Stop 26 indicates the dynamic nature of the magma chamber in which blocks of earlier cumulates occasionally foundered into the evolving cumulate pile. This in turn reflects either turbulent magma emplacement, or the periodic collapse of cumulates that formed on steep walls – or both.

3.32. Stop 27: North of Ramåa (B)

3.32.1. Location

Coordinates: 0629421 7010061. Tydal 1:50000 map.

3.32.2. Introduction

Rocks of the Treknattan Intrusion can also be studied here.

3.32.3. Description

The prominent SE-facing outcrop just to the south of the path is of olivine cumulates belonging to the Treknattan Intrusion. The outcrop has a distinct “patchy” appearance that reflects the role of the intercumulus minerals. Large (up to 20 cm across) plagioclase oikocrysts, that include hundreds of cumulus olivine grains, give rise to light-coloured patches, whereas generally smaller oikocrysts of clinopyroxene and/or hornblende give the darker brownish patches (Fig.96).

The outcrop has an unusual joint pattern that superficially resembles mud cracks. The pattern reflects the orientation of veins along which alteration of olivine to serpentine has taken place. Subsequent weathering has preferentially removed the softer, serpentinised material.



Fig.96. Olivine cumulates of the Treknattan Intrusion at Stop 27. The hammer shaft is on a large plagioclase oikocryst. The irregular-shaped, brownish patches represent oikocrysts of clinopyroxene and/or hornblende.

The olivine-rich rocks of the Treknattan intrusion form the brown-weathering, “whale-back” outcrops extending for some 700 m to the north (Enclosure 1). To the ESE the intrusion extends across the Ramåa valley, where it is poorly exposed, to the Treknattan area and beyond (Fig.97).

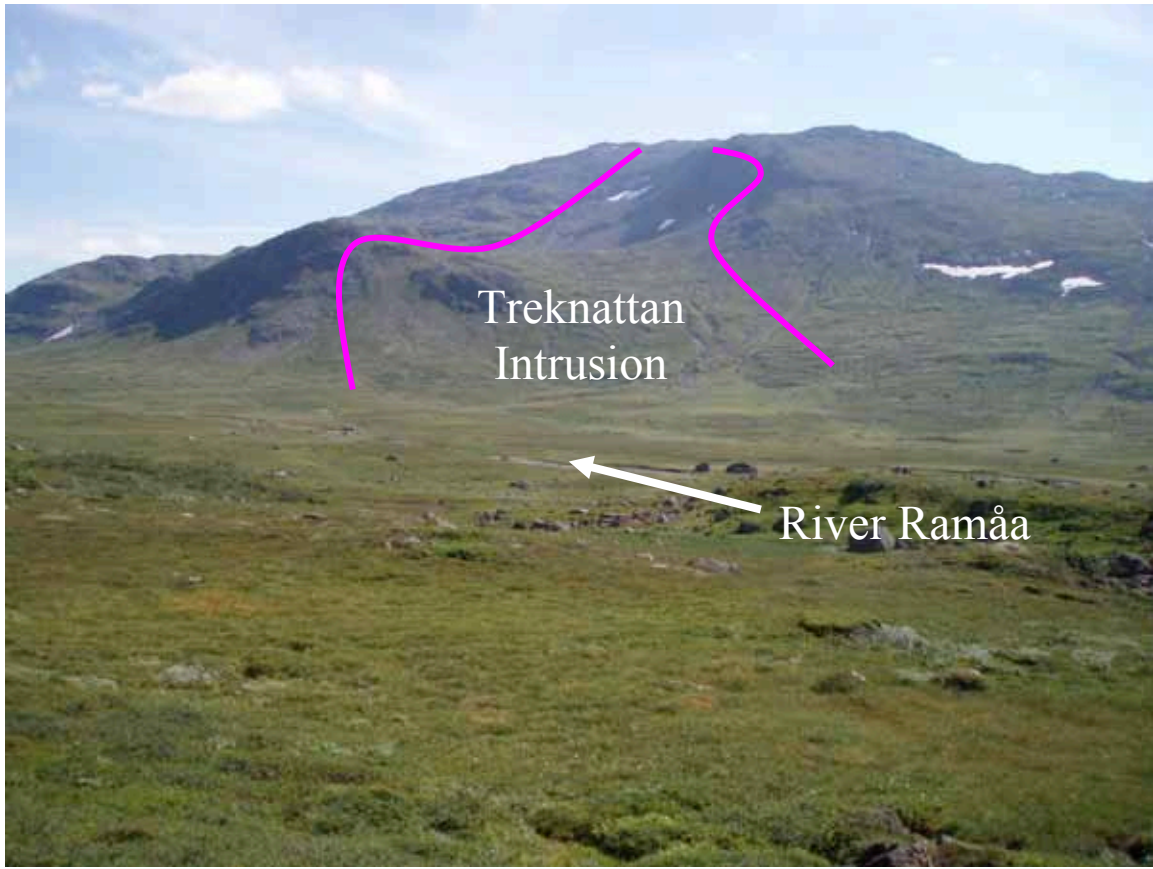


Fig.97. View of the Treknattan area to the ESE from Stop 27. The highest point is the summit of Fongen (1441 m). The Treknattan Intrusion is poorly exposed in the Ramåa valley. On the southern side of the valley the intrusion extends towards the summit of Fongen mountain. The olivine-rich rocks of the Treknattan body, that are more easily weathered than the layered gabbros and metabasaltic inclusions of the FHI, occupy the saddle-shaped area in the centre of the picture.

3.32.4. Significance of the outcrops

The Treknattan Intrusion is a basic-ultrabasic body that was discordantly emplaced into the northern part of the FHI. It was intruded after consolidation of the FHI but before deformation and metamorphism. The elongate shape of the Treknattan Intrusion, and its strongly discordant relationship to the FHI, indicate that it is an elongate, sub-cylindrical or ellipsoidal body with steep walls. In the Treknattan area the orientations of structures in the FHI are unaffected by emplacement of the Treknattan body. Emplacement was probably by dissolution and assimilation of the gabbroic host rocks, possibly accompanied by stoping.

It seems likely that the parental magmas to the Treknattan and Fongen-Hyllingen Intrusions are genetically related. There are several arguments in favour of this:

- a) There is a very close spatial and chronological relationship between the two intrusions.
- b) Both show the early sequence of crystallization of olivine (\pm Cr-spinel)-plagioclase-Ca-rich pyroxene.

- c) Both intrusions display a reaction relationship between olivine and Ca-poor pyroxene.
- d) The magmas represent water-rich, basaltic melts at different stages of evolution.
- e) Both magmas have relatively low initial $^{87}\text{Sr}/^{86}\text{Sr}$ ratios (FHI $\text{Sr}_i = 0.7031$; Treknattan $\text{Sr}_i = 0.7025$) indicating derivation from a moderately depleted mantle source.

The magmas parental to the two intrusions may have been derived from multiple magma chambers or a zoned magma chamber, rising to their present position through a common feeder conduit.

3.33. Introduction to Stops 28-31

We are here in the lower part of Stage IV in the Ruten area of the FHI (Fig.98; Enclosure 1). During crystallization of the early part of Stage IV there were several minor magma influxes that produced laterally continuous olivine-rich units, partly as a result of magma-mixing (Figs.98 & 99; Enclosure 1). Seven olivine-rich units have been identified, each of which is associated with a compositional reversal. In the area NE of Ruten (Stops 28-30) we see some unique load-cast structures and some features caused by slumping. To the south of Ruten (Stop 31) we examine Unit 7 (the Kvassåsen unit) which is the thickest and most impressive of the olivine-rich units.

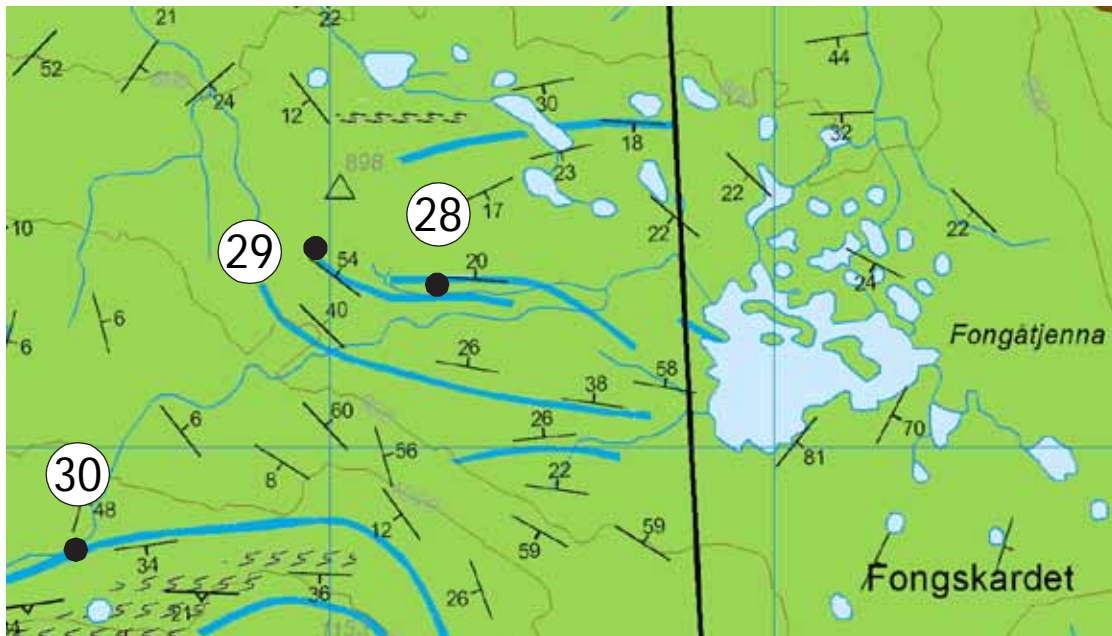


Fig.98. Locations of Stops 28 to 30.

3.34. Stop 28: Load features A

3.34.1. Location

Coordinates: 630610 7004159. Tydal 1:50000 map.

3.34.2. Introduction

One of the olivine-rich units here displays an unusual polygonal pattern in the plane of the layering. In conjunction with the outcrop at Stop 30 this feature has been interpreted as representing load structures, as described by Thy and Wilson (1980). These are the first convincing examples of igneous load casts ever described.



Fig.99. Stop 28. The olivine-rich unit in the foreground is ~1.2 m thick. The view to the north includes the summits of Fongen (left; ~4.5 km away) and Fongskaftet (right centre; ~3 km away).

3.34.3. Description

There are two olivine-rich units here, both of which dip to the north; they are located on the southern flank of a syncline (Enclosure 1). The one to the north (Fig.99) is ~1.2 m thick and consists dominantly of thin, laterally persistent, alternating layers of dunite and troctolite (\pm Ca-rich pyroxene). The dip-surface of the unit to the south exposes a very unusual pattern (Fig.100). A series of polygonal “cells” consisting of discrete altered plagioclase crystals in an olivine-rich matrix are surrounded by dark brown rims of dunite. The cells are up to 30 cm across (average ~20 cm) over an outcrop of ~6 m². Sporadic cm-sized oikocrysts of Ca-rich pyroxene are also present. The origin of these structures is discussed in connection with Stop 30.



Fig.100. Stop 28. Polygonal patterns in the plane of the layering in an olivine-rich unit. The lighter-coloured polygonal shapes consist of discrete, altered plagioclases in a darker, olivine-rich matrix. The “cells” are separated by continuous dunitic rims.

3.35. Stop 29: Slump structures in an olivine-rich unit

3.35.1. Location

Coordinates: 630045 7004233. Tydal 1:50000 map.

3.35.2. Introduction

One of the olivine-rich units here displays a series of slump structures. These bear witness to local deformation of the layering shortly after crystallisation, before deposition of overlying material. The most likely cause is the impact of roof xenoliths causing disruption of the crystallisation front.

3.35.3. Description

The upper ~20 cm of the olivine-rich unit here contains a series of deformation structures. One of them is illustrated in Fig.101. This fold is confined to the ca. 20 cm-thick upper part of the olivine-rich unit. The layers below and above are not deformed. Other deformation structures in this layer contain angular fragments of dunitic material.



Fig.101. Stop 29. Fold structure in the troctolitic upper part of an olivine-rich unit.

3.35.4. Significance of the outcrops

The fact that these deformation structures are restricted to an individual layer implies that they formed when the underlying layer was relatively consolidated and before the overlying layer had formed. The presence of fragmental portions implies that material was ripped up from an underlying layer. The turbulence required was probably caused by the impact on the magma chamber floor of a xenolith from the roof. The geometry of the deformation structures implies that movement was from the left in Fig.101. There is, however, no xenolith exposed in the vicinity of these structures. It could be hidden in the third dimension or have been eroded away.

3.36. Stop 30: Load features B

3.36.1. Location

Coordinates: 629259 7003725. Tydal 1:50000 map.

3.36.2. Introduction

This beautiful outcrop exposes some mushroom-like structures that are believed to represent igneous load casts (Fig.102).

3.36.3. Description

Following a stream uphill from Stop 29 we encounter an olivine-rich unit at about 1040 m above sea level. This is probably the same unit as the one containing the polygonal structures at Stop 28 that is repeated in a fold (Enclosure 1). This olivine-rich unit can be followed along strike and forms several beautiful brown-coloured outcrops. The unit contains cm-sized oikocrysts of Ca-rich pyroxene that are relatively resistant and stand out as small spheres in some outcrops.



Fig.102. Stop 30. A series of “mushroom” structures in a ~6 cm-thick layer in an olivine-rich unit.

At Stop 30 (Fig.102) a metagabbro layer is overlain by a ~6 cm-thick layer containing light-coloured, mushroom-shaped features in a dark dunitic matrix. There is a fairly constant spacing between the “mushrooms” that consist largely of altered plagioclase crystals. A total of ~15 “mushrooms” occur in a lateral distance of about 1.5 m. The “mushrooms” are about 5 cm high, which is about the same order of magnitude as their maximum width. Some examples of apparent detachment from the base are seen, but this could be the effect of the two-dimensional outcrop. Along strike (further downstream) this olivine-rich unit contains a variety of deformed mushroom-like structures.

The rocks in which the structures occur at Stops 28 and 30 were originally dunites (olivine adcumulates) and troctolites (olivine plagioclase adcumulates) but they have been affected by alteration processes. The compositions of the unaltered phases are Fo₆₉ and An₆₁. Plagioclase has been extensively altered to chlorite which occurs as a fine-grained aggregate. Tremolite and anthophyllite are developed around the altered plagioclase, often as radiating needles that penetrate the olivine. Immediately below the mushroom-bearing layer is a 3 mm-thick layer consisting of talc and dolomite with minor magnetite. Below this is a layer of bladed anthophyllites that are orientated roughly normal to the plane of the layer, and then a layer of aggregates of fine-grained chlorite and pale-green, pleochroic actinolite. The main metamorphic reaction appears to have been of the type:



There are only minor amounts of Na in the metamorphic minerals and most of the Na released from plagioclase was probably removed from the system with excess H₂O.

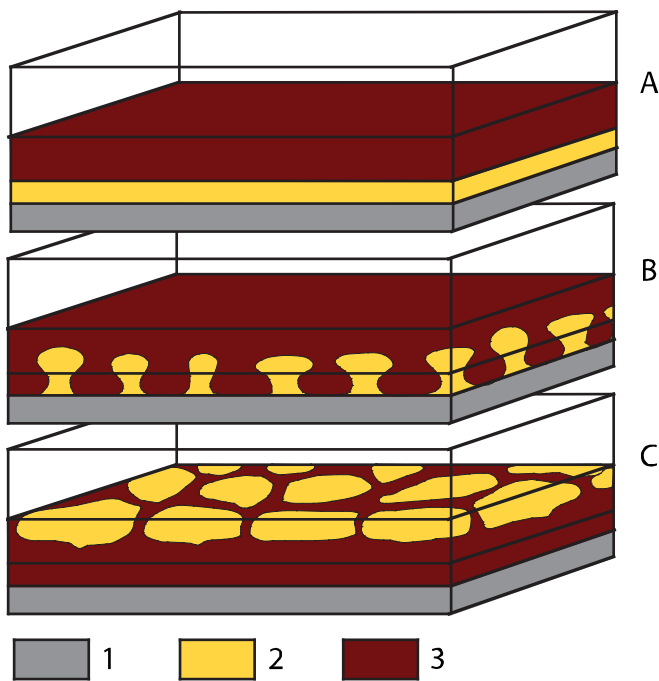


Fig.103. Schematic model showing possible development of the deformation structures in Figs100 & 102. 1 = largely consolidated gabbro. 2 = plagioclase-rich crystal mush. 3 = olivine-rich crystal mush (in contact with magma in A). The progressive deformation caused by density contrast between layers 2 and 3 is shown in stages from A to C. Stage B is equivalent to that in Fig.102, whereas stage C is equivalent to that in Fig.100. The diagram is very similar to those shown by Ankatell et al. (1970) for the experimental deformation of water-saturated sediments in a non-mobile system with reversed density gradients.

3.36.4. Significance of the outcrops

The structures that form the “mushrooms” and the polygonal patterns in the plane of the layering have been explained as representing igneous load casts by Thy and Wilson (1980). The original configuration was a mineral-stratified, plagioclase-olivine-liquid crystal mush. The structures were initiated by the density contrast between an upper, olivine-rich mush and a lower plagioclase-rich mush. The structures bear a remarkable resemblance to those produced by Dzulynski (1966) and Ankatell et al. (1970) in water-saturated sediments (Fig.103). If the polygonal, plagioclase-rich structures in Fig.103C were to merge, the geometry would consist of a laterally continuous olivine-rich layer overlain by a laterally continuous plagioclase-rich layer – opposite to the starting situation. Such inverted layer sequences would be very hard to identify in a layered intrusion.

A wide variety of post-depositional structures, including load structures similar to those described here, have been described from the Bushveld Intrusion by Lee (1981).

3.37. Stop 31: Olivine-rich unit 7 (The Kvassåsen unit)

3.37.1. Location

Coordinates: 629402 7000763. Tydal 1:50000 map. (Fig.104).

3.37.2. Introduction

The 7 olivine-rich units south of Ruten (Enclosure 1 and Fig.105) vary in thickness from 1-35 m and occur in a 1400 m-thick sequence. Units 1 to 6 can be traced for 100 – 1000 m along strike, whereas unit 7 can be followed for ~2000 m. Several thinner (<1 m), laterally impersistent units are also developed; these have not been numbered. The units are discontinuous on the map because they wedge out, are cut off by minor faults, or enter poorly exposed ground. No comparable units have been found in the lower part of Stage IV in the Hyllingen area. The olivine gabbros that envelop the units have meter-scale layering and a pale brown colour except where they have been metamorphosed to grey metagabbros. The olivine-rich units have cm-scale layers with dark reddish-brown to light brown colours that reflect their variable olivine content. The most olivine-rich layers, which commonly show variable alteration to serpentine and magnetite, alternate with troctolitic layers. The olivine-rich layers weather out preferentially, giving the outcrops a characteristic ribbed appearance. The olivine-rich units locally display slump structures (Stop 29) and load features (Stops 28 and 30).

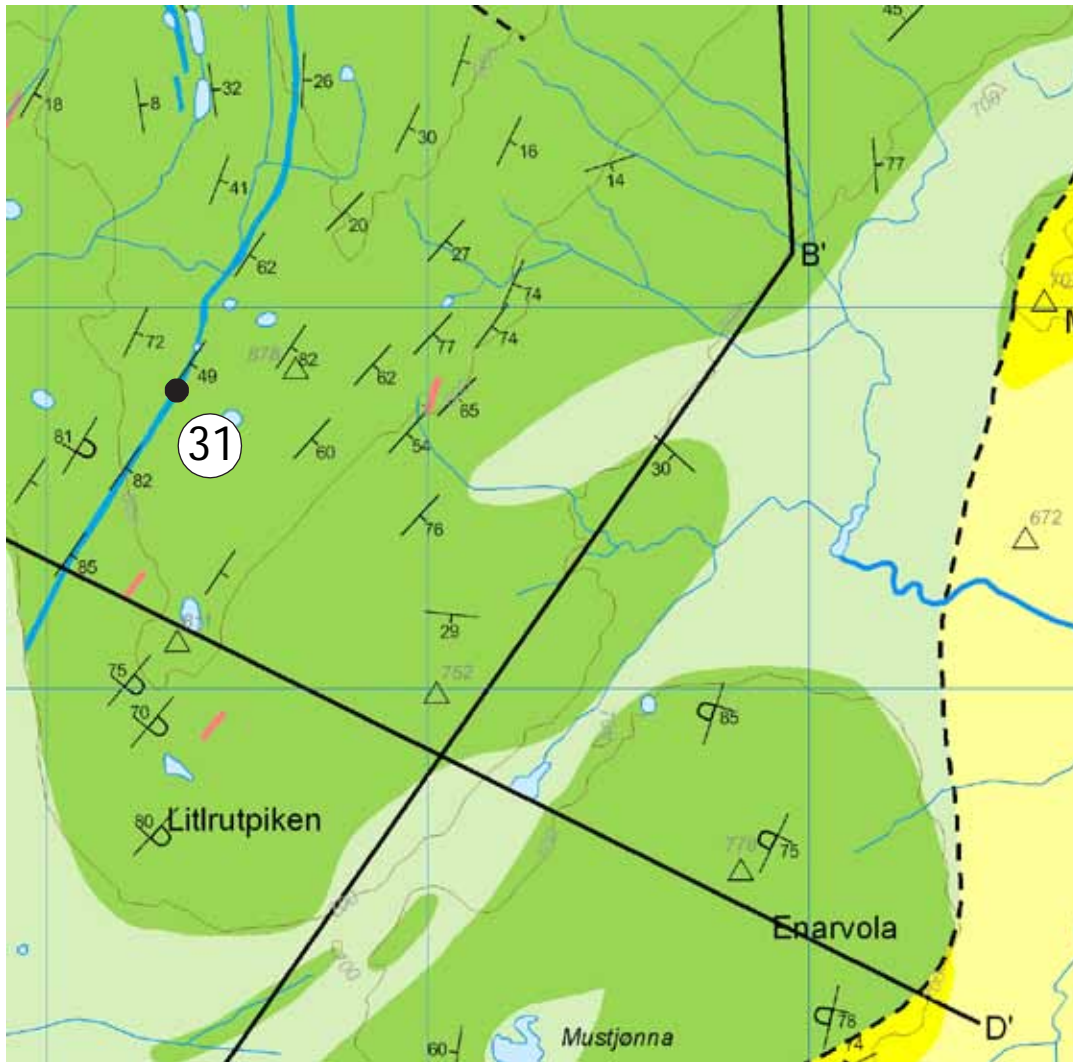


Fig.104. Location of Stop 31.

The lower 6 olivine-rich units are developed in a ~600 m-thick sequence of olivine gabbros (Fig.105). Some 25 m above unit 6, olivine in the olivine gabbros is replaced by Ca-poor pyroxene so that the rock becomes a gabbronorite. These gabbronorites persist for ~350 m where magnetite appears. These magnetite gabbronorites continue for ~100 m, after which they are abruptly overlain by olivine-rich unit 7 with a thickness of 23-35 m. This is in turn overlain by olivine gabbro (30 m), gabbronorite (130 m) and magnetite gabbronorite (>120 m). Plagioclase compositions become continuously more evolved (from $An_{55.5}$ to $An_{50.5}$) up through the interval between units 6 and 7. After the reversal associated with unit 7 (discussed below), plagioclases reach $An_{48.5}$ in the uppermost magnetite-bearing rocks. Highly magnesian olivine compositions (Fo_{74}) occur in unit 4. Here we examine unit 7 (the Kvassåsen unit) which is the thickest and most impressive of the olivine-rich units. The information concerning the olivine-rich units is mostly taken from Meyer & Wilson (1999).

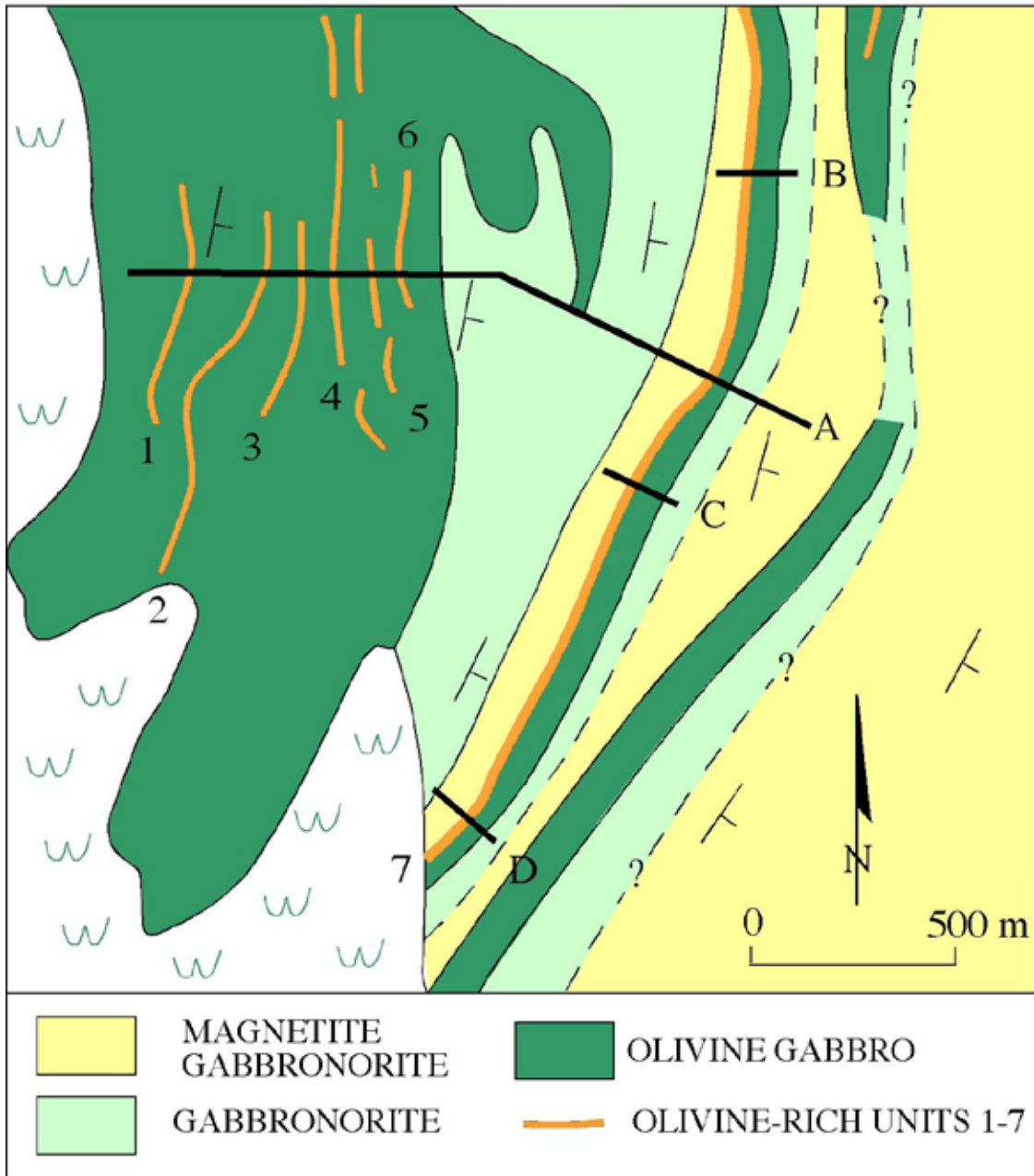


Fig.105. Simplified geological map of the area containing olivine-rich units 1-7. Based on Enclosure 1 and Meyer & Wilson (1999). Sample profiles A – D have been studied by Meyer & Wilson (1999).

3.37.3. Description

Unit 7 dips to the east ($40^\circ - 85^\circ$) along its entire strike length of ~ 2000 m (Figs.105 & 106) and varies in thickness from ~ 23 m in the north to ~ 35 m in the south. It consistently overlies magnetite gabbronorite. Unit 7 has been divided into 8 sub-units on the basis of variations in lithology, texture and the scale of modal layering (Fig.107). Three different layering scales are shown in Fig.107: cm-, dm- and m-scale. Determination of the scale in the field is usually straightforward but, for example, individual cm-scale may occur in m-

scale packages and estimation of their role can be subjective. The bulk composition of the unit is melanocratic olivine gabbro, but individual layers may be isomodal (e.g. dunite, troctolite or olivine gabbro) or modally graded (e.g. olivine-rich base and plagioclase-rich top). The sub-units are well developed in the lower part, but become less clear towards the top.



Fig.106. View to the north from near Stop 31 along the strike of olivine-rich unit 7. The approximate location of unit 7 is marked with a dashed line. The most olivine-rich part of unit 7 (sub-unit e in Fig.107) forms the brown-weathering rocks. Unit 7 dips to the east along its entire strike length.

The base of unit 7 is marked by a laterally persistent, massive 20-50 cm-thick pyroxenite layer (~80% Ca-poor and ~20% Ca-rich pyroxene) which is designated as sub-unit a. In most logs the pyroxenite is overlain by a thin (<1 m) sequence of olivine gabbro with cm-scale layering (sub-unit b). In the southern logs, this is followed by up to 2.4 m of quite massive olivine-rich gabbro with sub-spherical oikocrysts of Ca-rich pyroxene (sub-unit c). This sub-unit wedges out to the north and south and is overlain by 2-5 m of olivine gabbro with dm-scale modal layering (sub-unit d).

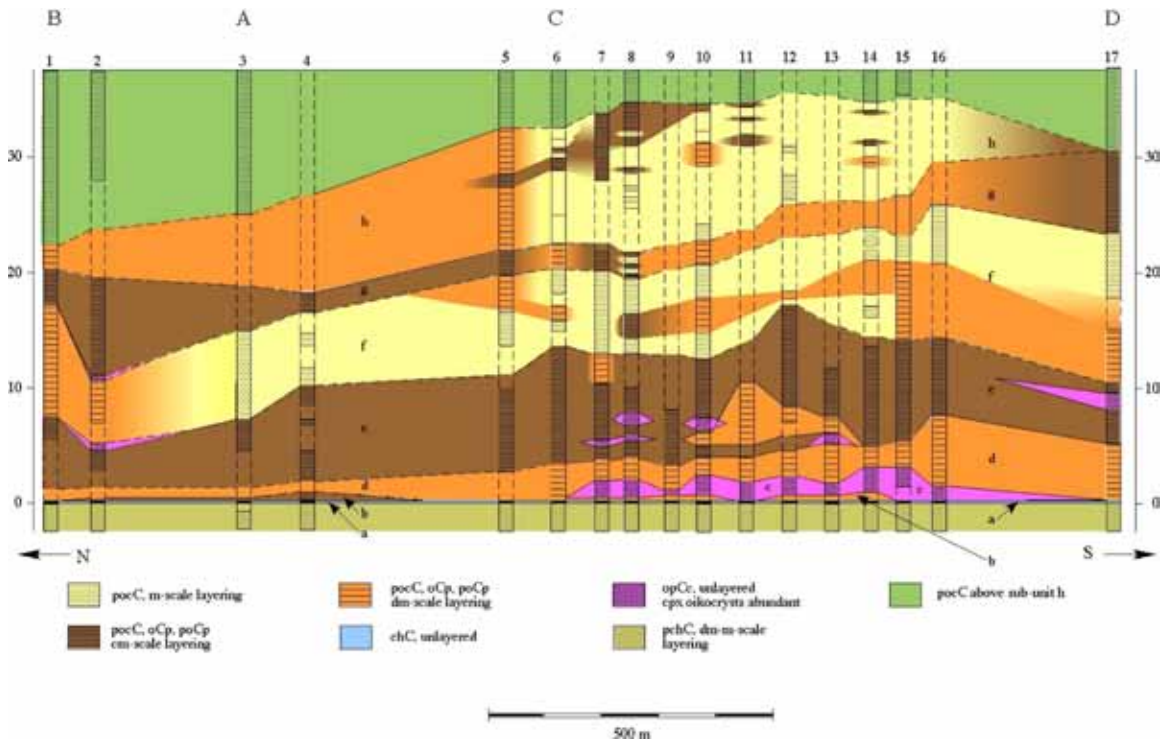


Fig.107. Lithological variations in unit 7 established on the basis of 17 logs. Datum is the lower level of the pyroxenite (chC) that defines the base of the unit. Unit 7 has been divided into 8 sub-units on the basis of the lithology and scale of layering. Vertical exaggeration = x 20. Cumulus phase notation: p = plagioclase; c = Ca-rich pyroxene; o = olivine; h = Ca-poor pyroxene; m = magnetite; C = cumulate. Abbreviations after C = intercumulus status. Numbers 1-17 are the log numbers. Stop 31 is in the vicinity of log 6.

Sub-unit e is the most distinctive part of unit 7 with laterally continuous isomodal to modally graded layers (5-20 mm thick) of dark brown dunite alternating with paler brown troctolite or olivine gabbro (Fig.108). It is developed in all logs but is locally intercalated with intervals with dm-scale layering and some unlayered intervals with Ca-rich pyroxene oikocrysts (similar to sub-unit c). Sub-unit e varies in thickness from ~5-10 m.

Identification and lateral correlation of sub-units is not unequivocal above sub-unit e. The cm-scale layered rocks of sub-unit e are overlain by olivine gabbro and troctolite with m- to dm-scale layers (sub-unit f); dunitic or pyroxenitic layers are locally developed. Sub-unit g comprises cm-scale layered olivine gabbros in most northern logs but the scale of layering increases to dm- and locally m-scale in the south, apart from log 17 where it again has cm-scale layering. Sub-unit h, which is generally poorly exposed, comprises olivine gabbros with cm- to dm-scale layering. The top of sub-unit h, which marks the upper limit of unit 7, is defined by the persistent occurrence of olivine gabbros with dm- to m-scale layering.

Partial alteration of olivine to serpentine is widespread. Veins of serpentine are commonly at an acute angle to the modal layering (Fig.109). This alteration is locally more pervasive (Fig.110).



Fig.108. Stop 31. Sub-unit e in olivine-rich unit 7 consists largely of alternating layers of dunite (dark brown) and troctolite (paler brown). Small-scale modal layering is beautifully developed. Looking south; stratigraphic up is to the left.

The fact that magnetite gabbros are abruptly overlain by thick olivine-rich unit 7 bears witness to a significant compositional reversal. The compositions of cumulus plagioclase (An_{54-51}) and Ca-rich pyroxene ($Mg\#cpx_{76-77}$) just below unit 7 are, however, only slightly more evolved than those in the olivine-rich unit itself (An_{57-52} and $Mg\#cpx_{79-76}$). Olivines are in the range Fo_{72-67} .

It is instructive to follow unit 7 along strike and study the many well-exposed features in this olivine-rich unit that formed as a result of magma mixing, as discussed below.

3.37.4. Significance of the outcrops

The olivine-rich units in Stage IV in the Ruten area are associated with cryptic regressions (Meyer & Wilson, 1999) and are interpreted as having formed in response to repeated events of magma addition. The most primitive cumulates previously recorded in the FHI occur at the Stage III/IV boundary in the Fongen area with An_{60} and $Mg\#cpx_{79}$ and a Sr_i value of 0.70308 ± 2 (Sørensen and Wilson, 1995). These are close to the most primitive compositions ($An_{59.2}$ and $Mg\#cpx_{80.5}$) in olivine-rich units 3 and 4 where the most magnesian olivine is $Fo_{73.6}$. These minerals crystallised from relatively uncontaminated replenishing magma. The most primitive compositions in unit 7 ($An_{55.9}$, $Mg\#cpx_{78.6}$ and $Fo_{71.8}$) are slightly more evolved. If the composition of the replenishing

magma was the same throughout formation of Stage IV, this implies that unit 7 was formed from a hybrid with a large proportion of new relative to resident magma.



Fig.109. Stop 31. Laterally persistent small scale layering in sub-unit e in olivine-rich unit 7. Stratigraphic up is to the right. Two small trough-like features are developed to the left of the hammer. Olivine in the dark-brown layers has been partially altered to serpentine. These layers weather out preferentially so that the paler brown, plagioclase-bearing layers stand out to give a striking ribbed appearance to the outcrops. Thin veins of serpentine are aligned at a slight angle to the modal layering below the hammer and elsewhere.

The modal proportion of olivine in layered cumulates in the Ruten area increases considerably in the olivine-rich units. The occurrence of a laterally persistent pyroxenite layer at the base of unit 7 is also a significant and unique feature in FHI. Both can be explained as a result of magma mixing. The resident magma just before formation of unit 7 was crystallising plagioclase + Ca-rich pyroxene + Ca-poor pyroxene (+ magnetite) on the appropriate cotectic curve. The replenishing magma is believed to have been close to the plagioclase + Ca-rich pyroxene + olivine cotectic. Mixing between these two magmas drove the melt composition into the Ca-poor pyroxene field in the An-Fo-SiO₂ phase diagram, resulting in the crystallisation of the thin basal layer of pyroxenite. Further mixing involving a large proportion of replenishing magma drove the hybrid composition close to that of the primitive end-member. This is discussed in more detail by Meyer & Wilson (1999).



Fig.110. Relatively pervasive alteration of olivine to serpentine in one of the olivine-rich units. Largely unaltered olivine remains brown. Serpentine is white. Magnetite produced during the metamorphic reaction forms black, metallic veins. Oikocrysts of Ca-rich pyroxene stand out as small resistant spheres.

4. ACKNOWLEDGEMENTS

Since I started work on Fongen-Hyllingen in 1973 I have received help, criticism and support from many people. It is not practically possible to name them all here. The research has been made possible by financial support from the Danish Natural Science Research Council and the Carlsberg Foundation. Accommodation during fieldwork was often provided by Trondheim Turistforening. The project was initiated when Niels Østerby Olesen put me on the path to Fongen. Most of the work has been carried out in cooperation with students from Aarhus University. I have many precious memories of time spent in the field with the “Fongen-Hooligans”, all of whom are named in Enclosure 1. Colleagues in Århus and elsewhere have helped in a variety of ways, and I am particularly grateful to Brian Robins, Odd Nilsen, Steve Sparks, Gurli Meyer, Frank Møller Nielsen, Henrik Schiellerup and Britta Paasch. Technical support has been provided with a smile by Lissie Jans, Inger Bech, Else Moltke Nielsen, Inger Tofte, Ingrid Aaes, Jette Villumsen and Inge Mortensen. I am very grateful to the Norwegian Geological Survey (NGU) for help during production of this work, especially Åse Rønningen for technical assistance with the geological map (Enclosure 1), Trond Slagstad (NGU) for technical production of the report and Gurli Meyer for a constructive review. Last, but not least, I must thank my wife and children – Pam, Emma and Daniel – for support and understanding, not least when Fongen fieldwork came before summer holidays.

5. REFERENCES

- Abrahamsen, N., Wilson, J.R., Thy, P., Olesen, N.Ø. & Esbensen, K.H. 1979. Palaeomagnetism of the Fongen-Hyllingen gabbro complex, southern Scandinavian Caledonides: plate rotation or polar shift? *Geophysical Journal of the Royal Astronomical Society* 59, 231-248.
- Abu El-Rus, M.A.A. 2003. Trace element modelling of magma evolution in the Fongen-Hyllingen Intrusion, Trondheim region, Norway. *Journal of Mineralogical and Petrological Sciences* 98, 47-75.
- Abu El-Rus, M.A.A., Wilson, J.R. & Sørensen, H.S. 2007. Magma evolution in the upper part (Stage IV) of the Fongen-Hyllingen Layered Intrusion, central Norway. *Journal of Mineralogical and Petrological Sciences* 102, 93-114.
- Ankatell, J.M., Cegla, J. & Dzulynski, S. 1970: On the deformational structures in systems with reversed density gradients. *Rocznik Polskiego Towarzystwa Geologicznego* 40, 3-30.
- Bird, D.K., Rosing, M.T., Manning, C.E. & Rose, N.M. 1985: Geological field studies of the Miki Fjord area, East Greenland. *Bulletin of the Geological Society of Denmark* 34, 219-235.
- Brandriss M.E. & Bird, D.K. 1999: Effects of H₂O on phase relations during crystallisation of gabbros in the Kap Edvard Holm complex, East Greenland. *Journal of Petrology* 40, 1037-1064.
- Brandriss M.E., Bird, D.K., O'Neil J.R. & Cullers, R.L. 1996: Dehydration partial melting, and assimilation of metabasaltic xenoliths in gabbros of the Kap Edvard Holm complex, East Greenland. *American Journal of Science* 296, 333-393.
- Bucher, K. & Frey, M. 1994: Petrogenesis of metamorphic rocks. Springer-Verlag. 318 pp.
- Campbell, I.H. 1978: Some problems with the cumulus theory. *Lithos* 11, 311-323.
- Carstens, C.W. 1920: Oversigt over Trondheimfeltets bergbygning. *Det Kongelige Norske Videnskabers Selskabs Skrifter* 1, 99-103.
- Dzulynski, S. 1966: Sedimentary structures resulting from convection-like patterns of motion. *Rocznik Polskiego Towarzystwa Geologicznego* 36, 3-21.
- Engell-Sørensen, O. 1985: Grænserelementer omkring den sydlige del (Hyllingen) af Fongen-Hyllingen mafiske kompleks, Norge. Unpublished M.Sc. thesis, University of Aarhus, 120 pp.
- Esbensen, K.H. 1978: Det synorogene, stratiforme gabbrokompleks, Fongen-Hyllingen Intrusionen, Sør-Trøndelag, Norge, sydlige skandinaviske Kaledonider: Magmatisk petrologi og geokemi. Unpublished M.Sc. thesis, University of Aarhus, 292 pp.
- Furnes, H., Roberts, D., Sturt, B.A., Thon, A & Gale, G.H. 1980: Ophiolite fragments in the Scandinavian Caledonides. *Proceedings of the International Ophiolite Symposium, Cyprus 1979*, 582-600.
- Gee, D.G. 1975a: A geotraverse through the Scandinavian Caledonides - Østersund to Trondheim. *Sveriges Geologiska Undersökning Series C*, 66 pp.

- Gee, D.G. 1975b: A tectonic model for the central part of the Scandinavian Caledonides. *American Journal of Science* 275A, 468-515.
- Grenne, T. & Lagerblad, B. 1985: The Fundsjø Group, central Norway - a Lower Palaeozoic island arc sequence: geochemistry and regional implications. In: Gee, D.G. & Sturt, B.A. (eds.): *The Caledonide Orogen - Scandinavia and Related Areas*, 746 - 760.
- Habekost, E.M. 1987: En petrologisk undersøgelse af metabasaltiske indeslutninger i Hyllingen Serien, den sydlige del af det lagdelte mafiske Fongen-Hyllingen Kompleks, Sør-Trøndelag, Norge. Unpublished M.Sc. thesis, University of Aarhus, 153 pp.
- Habekost, E.M. & Wilson, J.R. 1989: Raft-like metabasaltic inclusions in the Fongen-Hyllingen layered intrusive complex, Norway, and their implications for magma chamber evolution. *Journal of Petrology* 30, 1415-1441.
- Holm, D. H. 2003: Teksturelle variationer i en stor kontaktmetamorfoseret metabasaltisk inklusion (Summit Inklusionen) i Fongen-Hyllingen Intrusionen, Norge. Unpublished M.Sc. thesis, University of Aarhus, 136 pp.
- Homan, C.H. 1890: Selbu. Fjeldbygningen inden rektangelkartet Selbus omraade. Norges Geologiske Undersøgelse 2, 39 pp.
- Huppert, H.E., Sparks, R.S.J., Wilson, J.R., Hallworth, M.A., & Leitch, A.M. 1987: Laboratory experiments with aqueous solutions modelling magma chamber processes II. Cooling and crystallisation along inclined planes. In: Parsons, I. (ed.): *Origins of Igneous Layering*, 539-568. Dordrecht: Reidel Publishing Company.
- Hørbye, J.C. 1861: Notitser om Thydal. *Nyt Magazin for Naturvidenskaberne* 11, 220-225.
- Irvine, T.N. 1980: Magmatic infiltration metasomatism, double-diffusive fractional crystallization, and adcumulus growth in the Muskox intrusion and other layered intrusions. In: Hargraves, R.B. (ed.): *Physics of Magmatic Processes*, 325-384. Princeton, NJ: Princeton University Press.
- Irvine, T.N., Keith, D.W. & Todd, S.G., 1983: The J-M platinum-palladium reef of the Stillwater complex, Montana. *United States Geological Survey Professional Paper* 358, 106 pp.
- Jakobsen, N.N. 1985: Petrologien i to udvalgte områder i den sydlige del af Hyllingen Serien, Sør-Trøndelag, Norge. Unpublished M.Sc. thesis, University of Aarhus, 87 pp.
- Josephsen, K. 2003: Magmakammerprocesser i Fongen-Hyllingen Intrusionen, Norge: et detaljestudie af modallagdeling. Unpublished M.Sc. thesis, University of Aarhus, 110 pp.
- Kisch, H.J. 1962: Petrographical and geological investigations in the southwestern Tydal Region, Sør-Trøndelag, Norway *Academisch Proefschrift. University of Amsterdam*. 136 pp.
- Knudsen, L.G. 1990: Petrologien af den nordvestlige del af Fongen-Hyllingen Komplekset, Sør-Trøndelag, Norge: Treknattan området. Unpublished M.Sc. thesis, University of Aarhus, 137 pp.

- Kock-Hansen, K. 1997: En petrologisk undersøgelse af en lagdelt olivinrig enhed i Bierbekeområdet i Fongen-Hyllingen Intrusionen, Sør-Trøndelag, Norge. Unpublished M.Sc. thesis, University of Aarhus, 117 pp.
- Larsen, S.B. 1982: Petrologien af den sydlige del af Fongen-Hyllingen Komplekset - Hyllingen Serien - , Sør-Trøndelag, Norge. Unpublished M.Sc. thesis, University of Aarhus, 181 pp.
- Leshner, C.E., Rosing, M.T. & Bird, D.K. 1992: Metasomatic transformation of host lavas of the Miki Fjord Macrodyke, East Greenland. *EOS, Transactions, American Geophysical Union* 73, 640.
- Maaloe, S. 1978: The origin of rhythmic layering. *Mineralogical Magazine* 42, 337-345.
- McBirney, A.R. & Noyes, R.M. 1979: Crystallization and layering of the Skærgaard intrusion. *Journal of Petrology* 20, 487-544.
- Martin, D., Griffiths, R.W. & Campbell, I.H. 1987: Compositional and thermal convection in magma chambers. *Contribution to Mineralogy and Petrology* 96, 465-475.
- Meyer, G.B. 1994: Lagdelte olivinrige enheder i Rutenområdet i Fongen-Hyllingen Intrusionen, Sør-Trøndelag, Norge. Unpublished M.Sc. thesis, University of Aarhus, 130 pp.
- Meyer, G.B. 1999: Magmatic processes in two gabbroic complexes in the Central Scandinavian Caledonides. Unpublished Ph.D. thesis, University of Aarhus, 180 pp.
- Meyer, G.B. & Wilson, J.R. 1999: Olivine-rich units in the Fongen-Hyllingen Intrusion, Norway: implications for magma chamber processes. *Lithos* 47, 157-179.
- Morse, S.A. 1980: Basalts and phase diagrams. Springer-Verlag, Berlin. 493 pp.
- Möhl, H. 1877: Die Eruptivesteine Norwegens, mikroskopisch untersucht. *Nyt Magazin for Naturvidenskaberne* 23, 17-34.
- Naslund, H.R. 1986: Disequilibrium partial melting and rheomorphic layer formation in the contact aureole of the Basistoppen sill, East Greenland. *Contributions to Mineralogy and Petrology* 93, 359-367.
- Nielsen, K.Aa. 1991: En petrologisk og mineralkemisk undersøgelse af området omkring Tronshatten, Fongen-Hyllingen Komplekset, Norge. Unpublished M.Sc. thesis, University of Aarhus, 109 pp.
- Nilsen, O. 1973: Petrology of the Hyllingen gabbro complex, Sør-Trøndelag, Norway. *Norsk Geologisk Tidsskrift* 53, p. 213-232.
- Nilsen, O., Corfu, F. & Roberts, D. 2007: Silurian gabbro-diorite-trondhemite plutons in the Trondheim Nappe Complex, Caledonides, Norway: petrology and U-Pb geochronology. *Norwegian Journal of Geology* 87, 329-342.
- Olesen, N.Ø. 1974: Geological Map of the Heggset Area, the Trondheim region, University of Leiden.
- Olesen, N.Ø., Hansen, E.S., Kristensen & Thyrsted, T. 1973: A preliminary account on the geology of the Selbu-Tydal area, Trondheim region, Central Norwegian Caledonides. *Leidse Geologische Mededelingen* 49, 259-276.
- Paasch, B. 1991: Petrologien af den nordlige del af Fongen-Hyllingen komplekset, Norge: området nordøst for Fongen. Unpublished M.Sc. thesis, University of Aarhus, 98 pp.

- Parsons, I. (ed.) 1987: *Origins of Igneous Layering*. NATO Advanced Science Institute Series C: Mathematical and Physical Science 196. Dordrecht: Reidel Publishing Company. 666 pp.
- Roberts, D. & Sturt, B.A. 1980: Caledonide deformation in Norway. *Journal of the Geological Society of London* 137, 241 - 250.
- Roberts, D & Wolff, F.C. 1981: Tectonostratigraphic development of the Trondheim region Caledonides, Central Norway. *Journal of Structural Geology* 3, 487 - 494.
- Shelley, D. 1993: *Igneous and metamorphic rocks under the microscope*. Chapman & Hall. 445 pp.
- Sparks, R.S.J. 1985: Discordance in layered intrusions. *Nature* 315, 460.
- Svane, J.O. 1983: Geologien i Melshogna-Skaftet området. Den centrale del af Fongen-Hyllingen Komplekset, Tydal, Sør-Trøndelag, Norge. Unpublished M.Sc. thesis, University of Aarhus, 125 pp.
- Sørensen, H.S. 1990: En petrologisk og mineralkemisk undersøgelse af området nord for Fongskaftet, Fongen-Hyllingen komplekset, Norge. Unpublished M.Sc. thesis, University of Aarhus, 115 pp.
- Sørensen, H.S. 1994: Magmakammerprocesser belyst ved et studie af Fongen-Hyllingen komplekset, Trondheim regionen, Norge. Unpublished Ph.D. thesis, University of Aarhus, 178 pp.
- Sørensen, H.S. & Wilson, J.R. 1995. A strontium and neodymium isotopic investigation of the Fongen-Hyllingen layered intrusion, Norway. *Journal of Petrology* 36, 161-187.
- Sørensen H.S. & Wilson J.R. 1996: Petrology of the Treknattan intrusion in the Fongen-Hyllingen complex, Trondheim region, Norway: a late intrusion into an evolved layered complex. *Lithos* 38, 109-127.
- Tegner, C., Wilson, J.R. & Robins, B. 2005: Crustal assimilation in basalt and jotunite: Constraints from layered intrusions. *Lithos* 83, 299-316.
- Thayssen, F. 1998: En petrologisk og mineralkemisk undersøgelse af metamorfe bjergarter i den sydlige del af Fongen-Hyllingen Intrusionen, Norge. Unpublished M.Sc. thesis, University of Aarhus, 110 pp.
- Thjømøe, P.A. 1995: En geologisk undersøgelse af mafiske gange, ved Ramfjellet-Tofjellet området, Trondheim regionen, Norge. Unpublished M.Sc. thesis, University of Aarhus, 108 pp.
- Thy, P. 1977: En petrografisk og geokemisk undersøgelse af den centrale del (Ruten) af Fongen-Hyllingen gabbro komplekset, Tydal, Sør-Trøndelag, Norge. Unpublished M.Sc. thesis, University of Aarhus, 192 pp..
- Thy, P. & Wilson, J.R. 1980: Primary igneous load-cast deformation structures in the Fongen-Hyllingen Complex, Trondheim region, Norway. *Geological Magazine* 117, 363-371.
- Törnebohm, A.E. 1896: Grunddragen i det centrale Skandinaviens bergbygnad. Kongelig Svenska Vetenskaps-Akadamiene Handlingear 28, 212 pp.
- Vogt, J.H.L. 1889: Om fund af Dictyonema og Stinkkalk i Alunskifer. Foredrag 16. nov 1888. *Forhandlinger i videnskabs-selskabet i Christiania for 1888. Oversigt over møder*, 12.
- Wager, L.R. & Brown, G.M. 1968: *Layered Igneous Rocks*, 587 pp. Edinburgh: Oliver & Boyd.

- Wilson, J.R. 1985: Fe-Ti oxides in the Fongen-Hyllingen layered mafic intrusion. *Norges Geologiske Undersøkelse. Bulletin* 402, 73-78.
- Wilson, J.R. & Engell-Sørensen, O. 1986. Basal reversals in layered intrusions: evidence for emplacement of compositionally stratified magma. *Nature* 326, 616-618.
- Wilson, J.R. & Larsen, S.B. 1982: Discordant layering relations in the Fongen-Hyllingen basic intrusion. *Nature* 299, 625-626.
- Wilson, J.R. & Larsen, S.B. 1985: Two dimensional study of a layered intrusion: the Hyllingen Series, Norway. *Geological Magazine* 122, 97-121.
- Wilson, J.R. & Olesen, N.Ø. 1975: The form of the Fongen-Hyllingen gabbro complex, Trondheim region, Norway. *Norsk Geologisk Tidsskrift* 55, 423-439.
- Wilson, J.R. & Pedersen, S. 1982: The age of the synorogenic Fongen-Hyllingen Complex, Trondheim region, Norway. *Geologiska Föreningens i Stockholm Förhandlingar* 103, 429-435.
- Wilson, J.R. & Sørensen, H.S. 1996: The Fongen-Hyllingen layered intrusive complex, Norway. In: Cawthorn, R.G. (ed.): *Layered Intrusions*, 303-329. Amsterdam: Elsevier.
- Wilson, J.R., Esbensen, K.H & Thy, P. 1981a. Igneous petrology of the synorogenic Fongen-Hyllingen layered basic complex, south-central Scandinavian Caledonides. *Journal of Petrology* 22, 584-627.
- Wilson, J.R., Esbensen, K.H & Thy, P. 1981b. A new pyroxene fractionation trend from a layered basic intrusion. *Nature* 290, 325-326.
- Wilson, J.R., Hansen, B. & Pedersen, S. 1983: Zircon U-Pb evidence for the age of the Fongen-Hyllingen Complex, Trondheim region, Norway. *Geologiska Föreningens i Stockholm Förhandlingar* 105, 68-70.
- Wilson, J.R., Josephsen, K. & Holm, D.H. 2004. Den lagdelte Fongen-Hyllingen Intrusion, Norge. *Geologisk Tidsskrift* 1, 1-24.
- Wilson, J.R., Menuge, J.F., Pedersen, S. & Engell-Sørensen, O 1987. The southern part of the Fongen-Hyllingen layered mafic complex, Norway: emplacement and crystallisation of compositionally stratified magma. In: Parsons, I. (ed.) *Origins of Igneous Layering*. Nato ASI Series, 196 Dordrecht: D. Reide, 145-185.
- Wolff, F.C. & Roberts, D. 1980: Geology of the Trondheim region. *Norges Geologiske Undersøkelse Bulletin* 356, 117-167.